A TENSOR PRODUCT DECOMPOSITION OF THE MANY-ELECTRON HAMILTONIAN

by

Fredrick A. Senese

Dissertation submitted to the Faculty of the
Virginia Polytechnic Institute and State University
in partial fulfillment of the requirements for the degree of
DOCTOR OF PHILOSOPHY
in
Physical Chemistry

APPROVED:

Jimmy W. Viers, Chairman

John. C. Schug Jack D. Graybeal

Layne T. Watson Christopher Beattie

May, 1989
Blacksburg, Virginia

A TENSOR PRODUCT DECOMPOSITION OF THE MANY-ELECTRON HAMILTONIAN

by

Fredrick A. Senese

Committee Chairman: Jimmy W. Viers

Chemistry

(ABSTRACT)

A new direct full variational approach is described. The approach exploits a tensor (Kronecker) product construction of the many-electron Hamiltonian and has a number of computational advantages. Explicit assembly and storage of the Hamiltonian matrix is avoided by using the Kronecker product structure to form matrix-vector products directly from the molecular integrals. Computation-intensive integral transformations and formula tapes are unnecessary. The wavefunction is expanded in terms of spin-free primitive kets rather than Slater determinants or configuration state functions and is equivalent to a full configuration interaction expansion. The approach suggests compact storage schemes and algorithms which are naturally suited to parallel and pipelined machines.

Sample calculations for small two- and four-electron systems are presented. The preliminary ground state potential energy surface of the hydrogen molecule dimer is computed by the tensor product method using a small basis set.

Acknowledgements.

This work was supported by a generous grant of computer time from the Cornell Theory Center and the Cornell National Supercomputer Facility.

I would like to thank the members of my graduate committees for their guidance in the writing of this dissertation. Special thanks are due to Dr. Jimmy Viers and Dr. John Schug. Their candor, encouragement and assistance were deeply appreciated. This dissertation is founded on the work of Dr. Christopher Beattie of the Mathematics Department at Virginia Tech; without him this work would not have been possible.

Also, much is owed to Dr. George Sanzone and to Dr. Harold Bell, who have strongly influenced my research interests. The contribution of my wife can scarcely be expressed; her sense of humor and moral support were critical in the completion of this dissertation.

Contents

List of Tables

List of Figures

Chapter 1

Introduction

A central problem in theoretical chemistry is the approximation of the eigenvalues and eigenfunctions of the Hamiltonian operator for many-electron molecular systems.

$$\hat{\mathbf{H}}\Psi_i = E_i\Psi_i \tag{1.1}$$

where $\hat{\mathbf{H}}$ is the molecular Hamiltonian operator with domain $\mathcal{D}\hat{\mathbf{H}}$ dense in Hilbert space $\mathcal{H}$, Ψ_i is a dynamical state function which depends on particle space and spin coordinates, and E_i is the total energy of the system in the state described by Ψ_i. *Ab-initio* solutions of equation 1.1 can be used to predict a variety of molecular properties and energies (including polarizabilities, dipole moments, excitation energies, ionization potentials, electron affinities, binding energies, intermolecular interaction energies, transition probabilities and moments, atomic term level splittings, force constants, equilibrium molecular geometries, paramagnetic shielding tensors, hyperfine structure constants, charge densities, electric field gradients, and population analyses) [1].

This work introduces a new variational approach for the approximate solution of equation 1.1 which is equivalent to the method of full configuration interaction. Section 1.1 outlines three fundamental approximations which underly all further developments, and presents the form of the molecular Hamiltonian operator and its eigenfunctions under these approximations. Section 1.2 explains the motivation for fully variational electronic structure calculations and briefly describes two post-Hartree

Fock variational treatments which are closely related to the tensor product approach - the method of configuration interaction and the multistructure valence bond approach. Section 1.3 provides an overview of the tensor product approach, outlining its strengths and weaknesses with respect to the standard configuration interaction and multistructure valence bond methods. In Chapter 2, a Kronecker product form of the electronic Hamiltonian is obtained by exploiting the tensor product structure of the N-electron model space $\mathcal{V}^{[N]}$. In Chapter 3, the restriction of the eigenvector to physically relevant subspaces of $\mathcal{V}^{[N]}$ using Young projectors leads to a compact storage scheme for the eigenvector, which can be visualized by rectangular arrays of Weyl tableau. Chapter 4 explains how the tensor product Hamiltonian and the Weyl tableau construction can be exploited in the iterative solution of the large matrix eigenvalue problem. Chapter 5 presents applications of the tensor product approach to several small model systems, including calculations on the hydrogen molecule and the hydrogen molecular dimer $(H_2)_2$ for small basis sets. Chapter 6 concludes with a summary and suggestions for possible refinements and extensions of the method.

Throughout this work we use the following notation. Operators are denoted by hats (e. g., $\hat{\mathbf{H}}$); groups, spaces, and subspaces are represented by calligraphic letters (e. g., $\mathcal{S}_N, \mathcal{H}, \mathcal{V}$). Matrices are represented by bold face Latin letters; N-electron matrices are denoted by capital letters while one-electron matrices are lower case. Similarly N-electron and orbital functions are denoted by upper and lower case Greek letters, respectively.

1.1 The Electronic Problem

For all but the smallest systems, equation 1.1 can be solved only approximately. In this work (and in most treatments of electronic structure) the problem is simplified by:

1) separating the spin and spatial variables;

2) separating the electronic and nuclear motions;

3) restricting the domain of $\hat{\mathbf{H}}$ to a finite-dimensional model space $\mathcal{V}^{[N]} \subset \mathcal{H}$ (the "algebraic approximation" [95]).

The spin and spatial variables can uncoupled by neglecting relativistic effects. One then approximately solves equation 1.1 in the spatial variables only; the spin part of the problem leads to the requirement that the total state function be antisymmetric with respect to the exchange of space and spin coordinates for identical fermions (particles with half-integral spins). The total state function must also be symmetric with respect to exchange of space and spin coordinates for identical bosons (particles with integral spins); however once a separation of electronic and nuclear space and spin coordinates has been accomplished the nuclear spins have no direct effect on the electronic part of the problem, and we assume for simplicity that all nuclei have zero spin.

In molecules which contain only first row atoms, relativistic effects are usually small and can be treated as a perturbation of the nonrelativistic Hamiltonian if necessary. However, in heavier atoms the inner electrons move at relativistic velocities, resulting in a contraction of the inner shells which effectively screens the nuclear charge from the valence electrons. Thus nonrelativistic treatments become increasingly inadequate as nuclear charge increases [69, 90]. For a recent review of relativistic quantum mechanics see Pyykkö [70].

Neglecting all spin-spin and spin-orbit coupling terms that do not vanish in the nonrelativistic limit (and terms which represent the effects of external fields) the spin-free Hamiltonian has the form

$$\hat{\mathbf{H}} = \hat{\mathbf{T}}_{nuc} + \hat{\mathbf{T}}_{elec} + \hat{\mathbf{V}}_{nuc} + \hat{\mathbf{V}}_{elec} + \hat{\mathbf{V}}_{nuc-elec}. \tag{1.2}$$

Using atomic units and the molecular coordinate system of Figure 1.1, the individual kinetic and potential energy operators can be written

$$\hat{\mathbf{T}}_{nuc} = -\sum_{a=1}^{n} \frac{1}{2M_a} \nabla_a^2 \tag{1.3}$$

$$\hat{\mathbf{T}}_{elec} = -\frac{1}{2} \sum_{i=1}^{N} \nabla_i^2 \tag{1.4}$$

$$\hat{V}_{nuc} = \sum_{a>b}^{n} \frac{Z_a Z_b}{|R_a - R_b|} \tag{1.5}$$

$$\hat{V}_{elec} = \sum_{i>j}^{N} \frac{1}{|r_i - r_j|} \tag{1.6}$$

$$\hat{V}_{nuc-elec} = -\sum_{i=1}^{N} \sum_{a=1}^{n} \frac{Z_a}{|R_a - r_i|} \tag{1.7}$$

where $\hat{T}_{nuc}$ corresponds to the kinetic energy of the n nuclei with individual masses M_a, $\hat{T}_{elec}$ is the electronic kinetic energy operator, $\hat{V}_{nuc}$ represents the Coulombic repulsion between the n nuclei with individual charges Z_a, $\hat{V}_{elec}$ is the interelectronic Coulombic repulsion operator, and $\hat{V}_{nuc-elec}$ accounts for the electrostatic attraction between the electrons and the nuclei. The subscripts i and a of the Laplacian operators denote differentiation with respect to the coordinates of the i-th electron and the a-th nucleus, respectively; $|\mathbf{x}|$ denotes the Euclidean norm of the vector $\mathbf{x}$.

Further simplification of 1.1 can be achieved by noting that because nuclear masses are at least 3 orders of magnitude larger than the electronic mass, nuclear and electronic motions are approximately separable. Under the 'clamped nucleus' approximations [11, 12, 51] the nuclear masses are assumed to be infinite, so that $\hat{T}_{nuc}$ can be neglected and $\hat{V}_{nuc}$ is a constant. The remaining terms comprise the *electronic* Hamiltonian operator $\hat{H}_{elec}$ which can be written

$$\hat{H}_{elec} = \sum_{i=1}^{N} \hat{h}(i) + \sum_{i<j}^{N} \hat{g}(i,j), \tag{1.8}$$

where the one-electron operators $\hat{h}(i)$ include the electronic kinetic energy and nuclear attraction terms

$$\hat{h}(i) = -\frac{1}{2}\nabla_i^2 - \sum_{a}^{N_a} \frac{Z_a}{|r_i - R_a|} \tag{1.9}$$

and the two-electron operators $\hat{g}(i,j)$ are the usual Coulombic repulsion operators $|r_i - r_j|^{-1}$. Note that the forms of the one- and two-electron operators are identical for all electrons, and so $\hat{H}_{elec}$ is symmetric with respect to permutations of the electron labels as required by the physical indistiguishability of electrons. Thus permutation operators acting on the electron labels commute with the electronic Hamiltonian, a

fact that proves very useful in the selection of physically relevant eigenfunctions (see Chapter 3).

The high symmetry of atoms permits approximate solution of the spin-free electronic Schrödinger equation at this point by allowing a separation of angular and radial variables. The angular part of the problem is solved analytically; the radial part involves solution of a second order ordinary differential equation. For molecules of arbitrary symmetry this separation of variables is generally not possible. Approximate solutions in these cases are nearly impossible to obtain without restricting the domain of $\hat{\mathbf{H}}$ to a finite-dimensional model subspace $\mathcal{V}^{[N]}$ of the full Hilbert space H. If the subspace is nearly invariant under the action of the original Hamiltonian operator then the approximate eigenvalues and eigenvectors obtained from the model Hamiltonian matrix will yield accurate approximations to the nonrelativistic molecular energies and eigenstates. If $\{\Psi_i\}$ is a set of N-electron functions which forms a basis for the model subspace, the N-electron Schrödinger eigenfunctions Φ can be approximated by

$$\Phi \approx \sum_{i=1}^{D} c_i \Psi_i. \tag{1.10}$$

The linear expansion coefficients c_i can be determined variationally, by seeking the stationary points of the Rayleigh quotient

$$\varepsilon(\Phi) = \frac{\int \Phi^*(\mathbf{H}\Phi)d\tau}{\int \Phi^*\Phi d\tau}. \tag{1.11}$$

where the integrations are over all space and the energy functional $\varepsilon(\Phi)$ is a variational upper bound on the true ground state electronic energy. This procedure, called the ***Rayleigh-Ritz*** or *linear variation* method, reduces the Schrödinger equation to the general matrix eigenvalue problem

$$\mathbf{H}\,c = \varepsilon\,\mathbf{S}\,c. \tag{1.12}$$

S is the N-electron overlap matrix of scalar products

$$S_{ij} = \int \Psi_i^* \Psi_j d\tau = \langle i \mid j \rangle \tag{1.13}$$

and H is the matrix representation of $\hat{\mathbf{H}}$ restricted to an N-electron model space spanned by the $\{\Psi_i\}$, with elements

$$H_{ij} = \int \Psi_i^* \hat{\mathbf{H}} \Psi_j d\tau = \langle i \mid \hat{\mathbf{H}} \mid j \rangle. \tag{1.14}$$

where equations 1.13 and 1.14 introduce the Dirac bracket notation, which symbolizes the function Ψ_i by the *ket* $|i\rangle$ and its conjugate Ψ_i^* by the *bra* $\langle i|$. A bra and ket with an operator between them indicates a *bracket* (*e. g.*, the integral of equation 1.14). The ϵ are variational upper bounds on the true electronic energies.

The variational approach provides improvable, guaranteed upper bounds on the true energies with errors that are second order in the errors in the eigenfunction. A thorough discussion of the role of the variation principle in quantum chemistry is given by Epstein [27].

1.2 A Survey of Variational Electronic Structure Methods

No attempt will be made to provide a complete review of variational methods here. The literature on the Hartree-Fock and configuration interaction methods is vast, and a complete survey or theoretical exposition is beyond the scope of this dissertation; the reader is directed to a number of excellent reviews for further information. This section will highlight the strengths and weaknesses of these methods to provide a basis for comparison with the tensor product approach and to explain the motivation for full variational treatements of the electronic problem.

1.2.1 Orbital Models

The sum of one-electron operators $\hat{\mathbf{H}}_{bare} = \sum_{i=1}^{N} \hat{\mathbf{h}}(i)$ is an independent electron or 'bare nucleus' Hamiltonian whose eigenvalues and eigenvectors can be obtained very simply. The N-electron problem

$$\hat{\mathbf{H}}_{bare}\Phi(r_1, \ldots, r_N) = \epsilon\Phi(r_1, \ldots, r_N) \tag{1.15}$$

is decomposed into N one-electron problems

$$\hat{\mathbf{h}}(i)\phi(r_i) = \varepsilon_i\phi(r_i) \tag{1.16}$$

where $\phi(r_i)$ is a one-electron function (orbital) describing the independent motion of the i-th electron and ε_i is the corresponding one-electron energy, such that $\varepsilon = \sum_{i=1}^{N} \varepsilon_i$ and Φ is approximated by $\prod_{i=1}^{N} \phi_i$. This simplification motivates the independent electron models, which approximate $\hat{\mathbf{H}}$ as a sum of one-electron operators.

The relative contribution of the two-electron terms is too large to be neglected or treated as a perturbation of the bare nucleus Hamiltonian. However, the decomposition of the electronic Hamiltonian into one-electron operators can be accomplished by approximating $\hat{\mathbf{g}}(i,j)$ as effective one electron operator $v^{HF}(i)$ representing the potential experienced by the i-th electron in the average field created by the other $N-1$ electrons. The model Hamiltonian is then written as a sum of Fock operators $\hat{\mathbf{f}}(i) = \hat{\mathbf{h}}(i) + v^{HF}(i)$, and the approximate solution of 1.1 reduces to iterative solution of the coupled one-electron Hartree-Fock equations $\hat{\mathbf{f}}(i)\phi(r_i) = \varepsilon_i\phi(r_i)$ where ε_i is a one-electron energy. The motion of the i-th electron is uncorrelated with the motions of all other (different-spin) electrons and is described by the orbital $\phi(r_i)$. The Hartree-Fock approach is a nonlinear variational method in which the orbitals are varied at each step of the iteration until a self-consistent field is obtained. For computational details, see [2]. For general expositions of the method see the texts by March [55], Froese-Fischer [30], and Szabo and Ostland [86]. A survey of Hartree-Fock results is given by Richards *et. al.* [71] and Mulliken [1].

The Hartree-Fock approximation is capable of recovering a large fraction of the total nonrelativistic energy. For example, Hartree-Fock calculations can recover 98.9 percent of the total energy of LiH [95]. However the binding energy for this molecule is 1.1 percent of the total energy, and in general the error in Hartree-Fock total energies are the same order of magnitude as most energies of chemical interest (which are energy *differences*). In some cases the Hartree- Fock approximation leads to qualitatively incorrect predictions; for example, the dissociation of molecules is inadequately modelled. With a large basis set, the discrepancy between the Hartee-Fock and exact nonrelativistic energies is chiefly due to neglect of electron correlation. Löwdin [52]

defined the correlation energy as

$$E_{corr} = E_{nr} - E_{HF} \tag{1.17}$$

where the exact nonrelativistic energy E_{nr} is usually estimated by subtracting relativistic corrections from the true (experimental) energy. However, the interelectronic Coulombic repulsion can be strongly coupled with relativistic effects [31, 14], so that the correlation and nonrelativistic energies are not absolutely additive. Note also that the Hartree-Fock energy includes the effect of exchange correlation (that is, the statistical correlation of the motions of same-spin electrons). In general, E_{corr} denotes an effective correlation energy obtained as the difference between the the energies obtained by a correlated method and the Hartree-Fock method.

1.2.2 Configuration Interaction Methods

Let the Ritz trial functions $\{\psi_i\}$ be configuration functions, N-electron functions constructed from a basis of one electron functions $\{\phi_i\}$, $i = 1, \ldots, m$. Spin and symmetry-adapted linear combinations of these configuration functions correspond to states of the system with fixed orbital occupancies (electronic configurations). Expansion 1.10 represents a mixing or interaction of these configurations in the total wavefunction, so the Rayleigh-Ritz procedure with configuration functions is called the method of configuration interaction (CI). If all possible configuration functions are included in the expansion, the method of full configuration interaction (FCI) is obtained.

The method of full configuration interaction produces selected eigenvalue-eigenvector pairs of a finite dimensional restriction of the original molecular Hamiltonian in a subspace spanned by chosen N-electron configuration functions. Typically the N-electron functions are Slater determinants or spin and symmetry-adapted linear combinations of Slater determinants (configuration state functions), which are themselves constructed from a basis of 1-electron functions (atomic or molecular orbitals). FCI provides approximate eigenpairs of the time-independent Hamiltonian equation which become exact as the approximating subspaces become dense- a limit which is unattainable with any finite computation (or finite basis set). This characteristic makes FCI

energies and properties highly accurate benchmarks for the calibration of methods which incorporate further approximations [4]. For example, FCI aids in the selection of active orbital spaces in multiconfigurational self-consistent field calculations, and allows the effects of the truncation of expansions for expectation values in limited CI calculations to be gauged. Additionally, FCI is the only post-Hartree Fock method that is at once size consistent, extensive, and variational.

While conceptually simple, FCI is the most computationally demanding of all current treatments of electron correlation. The FCI wavefunction is written as a linear combination of N-electron trial functions; the expansion coefficients are then obtained variationally by solving a generalized matrix eigenvalue problem. In general, the number of terms in the expansion of the wavefunction is extremely large and governs the dimension of the resulting matrix eigenvalue problem. For molecules of arbitrary symmetry the number of variational FCI expansion coefficients required for an N-electron, m-level, spin S system in a basis of configuration state functions is given by Weyl's number [63, 64]

$$D(m,N,S) = \frac{2S+1}{m+1}\binom{m+1}{N/2-S}\binom{m+1}{N/2+S+1} \tag{1.18}$$

Because m must be much greater than N to recover a chemically significant fraction of the correlation energy, FCI rapidly becomes intractable as the number of electrons increases. For m much greater than N Weyl's number approaches

$$\frac{(2S+1)m^N}{(\frac{1}{2}N-S)!(\frac{1}{2}N+S+1)!} \tag{1.19}$$

Most configuration interaction calculations reduce the dimension of the problem by truncating the N-particle expansion. A large fraction of the correlation energy is usually recovered by including only single and double excitations from a set of reference configurations. Usually the neglect of configurations involving excitations of the inner shell electrons has little effect on chemical energies; chemical events do not involve the inner shells directly so their contribution to the correlation energy remains constant. However highly excited configurations can strongly interact with the single and double excitations, significantly affecting the interaction between the reference and singly and doubly excited states [17]. Thus simply restricting the CI

space to specific excitation classes sometimes proves inadequate and a more careful selection of configurations is required. There are a number of methods for selecting the most important configurations, either directly using perturbative approaches [16] or indirectly by careful choice of virtual orbitals [8].

If a full N-particle expansion of length L is truncated to $M < L$ terms, the eigenvalues $E_1^{(L)} \leq \cdots \leq E_L^{(L)}$ and $E_1^{(M)} \leq \cdots \leq E_M^{(M)}$ of the matrix representatives of $\hat{\mathbf{H}}$ in the subspaces spanned by the full and truncated expansion sets are related by the Cauchy interlace theorem [21]

$$E_i^{(L)} \leq E_i^{(M)} \leq E_{i+L-M}^{(L)} \tag{1.20}$$

(also known as MacDonald's separation theorem [54]). Full CI energies are always variationally lower (and hence more accurate) than truncated CI energies computed in an identical orbital subspace. Furthermore, the truncated CI energies converge very slowly to the FCI energies as the size of the N-electron expansion is increased, and limited CI calculations often must include a large number of configurations to provide chemically accurate results. An additional disadvantage of limited CI is that truncation of the CI expansion results in the loss of size consistency [95]. For example, a CI expansion for the hydrogen molecule which includes only single and double excitations from the reference configuration leads to exact (nonrelativistic) energies in the limit of basis set completeness. However, applying the same level of configuration mixing to a pair of infinitely separated hydrogen molecules does not lead to the correct energy, since triple and quadruple excitations must be included in the FCI expansion of the dimer. A perturbational analysis of the truncated CI expansion reveals that nonphysical terms involving the double excitations arise which do not vary linearly with N (corresponding to unlinked Brandow diagrams [95]). In the full expansion these nonphysical terms are cancelled by further nonphysical terms which involve the quadruple excitations. Thus truncated CI energies do not vary linearly with the number of electrons; in fact the energy becomes proportional to $N^{1/2}$ as N approaches infinity. Table 1.2.2 shows the percentage error in the total energy due to size inconsistency of double excitation CI for systems of noninteracting $(H_2)_2$ and He monomers [3].

Table 1.1: Size consistency errors in double-excitation CI calculations for collections of n noninteracting hydrogen molecules and helium atoms (taken from Bartlett).

n	Error H_2 (%)	Error He (%)
2	1.5	0.8
4	4.8	2.4
10	12.3	6.5
100	48.0	34.8
1000	79.1	70.8

The truncated CI expansion becomes an increasingly inadequate approximation as the number of particles is increased. The lack of size-consistency makes the accurate estimation of ionization energies and intermolecular interactions difficult. The nonphysical components of the truncated CI expansion are in some cases quite sensitive to variations in molecular geometry [97] and can produce aberrations in the shapes of potential energy surfaces and in the description of excited states.

The dimension and structure of the model Hamiltonian matrix **H** precludes the use of most methods based on basis transformation. Alternative methods for large, sparse matrix eigenvalue problems are based on various vector or subspace iterations (e.g., the Lanczos [45] and Davidson [25] methods). A kernel of most implementations of these large matrix methods involves formation of Hamiltonian matrix-vector products $x = \mathbf{H}y$, where the column vectors x and y in some sense approximate eigenvectors of **H**. In most full (and truncated) CI calculations this operation is the computational bottleneck encountered during iterative solution of the large-matrix eigenvalue problem.

Conventional (or *formula-* or *configuration-driven*) CI methods explicitly compute and store Hamiltonian matrix elements (or formulas for them) for the evaluation of x. The N electron functions are usually spin-adapted linear combinations of Slater determinants, and the Hamiltonian matrix elements are rather complex as a result. Conventional CI computes the information necessary for the construction of the matrix elements only once, at the beginning of the calculation. This information is recorded on a *symbolic formula tape* which consists of configuration labels, integral

indices, and spin-coupling coefficients in secondary storage. Brooks and Schaeffer [15] note that the time required to coinpute the formula tape is an order of magnitude longer than either the integral transformation or the solution of the Hamiltonian matrix eigenvalue problem.

While conventional CI allows flexibility in the selection of configurations for truncated CI expansions, calculations are severely I/O-bound. The number of Hamiltonian matrix elements which must be constructed increases as the square of the number of configurations. Even considering the sparsity of $\mathbf{H}$, the storage requirements for conventional full CI calculations are prohibitively large for systems with more than a few electrons when nonminimal basis sets are used. Even for truncated CI calculations, the construction of complete potential energy surfaces using conventional methods is very costly, despite the fact that the same formula tape can be used for many geometries.

Direct (or *integral-driven*) CI methods [74, 50, 75, 49] form the matrix-vector product directly from a list of molecular integrals by processing the integrals in a specific order and multiplying them by the appropriate CI coupling coefficients. Early direct CI calculations were applicable to wavefunctions composed of single and double excitations from a variety of specific reference functions; the formalism needed to apply the method to general reference functions and to include highly excited determinants seemed forbidding. Siegbahn [83] solved the former problem by separating the configuration space into two noninteracting subspaces– an "internal" space spanned a set of arbitrary reference configurations, and a larger "external" space spanned by the excited configurations. The result was a general direct CI procedure which could employ arbitrary reference functions.

Most modern direct CI methods employ the mathematical language of the unitary group by constructing the model Hamiltonian

$$\hat{\mathbf{H}}_{model} = \sum_{r,s}^{m} \sum_{i=1}^{N} |\phi_r(i)\rangle \, h_{rs} \, \langle \phi_s(i)| + \frac{1}{2} \sum_{r,s,t,u}^{m} \sum_{i<j}^{N} |\phi_t(i)\rangle \, |\phi_r(j)\rangle \, g_{rstu} \, \langle \phi_s(i)| \, \langle \phi_u(j)| \quad (1.21)$$

using the completeness relation and the fact that the matrix representatives of the one and two electron operators in $\mathcal{V}^{[N]}$ are independent of the particle indices. Orthonormality of the orbital basis leads to commutation relations among the basic

replacement operators $\hat{\mathbf{E}}_{rs} = \sum_{i=1}^{N} |\phi_r(i)\rangle \langle \phi_s(i)|$ which satisfy commutation relations identical to those of the generators of the unitary group. Application of the unitary group theory [65, 79] can then greatly simplify the calculation of the CI coupling coefficients, which are matrix elements of the replacement operators. The method leads to vector algorithms which have made possible many impressive full CI benchmarks [5]. The unitary group-driven direct CI methods of Siegbahn [81] and Knowles and Handy [42] are capable of treating large CI expansions (with up to 10^6 terms).

We briefly mention a very successful variational alternative to the configuration interaction methods. Configuration state functions are typically constructed from Hartree-Fock orbitals, since the latter are easily obtained and their use ensures that single excitations do not directly mix with the Hartree-Fock reference determinant (satisfying Brillouin's theorem [86]). However the Hartree-Fock orbitals are optimal only for single determinantal wavefunctions, since the virtual orbitals are optimized in an N-electron field while the occupied orbitals experience an averaged $N-1$ electron field [40]. This nonphysical feature of the Hartree-Fock orbitals often results in poorly convergent CI expansions. The multiconfigurational self-consistent field (MCSCF) methods remedy this problem by variationally optimizing both the configuration expansion coefficients of equation 1.10 and the orbital basis. In contrast the CI techniques vary only the expansion coefficients, and Hartree-Fock methods optimize only the orbitals[92]. The *complete active subspace* variant of MCSCF[82] selects all configurations which can be constructed from a set of doubly occupied *inactive* orbitals and a set of selected *active* orbitals, providing a chemically intuitive method for configuration selection. When the entire orbital set is active, complete active subspace MCSCF gives fully variational results. MCSCF methods which truncate the configuration expansion share the shortcomings of limited CI methods; they are not size-consistent and the quality of the results is highly dependent on the selection of configurations. For reviews of the MCSCF method see [20, 92]. For recent developments of the MCSCF method see [40, 47, 81].

1.2.3 Multistructure Valence Bond Methods

All of the self-consistent field and configuration interaction methods employ wavefunctions constructed from a basis of molecular orbitals. The multistructure valence bond methods use an overcomplete nonorthogonal basis of atomic orbitals to construct a wavefunction expanded in terms of spin-coupled *structures* (linear combinations of products of valence-bond orbitals, characterized by a particular coupling of spins to form a function with total spin S) rather than configuration state functions.

The spin-coupled multistructure valence bond approach of Gerratt and Raimondi [32] defines a set of effective one-electron operators $\hat{\mathbf{f}}(i)$ using the gradient of the single-structure valence bond wavefunction with respect to the orbital basis. When this gradient is zero, the effective operators satisfy the pseudo-eigenvalue equations

$$\hat{\mathbf{f}}(i)\phi_j(i) = \varepsilon_{j,i}\phi_j(i), j = 0, 1, \ldots \tag{1.22}$$

where $\phi_0(i)$ represents a ground-state valence-bond orbital and the remaining orbitals represent virtual valence-bond orbitals. These virtual orbitals correspond to negative energies and are localized; excited structures are formed by replacing the ground-state valence-bond orbitals in a reference structure with virtual orbitals. Assuming a maximum of n_{max} doubly occupied basis functions possible in any given structure, the total number of structures in a conventional valence bond calculation is given by [41]

$$g(N, m, S) = \sum_{n=0}^{n_{max}} \binom{m}{n} \binom{m-n}{N-2n} f_S^{N-2n} \tag{1.23}$$

where

$$f_S^N = \frac{(2S+1)N!}{(\frac{1}{2}N + S + 1)!(\frac{1}{2}N - S)!} \tag{1.24}$$

is the number of spin-coupling schemes possible within a single structure. The total number of structures thus increases as $\mathcal{O}(m!)$. The virtual orbitals obtained by the spin-coupled multistructure valence bond method produce a very rapidly convergent expansion; for example, an 80 structure expansion for BeH gives results comparable to CI calculations including some 3000 configurations [32].

1.3 Overview of the Tensor Product Approach

Here we introduce a first-quantized procedure which:

1) does not require an orthogonal orbital basis;

2) avoids integral transformations by using a wavefunction expanded in spin-free primitives rather than Slater determinants or configuration state functions;

3) leads to algorithms which are well suited to parallel and vector machine architectures;

4) can be used to treat ground and excited electronic states, open or closed shells, and systems of arbitrary symmetry.

5) is equivalent to full configuration interaction.

Most second-quantized CI and MCSCF procedures require orthonormalized orbital bases to ensure that the creation and annihilation operators obey the fundamental anticommutation relations. Valence-bond nonorthonormal bases provide a chemically intuitive description of molecular electronic structure. In limited variational procedures it is often more convenient to select *a priori* the most significant valence-bond structures than to select leading configurations built from molecular orbitals. In full variational procedures nonorthormal bases can lead to computational difficulties, and orthogonalization becomes necessary for larger problems. The tensor product approach does not require an explicitly orthogonalized basis and thus allows flexibility (although presently no provisions for truncation of the N-particle expansion are made).

More importantly, the ability to use nonorthogonal orbitals in conjunction with a wavefunction expanded in orbital products allows integral transformations to be avoided. Most direct CI procedures require transformation of the molecular integrals from an atomic orbital basis to a molecular orbital basis. The integral transformation is computationally expensive, requiring $\mathcal{O}(m^5)$ floating point operations for an m

level system. Additionally, the integral transformations have been an obstacle in the development of parallel CI codes because most extant transformation algorithms require considerable interprocessor communication. (However, efficient parallel integral transformations are possible if a large amount of shared memory is available [93].)

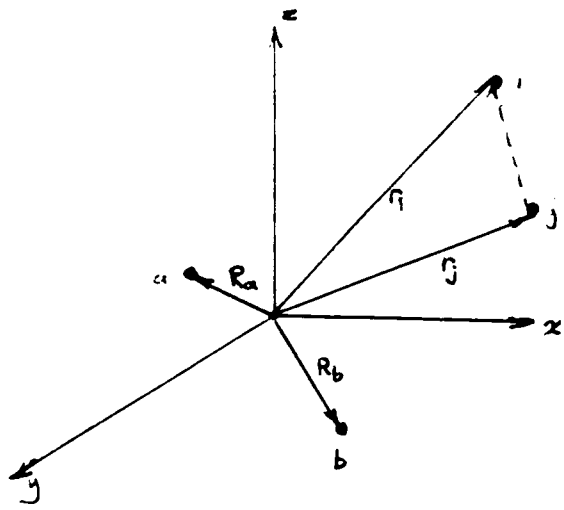

Figure 1.1. The molecular coordinate system. Here the nuclei are labelled by $a, b, \ldots$ and the electrons by $i, j, \ldots$

Chapter 2

The Tensor Product Construction

The one-to-one correspondence between physical observables and the set of self-adjoint operators in an abstract Hilbert space is a fundamental principle of quantum mechanics [91]. In section 1.1 the domain of the molecular Hamiltonian operator was restricted to a finite-dimensional model subspace $\mathcal{V}^{[N]} \subset \mathcal{H}$ by expanding the elements $\Phi \in \mathcal{H}$ with respect to a basis of N-electron functions. Several possible representations of $\hat{\mathbf{H}}$ are possible, depending on the choice of basis. We begin our development in the abstract Hilbert space itself, rather than in any particular representation space, since the properties we require are independent of the choice of the N-electron expansion set. We then show how an abstract separation of variables in the model N-electron space leads directly to a tensor product decomposition of the many-electron Hamiltonian.

The N-electron electronic Hamiltonian is defined on the N-particle subspace $\mathcal{H}^{(N)}$ of the full Fock space $\mathcal{F}$ [23]

$$\mathcal{F} = \bigoplus_{N=0}^{\infty} \mathcal{H}^{(N)} \tag{2.1}$$

where $\mathcal{H}^{(0)}$ is the one-dimensional Hilbert space of complex numbers. The elements of $\mathcal{F}$ are dynamical state functions Ψ of indeterminate particle number; equation 2.1 means that every Ψ can be uniquely written

$$\Psi = \sum_{N=0}^{\infty} \Phi^{(N)}, \tag{2.2}$$

where the functions $\Phi^{(N)} \in \mathcal{H}^{(N)}$ have fixed particle number N. If $P^{(N)}$ projects $\mathcal{F}$ into $\mathcal{H}^{(N)}$ then the expectation of $P^{(N)}$ for a system in a state described by Ψ can be physically interpreted as the probability that Ψ is an N-particle function.

$\mathcal{H}^{(N)}$ can be constructed from one-particle spaces as follows [9]. The orbital functions $\phi_i(1), i = 1, \ldots \infty$ are the elements of a one-particle Hilbert space $\mathcal{H}^{(1)}$. Define the space $\mathcal{H}^{(N)}$ as the linear span of all formal products

$$\Phi_{i_1,\ldots,i_N}(1,\ldots,N) \equiv \phi_{i_1}(1) \otimes \ldots \otimes \phi_{i_N}(N) \tag{2.3}$$

where the product operator $\otimes$ has the properties

$$\phi_i(1) \otimes (\phi_j(2) + \phi_k(2)) = \phi_i(1) \otimes \phi_j(2) + \phi_i(1) \otimes \phi_k(2) \tag{2.4}$$

$$(\phi_i(1) + \phi_j(1)) \otimes \phi_k(2) = \phi_i(1) \otimes \phi_k(2) + \phi_j(1) \otimes \phi_k(2) \tag{2.5}$$

$$(\alpha\phi_i(1)) \otimes (\beta\phi_j(2)) = \alpha\beta(\phi_i(1) \otimes \phi_j(2)). \tag{2.6}$$

where α and β are arbitrary scalars. The scalar product in $\mathcal{H}^{(N)}$ is defined as

$$\langle \Phi_{i_1,\ldots,i_N} \mid \Phi_{j_1,\ldots,j_N} \rangle = \prod_{k=1}^{N} \langle \phi_{i_k} \mid \phi_{j_k} \rangle \tag{2.7}$$

$\mathcal{H}^{(N)}$ can be written as an N-fold *tensor product space*

$$\mathcal{H}^{(N)} = \mathcal{H}^{(1)} \otimes \ldots \otimes \mathcal{H}^{(1)} \tag{2.8}$$

Consider any one-particle operator $\hat{\mathbf{f}}(1)$ which acts in $\mathcal{H}^{(1)}$. The one-particle operators can be used to construct an N- particle operator $\hat{\mathbf{f}}(1) \otimes \ldots \otimes \hat{\mathbf{f}}(N)$ which acts in $\mathcal{H}^{(N)}$, defined by [68, 9]

$$\hat{\mathbf{f}}(1) \otimes \ldots \otimes \hat{\mathbf{f}}(N)\Phi_{i_1,\ldots,i_N}(1,\ldots,N) = (\hat{\mathbf{f}}(1)\phi_{i_1}(1)) \otimes \ldots \otimes (\hat{\mathbf{f}}(N)\phi_{i_N}(N)) \tag{2.9}$$

If we use a basis of orbital functions $\phi_i, i = 1, \ldots, m$ that span a model space $\mathcal{V}$ of dimension m, the primitive N-particle functions [1]

$$|i\rangle = |i_1, \ldots, i_N\rangle = \phi_{i_1}(1)\phi_{i_2}(2)\cdots\phi_{i_N}(N), \quad 1 \le i_j \le m, \; 1 \le j \le N, \tag{2.10}$$

[1]Note that in the ket notation, the electronic variables are implicit in the position of the corresponding orbital indices.

span an N-fold tensor product space

$$\mathcal{V}^{[N]} = \mathcal{V}_1 \otimes \cdots \otimes \mathcal{V}_N \tag{2.11}$$

of dimension m^N. $\mathcal{V}^{[N]}$ is a subspace (of the domain of $\mathbf{H}$ dense in the Hilbert space $\mathcal{H}$) which holds all linear combinations of the elementary products of equation 2.3, where the orbital indices now range from 1 to m.

In $\mathcal{V}^{[N]}$ the i-th one electron operator can be written

$$\hat{\mathbf{I}}_1 \otimes \cdots \otimes \hat{\mathbf{I}}_{i-1} \otimes \hat{\mathbf{h}}(i) \otimes \hat{\mathbf{I}}_{i+1} \otimes \cdots \otimes \hat{\mathbf{I}}_N,$$

where $\hat{\mathbf{I}}_j$ is the identity operator in $\mathcal{V}_j$. The matrix representation of the bare nucleus Hamiltonian in $\mathcal{V}^{[N]}$ can be written

$$\mathbf{h} \otimes \mathbf{s} \otimes \cdots \otimes \mathbf{s} + \mathbf{s} \otimes \mathbf{h} \otimes \mathbf{s} \otimes \cdots \otimes \mathbf{s} + \cdots + \mathbf{s} \otimes \cdots \otimes \mathbf{s} \otimes \mathbf{h},$$

where $\mathbf{h}$ is the one-electron core Hamiltonian matrix $[\langle \phi_i \mid \hat{\mathbf{h}} \mid \phi_j \rangle]$ and $\mathbf{s}$ is the one-electron overlap matrix $[\langle \phi_i \mid \phi_j \rangle]$. Here $\otimes$ denotes a tensor or *Kronecker* product between matrices. Appendix A defines the Kronecker product and lists several relevant algebraic properties.

Similarly each two-electron operator $\hat{\mathbf{g}}(i,j)$ acts in $V_i \otimes V_j$ (rather than in $\mathcal{V}^{[N]}$); in $\mathcal{V}^{[N]}$ the two-electron operator acting on electrons 1 and 2 can be written

$$\hat{\mathbf{g}}(1,2) \otimes \hat{\mathbf{I}}_3 \otimes \cdots \otimes \hat{\mathbf{I}}_N,$$

where $\hat{\mathbf{g}}(1,2)$ acts only in the space $V_1 \otimes V_2$ (and is represented by the matrix g of two-electron integrals

$$g_{ij,kl} = \langle ij \mid kl \rangle = \int\int \phi_i^*(1)\phi_j^*(2)|r_1 - r_2|^{-1}\phi_k(1)\phi_l(2)d\tau_1 d\tau_2 \tag{2.12}$$

with ϕ_i, ϕ_k in $\mathcal{V}_1$ and ϕ_j, ϕ_l in $\mathcal{V}_2$). To describe the general operators $\hat{\mathbf{g}}(k,l)$ the isomorphism P_{kl} can be employed [28]:

$$\begin{aligned} P_{kl}\,\phi_{i_1}(1)\phi_{i_2}(2)\cdots\phi_{i_N}(N) &= \phi_{i_k}(1)\phi_{i_l}(2)\phi_{i_1}(3)\phi_{i_2}(4)\cdots \\ &\cdots\phi_{i_{k-1}}(k+1)\phi_{i_{k+1}}(k+2)\cdots\phi_{i_{l-1}}(l)\phi_{i_{l+1}}(l+1)\cdots\phi_{i_N}(N) \end{aligned} \tag{2.13}$$

Then in $\mathcal{V}^{[N]}$, $\hat{\mathbf{g}}(k,l)$ can be written

$$P_{kl}^{-1}[\hat{\mathbf{g}}(1,2)\otimes\hat{\mathbf{I}}_3\otimes\cdots\otimes\hat{\mathbf{I}}_N]\,P_{kl},$$

and its matrix representation is

$$P_{kl}^{-1}[\mathbf{g}\otimes\mathbf{s}\otimes\cdots\otimes\mathbf{s}]P_{kl}.$$

The complete tensor product decomposition[6] for $\mathbf{H}$ is

$$\mathbf{H}=\sum_{i=1}^{N}\mathbf{s}^{[i-1]}\otimes\mathbf{h}\otimes\mathbf{s}^{[N-i]}+\sum_{i<j}^{N}P_{ij}^{-1}(\mathbf{g}\otimes\mathbf{s}^{[N-2]})P_{ij}, \tag{2.14}$$

and the N-particle overlap matrix is

$$\mathbf{S}=\mathbf{s}^{[N]}=\bigotimes_{i=1}^{N}\mathbf{s}. \tag{2.15}$$

Like the unitary group model Hamiltonian, this model form H is cast in terms of the molecular integrals and can be used to develop direct variational procedures. Using the tensor product forms of $\mathbf{H}$ and $\mathbf{S}$, the general matrix eigenvalue problems for one-, two-, and three-electron systems can be written [7]

$$\mathbf{h}c=\epsilon\mathbf{s}c, \qquad (N=1)$$

$$(\mathbf{h}\otimes\mathbf{s}+\mathbf{s}\otimes\mathbf{h}+\mathbf{g})c=\epsilon(\mathbf{s}\otimes\mathbf{s})c, \qquad (N=2)$$

$$(\mathbf{h}\otimes\mathbf{s}\otimes\mathbf{s}+\mathbf{s}\otimes\mathbf{h}\otimes\mathbf{s}+\mathbf{s}\otimes\mathbf{s}\otimes\mathbf{h}$$
$$+\mathbf{g}\otimes\mathbf{s}+\mathbf{s}\otimes\mathbf{g}+P_{13}^{-1}(\mathbf{g}\otimes\mathbf{s})P_{13})c=\epsilon(\mathbf{s}\otimes\mathbf{s}\otimes\mathbf{s})c, \quad (N=3)$$

where we have used the fact that $P_{k,k+1}^{-1}[\mathbf{g}\otimes\mathbf{s}\otimes\cdots\otimes\mathbf{s}]P_{k,k+1}=\mathbf{s}^{[k-1]}\otimes\mathbf{g}\otimes\mathbf{s}^{[N-k-1]}$. The dependence on particle number can be made explicit as follows. Let ${}^{N}\mathbf{H}$ denote the N-electron Hamiltonian matrix. Then the one-electron part of ${}^{N+1}\mathbf{H}$ can be written

$$\begin{aligned}{}^{N+1}\mathbf{H}_{bare} &= \sum_{i=1}^{N+1}\mathbf{s}^{[i-1]}\otimes\mathbf{h}\otimes\mathbf{s}^{[N-i+1]}\\ &= \left(\sum_{i=1}^{N}\mathbf{s}^{[i-1]}\otimes\mathbf{h}\otimes\mathbf{s}^{[N-i]}\right)\otimes\mathbf{s}+\mathbf{s}\otimes(\mathbf{s}^{[N-1]}\otimes\mathbf{h})\end{aligned}$$

Since ${}^{N}\mathbf{H}_{bare}=\mathbf{s}^{[N-1]}\otimes\mathbf{h}+{}^{N-1}\mathbf{H}_{bare}\otimes\mathbf{s}$,

$${}^{N+1}\mathbf{H}_{bare}={}^{N}\mathbf{H}_{bare}\otimes\mathbf{s}+\mathbf{s}\otimes{}^{N}\mathbf{H}_{bare}-\mathbf{s}\otimes{}^{N-1}\mathbf{H}_{bare}\otimes\mathbf{s} \tag{2.16}$$

Similarly for the two electron part,

$$
\begin{aligned}
{}^{N+1}\mathbf{H} - {}^{N+1}\mathbf{H}_{bare} &= \left(\sum_{i<j}^{N} P_{ij}^{-1}(\mathbf{g} \otimes \mathbf{s}^{[N-2]})P_{ij}\right) \otimes \mathbf{s} + \sum_{i}^{N} P_{i,N+1}^{-1}(\mathbf{g} \otimes \mathbf{s}^{[N-1]})P_{i,N+1} \\
&= ({}^{N}\mathbf{H} - {}^{N}\mathbf{H}_{bare}) \otimes \mathbf{s} + \mathbf{s} \otimes ({}^{N}\mathbf{H} - {}^{N}\mathbf{H}_{bare}) \\
&\quad - \mathbf{s} \otimes ({}^{N-1}\mathbf{H} - {}^{N-1}\mathbf{H}_{bare}) \otimes \mathbf{s} + P_{1,N+1}^{-1}(\mathbf{g} \otimes \mathbf{s}^{[N-1]})P_{1,N+1}
\end{aligned}
$$

so the N-particle Hamiltonian can be written in terms of the $N-1$- and $N-2$-particle Hamiltonians as

$$
{}^{N}\mathbf{H} = {}^{N-1}\mathbf{H} \otimes \mathbf{s} + \mathbf{s} \otimes {}^{N-1}\mathbf{H} - \mathbf{s} \otimes {}^{N-2}\mathbf{H} \otimes \mathbf{s} + P_{1,N}^{-1}(\mathbf{g} \otimes \mathbf{s}^{[N-2]})P_{1,N} \qquad (2.17)
$$

Chapter 3

Structure and Storage of the Eigenvector

Up to this point the spin and spatial symmetries of the eigenvector have been neglected; the Hamiltonian construction presented in the last chapter is spin-free and can be applied to systems of arbitrary spatial symmetry. In practice it becomes imperative to exploit these symmetries in order to obtain a reduction of the many-particle eigenvector comparable to the reduction that can be achieved for the Hamiltonian. The full space spanned by the N-th rank tensors generated from the basis of m orbital functions has dimension m^N; storage of all ket expansion coefficients leads to storage requirements which are exponential in the number of electrons. Obviously full storage of the trial eigenvectors is impractical for systems with extended basis sets for more than a few electrons. We now turn to the closely related problems of finding an economical reduction of the trial eigenvectors and of restricting them to antisymmetric subspaces of $\mathcal{V}^{[N]}$. The necessary machinery for the decomposition of $\mathcal{V}^{[N]}$ is provided by the theory of the symmetric group and the spin-free formulation of quantum chemistry in section 3.1. There are three techniques which can be used to obtain spin-adapted eigenvectors [56, 67]:

1) the *Wigner operator* method, which requires construction of a matrix representation of the permutation group in the antisymmetric subspaces of $\mathcal{V}^{[N]}$;

2) the use of *orthogonal units* which can be constructed from the characters (traces) of the representation matrices;

3) the use of structure projectors, which are obtained without the use of either the representation matrices or their characters.

The last approach proves most convenient in this work. The physical motivation for the structure projectors and their construction from the Young tableau is discussed in section 3.2, using simple three- and four-electron systems to clarify the notation. In section 3.3, it is shown that spin-adaption using the structure projectors imposes constraints on the variational coefficients. The resulting structure of the spin-adapted eigenvector can be visualized using rectangular arrays of Weyl tableau.

3.1 Basic Concepts and Notation

In section 1.1 we noted that the spin-free electronic Hamiltonian is symmetric under any permutation of the electronic coordinates, satisfying the requirement that electrons be physically indistinguishable. For any permutation operator π which acts on the electronic labels, $\hat{H}_{elec} = \pi^{-1}\hat{H}_{elec}\pi$ and

$$[\hat{H}_{elec}, \pi] = 0, \quad \pi \in \mathcal{S}_N \tag{3.1}$$

where $\mathcal{S}_N$ denotes the group of $N!$ permutation operators, and $[\hat{A}, \hat{B}] \equiv \hat{A}\hat{B} - \hat{B}\hat{A}$. The spin-free primitive kets transform among themselves under permutations of the electronic variables and so form a basis for a reducible representation of the symmetric group. The N-electron space $\mathcal{V}^{[N]}$ spanned by the primitive kets can be decomposed into a direct sum of irreducible representation spaces $\mathcal{V}(\lambda)$ of $\mathcal{S}_N$:

$$\mathcal{V}^{[N]} = \mathcal{V}(\lambda_1) \oplus \mathcal{V}(\lambda_2) \oplus \cdots \oplus \mathcal{V}(\lambda_f), \tag{3.2}$$

where the λ_i label the irreducible representations. Because conjugate permutations have the same cyclic structure, the classes of the symmetric group is labelled by partitions of N:

$$\lambda_k = \left[\lambda_k^1, \lambda_k^2, \ldots, \lambda_k^N\right], \quad \lambda_k^1 \geq \lambda_k^2 \geq \cdots \geq \lambda_k^N \geq 0, \quad \sum_{i=1}^{N} \lambda_k^i = N,$$

with the λ_k^i equal to the lengths of the cycles which characterize the k-th permutation class. For example, the permutation classes of S_3 are

Class	*Partition*	*Permutations*
1	[1,1,1]	$(1)(2)(3) = I$ (identity)
2	[2,1]	$(12)(3)$, $(13)(2)$, $(1)(23)$
3	[3]	(123) (132)

The eigenfunctions of the spin-free Hamiltonian can be classified according to their permutation class and thus by corresponding partitions of N. The eigenfunction is said to belong to a particular permutation class $[\lambda]$ if it is a projection of a linear combination of permutation operators constructed from permutations in $[\lambda]$.

The projection operators can be constructed using Young's theory [22, 67, 57]. Each irreducible representation can be labelled with a Young frame, consisting of boxes arranged in rows with lengths corresponding to the characteristic cycle lengths λ^i. For example, the irreducible representations of S_3 can be associated with the partitions and frames

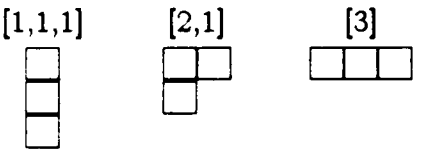

According to the Pauli principle, systems of fermions are described by state functions which belong to the antisymmetric (alternating) representations of the symmetric group S_N. Consequently all naturally occurring permutation states must have cyclic structures characterized by partitions $[\lambda]$ of the integers $1, \ldots, N$ which satisfy

$$[\lambda] = [\overbrace{\{i_1, i_2\}, \ldots, \{i_{2p-1}, i_{2p}\}}^{p \text{ groups of } 2}, \overbrace{\{i_{2p+1}\}, \ldots, \{i_N\}}^{N-2p \text{ groups of } 1}],$$

where $p = N/2 - S$ is the permutation quantum number and S is the spin quantum number. Equivalently, the physically relevant irreducible representation subspaces of $\mathcal{V}^{[N]}$ are labelled by Young frames with one or two columns.

A Young tableau can be constructed by placing each of the first N integers in a box of a Young frame. The tableau is called *standard* if the integers increase from left to right and from top to bottom; the number of standard tableaux associated

with a frame gives the dimension of the corresponding irreducible representation (Figure 3.1) These tableaux are concise sources of information about the irreducible representations. For example, they can be used to build the matrix representations of S_N and to form *structure projectors* which project primitive N-particle functions into the physically relevant subspaces. $\mathcal{V}^{[N]}$ must also be invariant to the symmetry operations of the molecular point group. Symmetries generated by the molecular geometry can lead to a further reduction of the eigenvector, and they may be exploited to simplify the formation of products involving the matrix of two-electron integrals (see section 4.3).

3.2 The Structure Projectors

The structure projector associated with a standard Young tableau T_χ^λ can be written

$$\hat{\mathbf{X}}_\chi^\lambda = \varrho(\hat{\pi}_{\chi 1})\hat{\mathbf{K}}_1^\lambda \hat{\pi}_{\chi 1} \tag{3.3}$$

where $\varrho(\hat{\pi})$ is the signature of the permutation operator $\hat{\pi}$ and $\hat{\pi}_{\chi 1}$ permutes the indices of T_χ^λ to obtain the standard tableau T_1^λ of Figure 3.1.

The unnormalized Young operators $\hat{\mathbf{K}}_1^\lambda$ are written as

$$\hat{\mathbf{K}}_1^\lambda = \hat{\mathbf{A}}_1^\lambda \hat{\mathbf{P}}_1^\lambda, \tag{3.4}$$

where $\hat{\mathbf{A}}_1^\lambda$ denotes an antisymmetric sum of products of permutations over indices in the columns of the tableau T_1^λ,

$$\hat{\mathbf{A}}_1^\lambda = \sum_{\hat{\pi}_1^\alpha, \hat{\pi}_1^\beta} \varrho(\hat{\pi}_1^\alpha \hat{\pi}_1^\beta)\hat{\pi}_1^\alpha \hat{\pi}_1^\beta, \tag{3.5}$$

and $\hat{\mathbf{P}}_1^\lambda$ denotes a product of symmetric sums of permutations over indices in tableau rows,

$$\hat{\mathbf{P}}_1^\lambda = \prod_{\hat{\pi}_1^r} (I + \hat{\pi}_1^r). \tag{3.6}$$

The column operators $\hat{\pi}_1^\alpha$ and $\hat{\pi}_1^\beta$ permute indices in the first (α) and second (β) columns of T_1^λ, respectively. The row operators $\hat{\pi}_1^r$ permute indices in the r-th row of T_1^λ, and $\hat{\mathbf{I}}$ is the identity operator.

3.3 Symmetry-Imposed Constraints on the Variational Coefficients

The eigenfunctions of the spin-free Hamiltonian are approximated as

$$\Phi = \sum_{j_1,\ldots,j_N=1}^{m} C_{j_1,\ldots,j_N} |j_1,\cdots,j_N\rangle. \tag{3.7}$$

Because all Φ which belong to an irreducible representation space labelled by λ satisfy $\Phi = \hat{\mathbf{X}}^{\lambda}\Phi$, symmetry adaptation places constraints on the variational coefficients $C_{j_1,\ldots,j_N}$. For example, consider the action of $\hat{\mathbf{X}}_1^{\lambda}$ and on primitives with invariance $\{2,1\}$ of the vector $\mathbf{c} = c_{111}|111\rangle \ldots c_{iij}|iij\rangle + c_{iji}|iji\rangle + c_{jii}|jii\rangle + \ldots + c_{mmm}|mmm\rangle$ for a 3-particle case:

$$\begin{aligned}
\hat{\mathbf{X}}_1^{\lambda}\mathbf{c} &= \ldots + c_{iij}(|iij\rangle - |jii\rangle) + c_{iji}(|iji\rangle - |jii\rangle) + c_{jii}(2|jii\rangle - 2|iij\rangle) + \ldots \\
&= \ldots \underbrace{(c_{iji} + c_{iij} - 2c_{jii})}_{c^1_{iij}}|iij\rangle + \underbrace{0}_{c^1_{iji}}|iji\rangle + \underbrace{(2c_{jii} - c_{iji} - c_{iij})}_{c^1_{jii}}|jii\rangle + \ldots
\end{aligned}$$

Note that in the structure projection $c^1_{iij} = -c^1_{jii}$ and $c^1_{iji} = 0$. The relationships among the coefficients can be visualized by inserting the orbital indices into the Young frame to generate *Weyl tableaux*[67]. Each Weyl tableau can be associated with a particular ket and its variational coefficient; for example,

$$C_{ijk} \Longleftrightarrow \begin{array}{|c|c|}\hline \mathrm{i} & \mathrm{j} \\ \hline \multicolumn{2}{|c|}{\mathrm{k}} \\ \cline{1-2}\end{array}\,.$$

All coefficients whose orbital indices are related by permutations over same-column indices have equal absolute values with relative signs equal to the parity of the permutations. That is, if $(j_1,\ldots,j_N) = \hat{\pi}_1^{\alpha}\hat{\pi}_1^{\beta}(k_1,\ldots,k_N)$, then

$$C_{j_1,\ldots,j_N} = \varrho(\hat{\pi}_1^{\alpha}\hat{\pi}_1^{\beta})C_{k_1,\ldots,k_N}.$$

When both columns of the Weyl tableau are of equal length, coefficients whose orbital indices are related by permutations exchanging Weyl tableau columns must be equal. For singlet systems, if $(j_1,\ldots,j_N) = \left(\prod_{\hat{\pi}_1^r}\hat{\pi}_1^r\right)(k_1,\ldots,k_N)$, then

$$C_{j_1,\ldots,j_N} = C_{k_1,\ldots,k_N}.$$

The set of all coefficients which are not mapped onto each other by permutations over same-column indices (or by column exchanges for systems with zero spin quantum number) are *unique* ket coefficients. The orbital indices corresponding to unique ket coefficients can be obtained very simply as follows: For each column of the Young frame, place all possible combinations of orbital indices in the boxes so that the indices increase going down the column and no orbital index appears in the same column twice (generating the columns of the Weyl tableau). Join the columns in all possible ways to obtain a rectangular array of Weyl tableaux. Each of these tableaux corresponds to a unique ket coefficient. The Weyl tableau generated for a doublet 3-electron system and a closed shell 4-electron system are given in Figure 2. Note that for closed shell systems, pairs of kets corresponding to pairs of Weyl tableau with identical (but interchanged) columns have identical coefficients. The canonically indexed vector of unique ket coefficients (the "packed" eigenvector) for the 3 electron system is given in Figure 3.3.

The number of unique kets $q(m, N, S)$ is

$$q(m, N, S) = \begin{cases} \frac{1}{2}\binom{m}{N_\alpha}\left[\binom{m}{N_\beta}+1\right], & \text{for } S=0, \\ \binom{m}{N_\alpha}\binom{m}{N_\beta}, & \text{otherwise.} \end{cases}$$

Typical values of $q(m, N, S)$ and $D(m, N, S)$ for small systems are given in Table 3.2. Note that $q(m, N, S)$ is larger than Weyl's number because of linear dependencies among some of the unique ket coefficients in the spin-adapted eigenvector. When m is much greater than N, the ratio q/D approaches $\frac{1}{2}(\frac{1}{2}N+1)$ for singlet systems and $(\frac{1}{2}N+S+1)/(2S+1)$ when the spin quantum number is nonzero. A similar situation exists in the two-box Weyl tableau expansions used in Clifford algebra unitary group approaches [65]; in both cases the substantial simplification in the structure of the model Hamiltonian compensates for the increase in dimension.

Table 3.1: The full, C, and packed, $\tilde{C}$ spin-adapted eigenvectors for $N = 3$, $m = 3$, $S = 1/2$.

Index i	Ket	C_i	$\tilde{C}_i$
1	$\|111\rangle$	0	c_{112}
2	$\|112\rangle$	c_{112}	c_{113}
3	$\|113\rangle$	c_{113}	c_{213}
4	$\|121\rangle$	0	c_{122}
5	$\|122\rangle$	c_{122}	c_{123}
6	$\|123\rangle$	c_{123}	c_{223}
7	$\|131\rangle$	0	c_{132}
8	$\|132\rangle$	c_{132}	c_{133}
9	$\|133\rangle$	c_{133}	c_{233}
10	$\|211\rangle$	$-c_{112}$	
11	$\|212\rangle$	0	
12	$\|213\rangle$	c_{213}	
13	$\|221\rangle$	$-c_{122}$	
14	$\|222\rangle$	0	
15	$\|223\rangle$	c_{223}	
16	$\|231\rangle$	$-c_{132}$	
17	$\|232\rangle$	0	
18	$\|233\rangle$	c_{233}	
19	$\|311\rangle$	$-c_{113}$	
20	$\|312\rangle$	$-c_{213}$	
21	$\|313\rangle$	0	
22	$\|321\rangle$	$-c_{123}$	
23	$\|322\rangle$	$-c_{223}$	
24	$\|323\rangle$	0	
25	$\|331\rangle$	$-c_{133}$	
26	$\|332\rangle$	$-c_{233}$	
27	$\|333\rangle$	0	

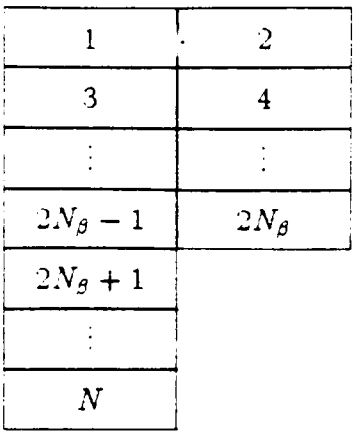

Figure 3.1: The standard Young tableau T_1^λ. N_α and N_β are the numbers of boxes in the first (α) and second (β) columns, respectively.

Table 3.2: Full space and subspace dimensions for typical systems with N electrons, m basis functions, and $S = 0$.

m	N	Full Space Dimension m^N	Number of Determinants	Number of Unique Kets $q(m, N, S)$	Weyl's Number $D(n, N, S)$
10	4	10000	4845	1035	825
20	4	160000	91390	18145	13300
30	4	810000	487635	94830	67425
40	4	2560000	1581580	304590	213200
50	4	6250000	3921225	750925	520625
20	8	2.56×10^{10}	76904685	11739435	5799465
30	8	6.56×10^{11}	2.56×10^{9}	3.76×10^{8}	1.72×10^{8}
40	8	6.55×10^{12}	2.89×10^{10}	4.18×10^{9}	1.85×10^{9}
10	10	1.00×10^{10}	184756	31878	19404
50	10	9.77×10^{16}	1.73×10^{13}	2.24×10^{12}	8.3×10^{11}
75	10	5.63×10^{18}	1.17×10^{15}	1.48×10^{14}	5.3×10^{13}

$\alpha \backslash \beta$	1	2	3
12	$\begin{array}{|c|c|}\hline 1&1\\\hline 2\\\cline{1-1}\end{array}$	$\begin{array}{|c|c|}\hline 1&2\\\hline 2\\\cline{1-1}\end{array}$	$\begin{array}{|c|c|}\hline 1&3\\\hline 2\\\cline{1-1}\end{array}$
13	$\begin{array}{|c|c|}\hline 1&1\\\hline 3\\\cline{1-1}\end{array}$	$\begin{array}{|c|c|}\hline 1&2\\\hline 3\\\cline{1-1}\end{array}$	$\begin{array}{|c|c|}\hline 1&3\\\hline 3\\\cline{1-1}\end{array}$
23	$\begin{array}{|c|c|}\hline 2&1\\\hline 3\\\cline{1-1}\end{array}$	$\begin{array}{|c|c|}\hline 2&2\\\hline 3\\\cline{1-1}\end{array}$	$\begin{array}{|c|c|}\hline 2&3\\\hline 3\\\cline{1-1}\end{array}$

Weyl tableau construction of the eigenvector: $N = 4$, $m = 4$, $S = 0$.

$\alpha \backslash \beta$	12	13	14	23	24	34
12	$\begin{array}{|c|c|}\hline 1&1\\\hline 2&2\\\hline\end{array}$	$\begin{array}{|c|c|}\hline 1&1\\\hline 2&3\\\hline\end{array}$	$\begin{array}{|c|c|}\hline 1&1\\\hline 2&4\\\hline\end{array}$	$\begin{array}{|c|c|}\hline 1&2\\\hline 2&3\\\hline\end{array}$	$\begin{array}{|c|c|}\hline 1&2\\\hline 2&4\\\hline\end{array}$	$\begin{array}{|c|c|}\hline 1&3\\\hline 2&4\\\hline\end{array}$
13		$\begin{array}{|c|c|}\hline 1&1\\\hline 3&3\\\hline\end{array}$	$\begin{array}{|c|c|}\hline 1&1\\\hline 3&4\\\hline\end{array}$	$\begin{array}{|c|c|}\hline 1&2\\\hline 3&3\\\hline\end{array}$	$\begin{array}{|c|c|}\hline 1&2\\\hline 3&4\\\hline\end{array}$	$\begin{array}{|c|c|}\hline 1&3\\\hline 3&4\\\hline\end{array}$
14			$\begin{array}{|c|c|}\hline 1&1\\\hline 4&4\\\hline\end{array}$	$\begin{array}{|c|c|}\hline 1&2\\\hline 4&3\\\hline\end{array}$	$\begin{array}{|c|c|}\hline 1&2\\\hline 4&4\\\hline\end{array}$	$\begin{array}{|c|c|}\hline 1&3\\\hline 4&4\\\hline\end{array}$
23				$\begin{array}{|c|c|}\hline 2&2\\\hline 3&3\\\hline\end{array}$	$\begin{array}{|c|c|}\hline 2&2\\\hline 3&4\\\hline\end{array}$	$\begin{array}{|c|c|}\hline 2&3\\\hline 3&4\\\hline\end{array}$
24					$\begin{array}{|c|c|}\hline 2&2\\\hline 4&4\\\hline\end{array}$	$\begin{array}{|c|c|}\hline 2&3\\\hline 4&4\\\hline\end{array}$
34						$\begin{array}{|c|c|}\hline 3&3\\\hline 4&4\\\hline\end{array}$

Figure 3.2: Weyl tableau construction of the eigenvector: $N = 3$, $m = 3$, $S = 1/2$.

Chapter 4

Computational Techniques

In this chapter we describe how the tensor product decomposition of the Hamiltonian and the structure of the spin-adapted eigenvectors can be exploited in the numerical solution of equation 1.12. First, we simplify the calculation by reducing the general matrix eigenvalue problem to standard form, using one of the congruence transformations described in section 4.1. Given the magnitude of $q(m, N, S)$ for even modest values of m and N and the structure of the Hamiltonian matrix, matrix eigenvalue methods based on matrix transformations (for example the Jacobi and QR methods) are impractical for tensor product variational calculations for systems with nonminimal basis sets or with more than three or four electrons. However, several of the subspace and vector iterative methods can be profitably applied; these are described in section 4.2. All methods involve certain basic linear algebraic kernals, such as the formation of dot products and Hamiltonian matrix-matrix multiplications. In section 4.3 we show how algorithms for these kernals can exploit the structure of the Hamiltonian matrix and the spin-adapted vectors in scalar, vector, and parallel environments. Several of the iterative large matrix eigenvalue algorithms require starting estimates of the eigenvalues and eigenvectors of interest; section 4.4 discusses how these estimates can be obtained.

4.1 The Standard Matrix Eigenvalue Problem

Although the general eigenvalue problem can be solved directly, the solution can often be obtained more economically by first converting the problem to standard form. For example, the Rayleigh quotient iteration described in section 4.2 can be formulated for either the general ($\mathbf{H}C = \varepsilon \mathbf{S}C$) or the standard ($\mathbf{H}'C' = \varepsilon C'$) matrix eigenvalue problems. The general solution requires the formation of large matrix-vector products involving $\mathbf{S}$ and $\mathbf{H}$ at each iteration while the standard solution requires only products involving $\mathbf{H}'$.

The reduction of the general matrix eigenvalue problem to standard form can always be accomplished in principle (although ill-conditioning of the overlap matrix can make the reduction difficult in practice). Note that all eigenvalues of s are positive, since if $\mathbf{u}^i$ is the i-th eigenvector of $\mathbf{s}$ the corresponding eigenvalue d_i can be written

$$\begin{aligned} d_i &= \sum_{j,k=1}^{m} u_j^{i*} s_{jk} u_k^i \\ &= \sum_{j,k=1}^{m} u_j^{i*} u_k^i \int \phi_j^*(r)\phi_k(r)dr \\ &= \int \left\| \sum_{j=1}^{m} u_j^i \phi_j(r) \right\|^2 dr \end{aligned}$$

which is always greater than zero. This property guarantees that the Hamiltonian and N-particle overlap matrices can be simultaneously diagonalized, since if the spectral decomposition of the one electron overlap matrix is written $\mathbf{s} = \mathbf{udu}^\dagger$ then

$$\begin{aligned} \mathbf{S} &= (\mathbf{udu}^\dagger)^{[N]} \\ &= (\mathbf{u} \otimes \ldots \otimes \mathbf{u})(\mathbf{d} \otimes \ldots \otimes \mathbf{d})(\mathbf{u} \otimes \ldots \otimes \mathbf{u})^\dagger \\ &= \mathbf{UDU}^\dagger \end{aligned}$$

where $\mathbf{D}$ must be real. Because $\mathbf{D}^{-1/2}\mathbf{U}^\dagger\mathbf{SUD}^{-1/2} = \mathbf{I}$, if the spectral decomposition of the Hamiltonian matrix is $\mathbf{H} = \mathbf{VEV}^\dagger$, the matrix $\mathbf{W} = \mathbf{UD}^{-1/2}\mathbf{V}$ will diagonalize both $\mathbf{H}$ and $\mathbf{S}$. There are many possible choices for $\mathbf{W}$ since $\mathbf{W}$ right-multiplied by any nonsingular diagonal matrix will also diagonalize $\mathbf{H}$ and $\mathbf{S}$[66].

The reduction to standard form can be accomplished by a congruence transformation $\mathbf{H}' = \mathbf{Z}^{\dagger}\mathbf{H}\mathbf{Z}$, $\mathbf{Z} = \otimes_{i=1}^{N} \mathbf{z}$, where $\mathbf{z}$ is an invertible matrix which satisfies

$$\mathbf{I} = \mathbf{z}^{\dagger}\mathbf{s}\mathbf{z}. \tag{4.1}$$

The eigenvalues of $\mathbf{H}'$ and $\mathbf{H}$ are identical and the corresponding eigenvectors are related by a factor of $\mathbf{Z}^{-1}$. There are several choices for z which can accomplish the reduction to standard form:

1) $\mathbf{z} = \ell^{-\dagger}$, where $\mathbf{s} = \ell\ell^{\dagger}$ (Cholesky decomposition);

2) $\mathbf{z} = \mathbf{s}^{-1/2} = \mathbf{u}^{\dagger}\mathbf{d}^{-1/2}\mathbf{u}$ (symmetric orthogonalization);

3) $\mathbf{z} = \mathbf{u}\mathbf{d}^{-1/2}$ (canonical orthogonalization).

The Cholesky factor ℓ preserves the profile of the overlap matrix[66]. Figure4.1 shows the structure of the overlap matrix and its Cholesky factor for a hydrogen molecular dimer calculation at the [3s2p] level. The structure of the Cholesky factor can be exploited in the formation of matrix-vector products $\ell^{\dagger}x$ and $(\ell \otimes \ell)x$, particularly in calculations which involve systems of weakly interacting monomers and large basis sets of nonorthogonal orbitals. The Cholesky decomposition is easier to compute than the canonical or symmetric orthogonalizations, requiring $\mathcal{O}(m^3/6)$ versus $\mathcal{O}(15m^3)$ floating point operations (using the QR algorithm [33] to accomplish the symmetric orthogonalization). The symmetric orthogonalization preserves the structure of the spin-adapted vectors, an advantage which is not shared by the Cholesky decomposition or canonical orthogonalization. For any spin-adapted vector x, $\mathbf{S}^{-1/2}x$ is also spin-adapted since the overlap matrix (and all of its powers) commutes with the structure projectors.

The canonical orthogonalization proves convenient when the basis set is nearly degenerate (resulting in small ($< 10^{-4}$) eigenvalues d_{ii}). If $\mathbf{u}$ is chosen so that the eigenvalues of $\mathbf{s}$ decrease down the diagonal of $\mathbf{d}$, then all d_{ii} below a chosen threshold can be discarded by simply truncating the transformation matrix.

The general eigenvalue problem $\mathbf{H}\,c = E\,\mathbf{S}\,c$ becomes

$$\mathbf{H}'b = \mathbf{Z}^{\dagger}\mathbf{H}\mathbf{Z}b = \epsilon b, \quad b = \mathbf{Z}^{-1}c, \tag{4.2}$$

where the structure of $\mathbf{H}'$ is

$$\mathbf{H}' = \sum_{i=1}^{N} \mathbf{I}^{[i-1]} \otimes (\mathbf{z}^t h \mathbf{z}) \otimes \mathbf{I}^{[N-i]} + \sum_{i<j}^{N} P_{ij}^{-1} \left[(\mathbf{z}^t \otimes \mathbf{z}^t) g (\mathbf{z} \otimes \mathbf{z}) \otimes I^{[N-2]} \right] P_{ij}. \quad (4.3)$$

4.2 Large Symmetric Matrix Eigenvalue Algorithms

The size and structure of $\mathbf{H}'$ dictates an iterative solution. In this section we briefly describe several large symmetric matrix eigenvalue algorithms which do not alter the Hamiltonian matrix (preserving the tensor-product form) and which can supply ground state (and in some cases, low-lying excited state) eigenvalue and eigenvector estimates.

4.2.1 Vector Iterations

We first describe the *power method*, a classical method for locating the dominant eigenvalue and corresponding eigenvector of a matrix. Consider the n-term *Krylov sequence*

$$\{\tilde{b}^{(0)}, \mathbf{H}'\tilde{b}^{(0)}, \mathbf{H}'\mathbf{H}'\tilde{b}^{(0)}, \ldots, \mathbf{H}'^{n}\tilde{b}^{(0)}\}. \quad (4.4)$$

for a spin-adapted trial eigenvector $\tilde{b}^{(0)}$ of $\mathbf{H}'$. The power method gives a limit to this sequence which is an unnormalized eigenfunction corresponding to the largest eigenvalue of $\mathbf{H}'$. To demonstrate this consider a system with the physical eigenvalues of $\mathbf{H}'$ ordered as

$$|\epsilon_1| > |\epsilon_2| \geq |\epsilon_3| \geq \ldots \geq |\epsilon_p| \geq 0; \quad (4.5)$$

(the method can also be extended to some systems with degenerate ground states). Define

$$\tilde{b}^{(n)} = \frac{\mathbf{H}'\tilde{b}^{(n-1)}}{\|\mathbf{H}'\tilde{b}^{(n-1)}\|_\infty} \quad (4.6)$$

where the infinity-norm of a vector x of length n is defined as $\|x\|_\infty = \max_{1 \leq i \leq n} |x_i|$. Let the orthonormalized eigenvectors $b_1, b_2, \ldots b_p$ of $\mathbf{H}'$ form a basis for a physically relevant subspace of $\mathcal{H}$. The initial trial vector $\tilde{b}^{(0)}$ can be expanded in this basis:

$$\tilde{b}^{(0)} = \sum_{i=1}^{p} \alpha_i b_i. \quad (4.7)$$

If $\tilde{b}^{(0)}$ is an adequate approximation of the ground state eigenvector b_1, α_1 is nonzero. The product $\mathbf{H}'\tilde{b}^{(0)}$ has components $\{\varepsilon_1\alpha_1 b_1, \ldots, \varepsilon_p\alpha_p b_p\}$ and by the ordering of eigenvalues in equation 4.5,

$$\|\varepsilon_1\alpha_1 b_1\|_\infty / \|\varepsilon_i\alpha_i b_i\|_\infty > \|\alpha_1 b_1\|_\infty / \|\alpha_i b_i\|_\infty \tag{4.8}$$

for all $i \neq 1$. The component of the trial vector which points towards the dominant eigenvector has been enriched.

The power method is simple but not often used in practice. The iteration converges linearly at a rate governed by the ratio $|\varepsilon_2/\varepsilon_1|$. A poorly chosen initial eigenvector estimate (for which α_1 is close to zero) will converge very slowly (or not at all if $\alpha_1 = 0$). Eigenvalue (and eigenvectors) other than the dominant one can be obtained by a "deflation" of $\mathbf{H}'$ which removes ε_1 as an eigenvalue [94], or by *inverse iteration*.

Inverse iteration applies the power method to the inverse of $\mathbf{H}'$ with origin shifted by $-\tilde{\varepsilon}\mathbf{I}$, where $\tilde{\varepsilon}$ approximates some target eigenvalue ε_j of $\mathbf{H}'$ [33]. Given a spin-adapted trial vector $\tilde{b}^{(0)}$ which adequately approximates the corresponding eigenvector b_j, consider the sequence of trial vectors $\tilde{b}^{(n)}$ obtained by solving

$$(H - \tilde{\varepsilon}\mathbf{I})c = \tilde{b}^{(n-1)}, \tag{4.9}$$

and normalizing,

$$\tilde{b}^{(n)} = c/\|c\|_\infty. \tag{4.10}$$

$\tilde{b}^{(n)}$ converges linearly to b_j as n approaches infinity.

The precise solution of equation 4.9 is difficult since the matrix $H - \tilde{\varepsilon}\mathbf{I}$ is very ill-conditioned if $\tilde{\varepsilon}$ is a good eigenvalue estimate; the error

$$\Delta = c - (H - \tilde{\varepsilon}\mathbf{I})^{-1}\tilde{b}^{(n-1)} \tag{4.11}$$

is the same order of magnitude as the solution. However it can be shown that the error vector points almost entirely in the direction of the eigenvector whose corresponding eigenvalue is approximated by $\tilde{\varepsilon}$ [66].

The *Rayleigh quotient iteration* accelerates the inverse iteration by replacing the shift with the energy functional of the new trial eigenvector. Given an initial eigenvector estimate $\tilde{b}^{(0)}$ with Rayleigh quotient $\tilde{\varepsilon}^{(0)}$, each iteration consists of the following:

1. Form $\tilde{\epsilon}^{(n)} = (\tilde{b}^{(n)})^T \mathbf{H}' \tilde{b}^{(n)} / (\tilde{b}^{(n)})^T \tilde{b}^{(n)}$;

2. Solve $(\mathbf{H}' - \tilde{\epsilon}^{(n)}\mathbf{I})c = \tilde{b}^{(n)}$;

3. Normalize the new trial vector: $\tilde{b}^{(n)} = c/\|c\|$;

4. Test for convergence.

Step 1 requires an additional matrix multiplication over the inverse iteration, but the first step is far less costly than the second step. A single Rayleigh quotient iteration is not much more expensive than a single inverse iteration for this problem. The rate of convergence becomes cubic; after only a few iterations, the number of significant digits in the approximate eigenvector triple every iteration.[33]. However, the matrix $\mathbf{H}' - \tilde{\epsilon}^{(n)}\mathbf{I}$ now changes with every iteration, and $\tilde{\epsilon}^{(n)}$ does not always converge to the eigenvalue closest to $\tilde{\epsilon}^{(0)}$ as n approaches infinity; the initial vector must be "sufficiently close" to the target eigenvector. Defining the residual vector

$$r^{(n)} = (\mathbf{H}' - \tilde{\epsilon}^{(n)}\mathbf{I})\tilde{b}^{(n)} \tag{4.12}$$

it can be shown that when the norm of $r^{(n)}$ is less than $\frac{1}{4}$ of the minimum gap between the target eigenvalue ϵ_j and its adjacent eigenvalues, then $\tilde{\epsilon}^{(n)}$ will converge to ϵ_j [94]. However the minimum gap is usually unknown.

This situation is in marked contrast to the inverse iteration, which will always converge to the eigenvector whose eigenvalue is closest to the shift $\tilde{\epsilon}$, given any initial eigenvector estimate which is not orthogonal to the eigenvector being sought. Inverse iteration can be used to refine an initial eigenvector estimate until it is sufficiently close to the target eigenvector; then we can switch to the more rapidly convergent Rayleigh quotient iteration.

Our code presently employs "TLIME", a two-tiered inverse iteration/Rayleigh quotient scheme developed by Szyld [87]. Szyld's method guarantees superlinear convergence to an eigenvalue on a specified interval $(\tilde{\epsilon} + \Delta\tilde{\epsilon}, \tilde{\epsilon} - \Delta\tilde{\epsilon})$, if any eigenvalues exist in the interval. When the interval does not hold any eigenvalues, the method will converge to the eigenvalue closest to $\tilde{\epsilon}$. The method begins by applying inverse

iteration until a switching criterion is satisfied, and then continues with Rayleigh quotient iteration. Define a residual for the inverse iteration analogous to 4.12,

$$q^{(n)} = (\mathbf{H}' - \tilde{\epsilon}\mathbf{I})\tilde{b}^{(n)}, \tag{4.13}$$

Since $\tilde{b}^{(n)}$ converges to an eigenvector b_j as n approaches infinity, the norm of $q^{(n)}$ provides an upper bound on the gap between the shift and the eigenvalue ϵ_j closest to it. The bound will not worsen as the iteration progresses [87], so

$$\|q^{(0)}\| \geq \|q^{(1)}\| \geq \ldots \geq \|q^{(n)}\| \geq |\tilde{\epsilon} - \epsilon_j|. \tag{4.14}$$

Thus the target eigenvalue is on the interval $(\tilde{\epsilon} - \|q^{(n)}\|, \tilde{\epsilon} + \|q^{(n)}\|)$, and so if $\|q^{(n)}\| < \Delta\tilde{\epsilon}$, then $\epsilon_j \in (\tilde{\epsilon} + \Delta\tilde{\epsilon}, \tilde{\epsilon} - \Delta\tilde{\epsilon})$. From equations 4.12 and 4.14, $\|r^{(n)}\|^2 = \|q^{(n)}\|^2 - (\tilde{\epsilon} - \tilde{\epsilon}^{(n)})^2$ so $\|r^{(n)}\| \leq \|q^{(n)}\|$. If $\Delta\tilde{\epsilon}$ is less than $\frac{1}{4}$ of the minimum gap between the target eigenvalue and its adjacent eigenvalues, the Rayleigh quotient iteration will cubically converge to an eigenvalue on $(\tilde{\epsilon} + \Delta\tilde{\epsilon}, \tilde{\epsilon} - \Delta\tilde{\epsilon})$. This motivates a switch from inverse iteration to the Rayleigh quotient iteration when

$$\|q^{(n)}\| \leq \Delta\tilde{\epsilon}. \tag{4.15}$$

Since the minimum gap is not known, one can not be certain that the eigenvector is "sufficiently close" to the true eigenvalue. The Rayleigh quotient is carefully monitored. If it leaves $(\tilde{\epsilon} + \Delta\tilde{\epsilon}, \tilde{\epsilon} - \Delta\tilde{\epsilon})$, the algorithm switches back to inverse iteration.

Notice that if the interval does not contain an eigenvalue, the switching criterion 4.15 is never satisfied and only inverse iterations would be performed. In this case TLIME will switch to Rayleigh quotient iterations if the relative change in the Rayleigh quotient between iterations becomes smaller than some preset tolerance. A minimum number of inverse iterations are forced to prevent the the procedure from prematurely switching to the Rayleigh quotient iteration.

The minimum gap length for the target eigenvalue determines the rate of convergence in both the inverse and Rayleigh quotient iterations. Since the eigenvalues of $\mathbf{H}'$ tend to be closely spaced, convergence of any of the vector iterations tends to be slow. Fortunately excellent estimates of ground state eigenvalues and eigenvectors can be easily obtained, and only a few iterations are usually necessary for convergence.

However, obtaining these estimates for excited state eigenvalues and eigenvectors is more difficult.

The feasibility of both the inverse and Rayleigh quotient iterations also depends on the difficulty of solving systems involving $\mathbf{H}' - \tilde{\varepsilon}\mathbf{I}$. As noted previously, factorization of this matrix is impractical. TLIME iteratively solves these systems using the large sparse symmetric linear equation solver SYMMLQ [61], based on a conjugate gradient procedure.

4.2.2 Subspace Iterations

The iterative subspace methods variationally approximate the eigenvector at each iteration n within a subspace of dimension d spanned by a set of vectors $\left\{v_i^{(t)}\right\}_{i=1}^{d}$ [25].

Coordinate relaxation methods (e.g. the Cooper-Nesbet algorithm [24, 59] used by Saxe *et al.*[75] in their classic double zeta FCI water study) use subspaces of small fixed dimension. The Cooper-Nesbet method requires the storage of only one CI vector, but convergence can be rather slow and the method is better suited to conventional rather than direct CI. The root-shifting optimal relaxation method developed by Shavitt *et. al.*[80] has been used in a number of CI calculations. The optimal relaxation methods correct the trial eigenvector $\tilde{b}^{(n)}$ at each step using

$$\tilde{b}^{(n+1)} = \tilde{b}^{(n)} + \lambda_j \vec{e_j}, \tag{4.16}$$

where $\vec{e_j}$ is a unit vector and λ is chosen to minimize the energy functional $\tilde{\varepsilon}^{(n+1)}$. If only the j-th component of the eigenvector is varied, the solution of $\partial\tilde{\varepsilon}^{(n+1)}/\partial\tilde{b}_j = 0$ is

$$\lambda_j = (\tilde{\varepsilon}^{(n+1)} - H'_{jj})^{-1} v_j \tag{4.17}$$

where $\vec{v} = (\mathbf{H}' - \tilde{\varepsilon}^{(n+1)}\mathbf{I})\tilde{b}^{(n)}$. Bender and Davidson's [8] variation allows several components of $\tilde{b}^{(n)}$ to be changed simultaneously; Shavitt *et. al.* further extend 4.17 to allow excited-state eigenvalues and eigenvectors to be obtained (by shifting all lower eigenvalues[26]). Unfortunately, the method can not compute isolated eigenstates (all lower-energy states must be known). Additionally, near-degenerate states cause convergence problems.

The Lanczos method [45] employs the Rayleigh-Ritz procedure within a sequence of nested Krylov subspaces which increase in dimension by one with each iteration:

$$\mathcal{K}^{(1)} \subset \mathcal{K}^{(2)} \subset \ldots \subset \mathcal{K}^{(n)} \tag{4.18}$$

where $\mathcal{K}^{(i)}$ is the subspace of $\mathcal{V}^{[N]}$ spanned by the first i elements of the Krylov sequence 4.4. The motivation for the method comes from the fact that $\mathcal{K}^{(n)}$ will be nearly invariant under $\mathbf{H}'$ as n becomes large, since for sufficiently large n $\mathbf{H}'^{n}v$ becomes approximately proportional to $\mathbf{H}'^{n-1}v$, and thus will contain good approximations of the eigenvectors of $\mathbf{H}'$. The Krylov subspaces have a number of additional advantages. The restriction of $\mathbf{H}'$ to the Krylov subspace $\mathcal{K}^{(n)}$ can be written

$$\mathbf{T}^{(n)} = \mathbf{V}^{(n)\dagger}\mathbf{H}'\mathbf{V}^{(n)} \tag{4.19}$$

where the columns of $\mathbf{V}^{(n)}$ are the *Lanczos vectors* $\{v_i\}_{i=0}^{n}$ which form an orthonormal basis for $\mathcal{K}^{(n)}$. The Lanczos vectors can be computed recursively to generate a tridiagonal $\mathbf{T}$ matrix whose eigenvalues belong to the spectrum of $\mathbf{H}'$.

However, in the basic Lanczos procedure round-off errors destroy the orthogonality of the basis vectors as the iteration proceeds. Several modifications to the algorithm circumvent this problem, by completely, selectively, or periodically reorthogonalizing the Lanczos vectors [66].

The Davidson method [25] also increases the dimension of the approximating subspace by one with each new iteration but attempts to improve convergence by using perturbation theory to select each new element of the spanning set.

An important feature of these iterative large matrix eigenvalue algorithms is that the Hamiltonian matrix is referenced only via a subroutine which forms Hamiltonian matrix-vector products, allowing the tensor product structure to be used advantageously.

4.3 Formation of the Model Hamiltonian Matrix-Vector Product

In each step of the vector or subspace iterations, Hamiltonian matrix-vector products are required:

$$x = \mathbf{H}y = \mathbf{H}_{bare}y + (\mathbf{H} - \mathbf{H}_{bare})y$$

where $\mathbf{H}_{bare}y$ and $(\mathbf{H} - \mathbf{H}_{bare})y$ are the one and two-electron parts of the product and x and y are symmetry-adapted vectors. The formation of the two-electron part

$$\sum_{i<j}^{N} P_{ij}^{-1}[(z^t \otimes z^t)\, g\, (z \otimes z) \otimes I^{[N-2]}]P_{ij}y$$

is the rate-limiting step. The expression for $(\mathbf{H}-\mathbf{H}_{bare})$ in terms of pair transpositions $p_{ij}(c_1 \otimes \cdots \otimes c_i \otimes \cdots \otimes c_j \otimes \cdots \otimes c_N) = (c_1 \otimes \cdots \otimes c_j \otimes \cdots \otimes c_i \otimes \cdots \otimes c_N)$ leads to

$$\sum_{i<j}^{N} p_{i+1,j}(\mathbf{I}^{[i-1]} \otimes (z^t \otimes z^t)\, \mathbf{g}\, (z \otimes z) \otimes \mathbf{I}^{[N-i-1]})p_{i+1,j}\, y,$$

which suggests a convenient reduction of the problem. If x and y are partitioned into subvectors x^{kl} and y^{kl} of length m^2 which cycle indices k and l while holding all other indices constant, the two-electron matrix vector product can be reduced to forming

$$x^{kl}_{I''} = (z^t \otimes z^t)\, g\, (z \otimes z) y^{kl}_{I''}$$

for all subvectors $x^{kl}_{I''}$ and $y^{kl}_{I''}$, where I'' labels the set of noncycling indices. The transformation of g should be performed implicitly (by preserving the factored form of the transformation matrix) to minimize errors due to finite precision arithmetic. For example, the multiplication involving canonical orthogonalization consists of the steps

1) Solve $(d \otimes d)^{1/2}a = y^{kl}_{I''}$ for a.

2) Form $b = (u \otimes u)a$.

3) Form $c = gb$.

4) Solve $(u \otimes u)d = c$ for d.

5) Solve $(d \otimes d)^{1/2} x_{p'}^{kl} = d$.

It is more efficient to form matrix-vector products in tensor product spaces (step 2) and solve linear systems with coefficient matrices which are tensor product matrices (step 4) without explicitly forming the large $(m^2 \times m^2)$ tensor product matrices. In step 2 above we exploit the fact that U can be written as a sum of elementary matrices

$$U = \sum_{i,j}^{m} u_{ij} E_{ij},$$

where E_{ij} is an $m \times m$ matrix with element ij equal to unity and all other elements equal to zero. Since $E_{ij} = e_i \otimes e_j^t$ (where e_i and e_j are unit vectors), the tensor product $U \otimes U$ can be written in terms of elementary tensor products

$$U \otimes U = \sum_{i_1,j_1}^{m} u_{i_1,j_1} e_{i_1} \otimes e_{j_1}^t \otimes \sum_{i_2,j_2}^{m} u_{i_2,j_2} e_{i_2} \otimes e_{j_2}^t,$$

which is a twice contravariant and twice covariant tensor. The vector

$$w = \sum_{j_1,j_2}^{m} w_{j_1,j_2} e_{j_1} \otimes e_{j_2}^t$$

and the matrix-vector product is then

$$z = (U \otimes U)w = \sum_{i_1,i_2,j_1,j_2}^{m} u_{i_1,j_1} u_{i_2,j_2} w_{j_1,j_2} e_{i_1} \otimes e_{i_2}^t,$$

which is (formally) the contraction of contravariant and covariant components within each of the two one-particle spaces. Pereyra and Scherer [68] have outlined general algorithms for solution of systems of linear equations involving nonsingular tensor product matrices which are based on triangular decompositions of the factor matrices coupled with tensor contractions. Multiplication by the two-factor tensor products $(\mathbf{z} \otimes \mathbf{z})$ can be accomplished by noting that for matrices $\mathbf{A}$, $\mathbf{B}$, and $\mathbf{C}$,

$$(\mathbf{B}^t \otimes \mathbf{A})\,\mathbf{vec}\,\mathbf{C} = \mathbf{vec}\,\mathbf{ACB}, \tag{4.20}$$

where the vec operator produces a vector of length pq from a $p \times q$ matrix by concatenating the matrix's columns (see Appendix A). Because the subvectors contain two cycling indices they can be naturally written as matrices $y_{p'}^{kl} = \mathbf{vec}\, Y_{p'}$.

While there are a large number of subvectors, they possess the same spin symmetries as their component kets, e.g.,

$$y^{\alpha i}_{J''} = \varrho(\pi^{\alpha}\pi^{\beta})y^{\beta i}_{J''}$$

where $\pi^{\alpha}\pi^{\beta}I = J$. Exploiting these symmetries significantly reduces the number of subvectors which must be explicitly gathered and premultiplied by the transformed two-electron integral matrix.

Paging activity can be minimized during the gathering of subvector elements from the packed eigenvector by organizing the eigenvector as a rectangular array (square and symmetric for singlet systems) with rows (columns) corresponding to lexically ordered combinations of orbital indices over the first (second) column in the appropriate Young frame as in Figure 3.2. For example, for each fixed set of β (odd) indices, we obtain all necessary elements which are indexed by fixed and cycling α (even) indices. To address individual elements of the eigenvector array we use Handy and Knowles' addressing function [42]:

$$address(i_1, \ldots, i_N) = 1 + \sum_{k=1}^{N} A_{k,i_k} \tag{4.21}$$

which computes the lexicographic index of an ordered combination of orbital indices. Here $\{i_k\}$ is a strictly ascending orbital indices drawn from a single column of the Weyl tableau (i. e., indices drawn from columns α and β of the tableau give its row and column indices in the eigenvector array, respectively). The array **A** is given by

$$\begin{aligned} A_{kl} &= \textstyle\sum_{i=m-l+1}^{m-k} \left[\binom{i}{N-k} - \binom{i-1}{N-k-1}\right] && \text{when} \quad m-N+k \geq l \geq k, k < N; \\ A_{Nl} &= l - N && \text{when} \quad m \geq l \geq N \end{aligned}$$

The subvectors of y can be constructed, effectively multiplied by $(z \otimes z)^t g(z \otimes z)$, and scattered to different subvectors of x with indices dictated by spin symmetry. This procedure has several advantages in parallel environments:

1) Subvectors which differ by 3 or more noncycling indices can be constructed from distinct portions of the packed vector. In parallel mode, this means that it is possible to simultaneously gather several subvectors from a packed vector in shared memory without contention.

2) Each of the transformed two electron integral matrix-subvector multiplications involves the same number of floating point operations. The matrix-vector multiplications can be apportioned evenly among the processors so that the load balancing should be very good.

3) The independence of the individual subvector problems suggests that interprocessor communication will be minimal.

4) The generation of the molecular integrals in parallel in loosely coupled processor arrays leaves integrals over different shells distributed among the different processors. In the tensor product method this poses no great difficulty because there is no need to perform integral transformation (involving sorting and redistribution of the integrals among the processors).

The overhead required to form the subvectors relative to the time required for individual subvector term calculations will determine the feasibility of parallel tensor product calculations.

4.4 Choice of The Initial Eigenvector Estimate

It was noted in Chapter 3 that the eigenvectors of the tensor product Hamiltonian are not restricted to any particular permutation class. Thus the ground state energy often does not correspond to the lowest eigenvalue of $\mathbf{H}'$. Given the cost of the Hamiltonian-matrix vector multiply, the choice of a good initial eigenvector estimate becomes critical as the particle number and basis set size increase.

When ϵ is the SD-CI ground state energy (corrected for size-consistency errors), and $\tilde{b}^{(0)}$ is constructed from the Hartree-Fock wavefunction, a single inverse iteration and one or two Rayleigh quotient iterations were sufficient for convergence in the hydrogen dimer calculations described in Chapter 5.

The bare nucleus Hamiltonian can provide eigenvalue estimates which are guaranteed (albeit very crude) lower bounds on the true eigenvalues. The bare nucleus term

of $\mathbf{H}'$ can be written as a Kronecker sum [1] of the transformed one-electron matrices:

$$\mathbf{H}'_{bare} = \sum_{i=1}^{N} I^{[i-1]} \otimes (z^t h z) \otimes I^{[N-i]} \tag{4.22}$$

$$= \bigoplus_{i=1}^{N} z^t h z \tag{4.23}$$

The eigenvalues of $\mathbf{H}'_{bare}$ are sums of the eigenvalues of $z^t h z$, and the eigenvectors are Kronecker products of the corresponding eigenvectors.

A more physically realistic starting vector is the single determinantal Hartree-Fock wavefunction. The initial guess corresponds to a Hartree-Fock determinant, spin-projected as necessary using Matsen's structure projectors. The correct spin symmetry should in principle be preserved throughout the iterative solution of the matrix eigenvalue problem because all of the operators employed are spin-free, and the same integral matrices are used throughout; in practice, the nonassociativity of floating point operations in finite precision arithmetic may cause the vector to leak into nonphysical subspaces. In this case spin projection of the vector over the course of the eigenvalue iteration may be necessary occasionally.

Given a set of occupied Hartree-Fock orbitals $\varphi_{i_k}, k = 1, \ldots, N$ such that

$$\varphi_i(\mathbf{r}) = \sum_{k=1}^{m} a_{ki} \phi_k(\mathbf{r}) \tag{4.24}$$

the elements of the corresponding packed eigenfunction for a closed shell system can be simply generated by forming

$$c_{j_1,\ldots,j_N} = \prod_{k=1}^{N} a_{j_k i_k} \tag{4.25}$$

where the set $\{i_k\}$ indexes the occupied molecular orbitals.

[1] see Appendix A.

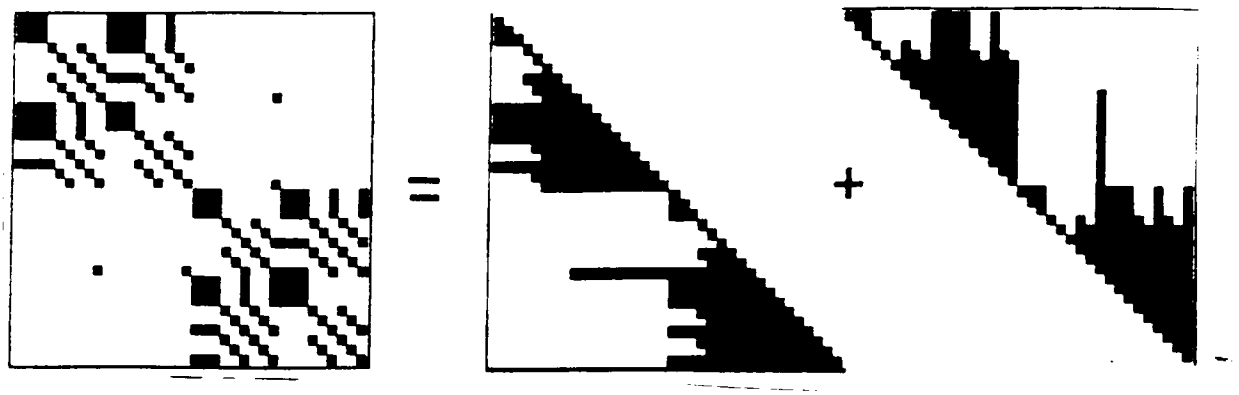

Figure 4.1: The structure of the overlap matrix and its corresponding Cholesky factor for a weakly interacting (R = 20.0) pair of [3s2p] hydrogen molecules in the T-configuration

Chapter 5

Applications

In this chapter we demonstrate the tensor product method using sample calculations for a few small model systems. In section 5.1, potential energy curves for the ground and low-lying excited states of H_2 are presented. Section 5.2 describes a fully variational double-zeta potential energy surface for the hydrogen molecular dimer. The surface consists of 136 configurations at varying orientations and intermolecular separations from 3.0-11.0 bohrs. Extension of these calculations to larger basis sets will allow the construction of highly accurate anisotropic pair potentials to study structure, phase transitions and many-body effects in hydrogen crystals, topics with potential applications in controlled hydrogen fusion technologies.

All tensor product calculations were done on an IBM 3090/600VF mainframe, using the software described in Appendix D. The molecular one- and two-electron integrals were computed using the POLYATOM package. Hartree-Fock and configuration interaction calculations were performed using GAUSSIAN 82 [10].

5.1 Ground and Excited States of H_2

The hydrogen molecule has been extensively studied and provides a first testing ground for any theoretical treatment of electron correlation. The most precise theoretical H_2 energies and wavefunctions have been computed by Kolos *et. al.*[43]. Their fully correlated wavefunction composed of gaussian geminals which depend explicitly

on the interelectronic distances. The corresponding energy is about 40 microhartrees above the exact nonrelativistic Born-Oppenheimer energy.

The goal of the following calculations is to demonstrate and verify the tensor product method rather than attempt to approach the nonrelativistic limit; accordingly an economical basis set is employed. Both ground and excited states are of interest so the basis set is not optimized with respect to any particular state. The basis set consists of linear combinations (or "contractions") of primitive Cartesian Gaussian functions

$$g_{i,j,k}(\zeta) = Ax^i y^j z^k \exp(-\zeta_{i,j,k} r^2) \tag{5.1}$$

where A is a normalization factor, r is the electronic position vector (relative to the orbital center), i,j, and k, are positive integers whose sum is the angular momentum quantum number of the orbital function, and ζ is the orbital exponent. The orbitals

$$\begin{aligned} \phi_{1s} &= \sum_{n=1}^{3} a_n g_{000}(\zeta_n) \\ \phi_{2s} &= g_{000}(\zeta_4) \end{aligned}$$

are centered on hydrogen atom $c = a$ or b, using the contraction coefficients a_n and the exponents given in table 5.1. This *double zeta* basis is a 3-1 contraction of Huzinaga's 4*s* basis [36], which was obtained by a least squares fit to hydrogenic Slater-type orbitals. A more precise basis set would include *diffuse* functions (with small orbital exponents), *polarization* functions (with angular momentum quantum numbers greater than zero), and possibly functions centered at locations other than the nuclear centers (typically, at bond midpoints). Table 5.2 compares restricted Hartree-Fock (RHF) and full configuration interaction calculations in the double zeta basis of Table 5.1 with more extensive basis sets containing additional *s* and *p* functions.

The tensor product decomposition of the Hamiltonian for this two electron system is given by

$$(\mathbf{h} \otimes \mathbf{s} + \mathbf{s} \otimes \mathbf{h} + \mathbf{g})c = \varepsilon(\mathbf{s} \otimes \mathbf{s})c \tag{5.2}$$

For such a small system H′ can be diagonalized (e. g., using the Householder-QR-Wilkinson algorithm [33]) to obtain ground and excited state energies and eigenvectors to independently check the convergence of the large-matrix methods described in

Table 5.1: Exponents and contraction coefficients of the double zeta basis set employed in the sample H_2 and $(H_2)_2$ surfaces.

n	Exponent ζ_n	Contraction Coefficient a_n
1	13.3615	0.032828
2	2.01330	0.231208
3	0.453757	0.817238
4	0.123317	1.000000

section 4.2. Table 5.3 presents ground state full CI energies and the energies of the lowest 3 states at various internuclear separations R, obtained by diagonalizing the tensor-product Hamiltonian. Figure 5.1 shows the potential energy curves lowest 4 eigenstates.

Table 5.2: H_2 total energies in hartrees (R = 1.4 a. u.)

Basis	RHF	FCI
[3s1p]	-1.128618	-1.155854
[4s1p]	-1.129062	-1.156858
[3s2p]	-1.132717	-1.168271
[4s2p]	-1.132968	-1.168858
[4s3p]	-1.133140	-1.170492

The 3s and 4s sets are 3-1-1 and 3-1-1-1 contractions of Huzinaga's 5s and 6s sets, respectively; the 1p, 2p, and 3p functions have exponents {0.15}, {1.0, 0.08}, and {1.0, 0.15, 0.08}, respectively.

Table 5.3: H_2 ground and low-lying excited-state total energies (in Hartrees) at various internuclear separations.

R(bohr)	$^1\Sigma_g^+$(FCI)[1]	$^1\Sigma_g^+$(TP)	$^3\Sigma_u^+$(TP)	$^1\Sigma_u^+$(TP)
1.10	-1.1150620	-1.1150619	-.6403517	-0.5418460
1.20	-1.1335792	-1.1335791	-.6897202	-0.5789991
1.30	-1.1438653	-1.1438652	-.7301348	-0.6064784
1.35	-1.1466918	-1.1466916	-.7477283	-0.6174041
1.40	-1.1482871	-1.1482870	-.7638760	-0.6267924
1.45	-1.1488411	-1.1488409	-.7787549	-0.6348518
1.50	-1.1485147	-1.1485146	-.7925118	-0.6417625
1.55	-1.1474455	-1.1474453	-.8052704	-0.6476806
1.60	-1.1457511	-1.1457509	-.8171340	-0.6527419
1.70	-1.1408787	-1.1408785	-.8385211	-0.6607539
1.85	-1.1310077	-1.1310076	-.8657243	-0.6688704
2.00	-1.1194081	-1.1194080	-.8882258	-0.6739444
2.25	-1.0988838	-1.0988836	-.9176830	-0.6788167
2.50	-1.0791241	-1.0791239	-.9395081	-0.6816051
3.00	-1.0464614	-1.0464612	-.9676407	-0.6839020
3.50	-1.0245185	-1.0245183	-.9828509	-0.6814980
4.00	-1.0115883	-1.0115881	-.9908385	-0.6744419
5.00	-1.0013692	-1.0013691	-.9968545	-0.6517242
6.00	-0.9991104	-0.9991103	-.9982143	-0.6258778

FCI- full configuration interaction energies, computed with GAUSSIAN 82.

TP- tensor product full variational energies.

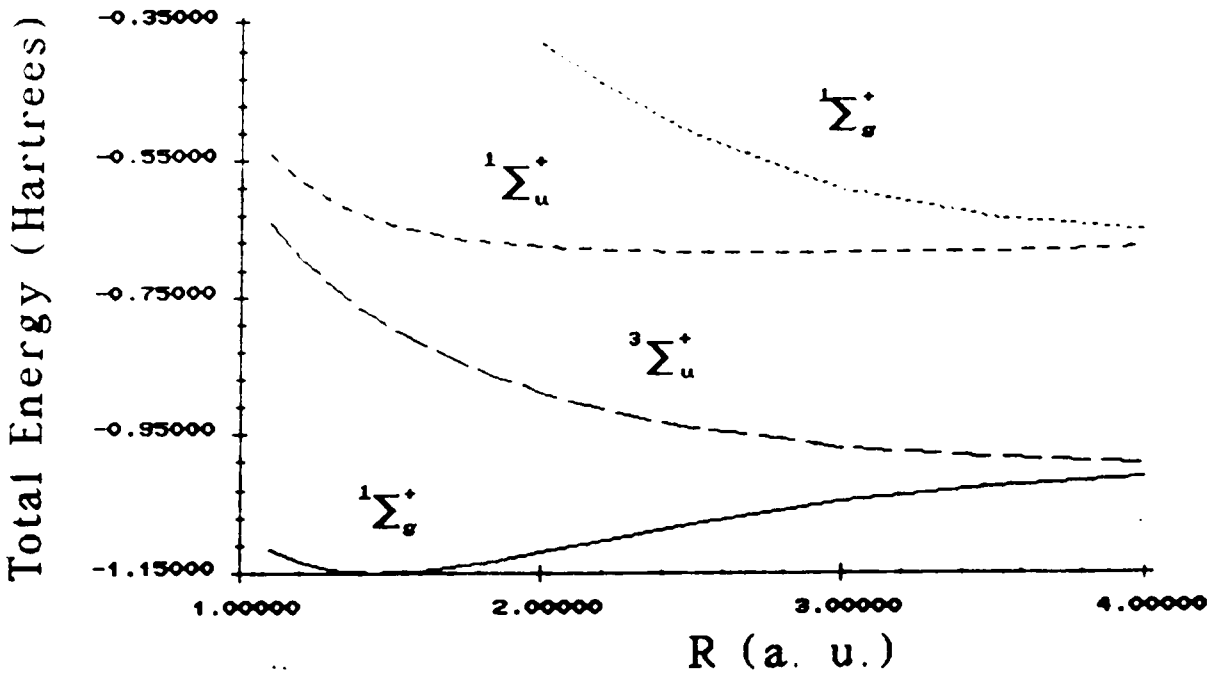

Figure 5.1: Ground and excited state potential energy curves for double-zeta H_2 computed by the tensor product approach

Note that the term symbols labelling the eigenstates follow the usual notation for linear $D_{\infty h}$ and $C_{\infty v}$ molecules[1]. The spin multiplicity of the eigenstates is determined by application of the singlet and triplet structure projectors

$$\hat{\mathbf{X}}^{[2]} = \frac{1}{\sqrt{2}}\{\hat{\mathbf{I}} + \hat{\pi}\} \tag{5.3}$$

and

$$\hat{\mathbf{X}}^{[1,1]} = \frac{1}{\sqrt{2}}\{\hat{\mathbf{I}} - \hat{\pi}\}, \tag{5.4}$$

respectively, where $\hat{\pi}$ exchanges the electron labels. Similarly, the symmetry of the wavefunctions can be assigned by observing the action of symmetry operations (e. g., the inversion operator simultaneously exchanges orbitals centered on *a* with corresponding orbitals on center *b*. For example, for an ***ungerade*** eigenvector the coefficients of the kets $|1s_a 2s_a 1s_b 2s_b\rangle$ and $|1s_b 2s_b 1s_a 2s_a\rangle$ have equal absolute values but opposite signs). The $^1\Sigma_{g1}^+$ and $^3\Sigma_u^+$ states converge to twice the energy of an isolated double zeta hydrogen atom at large internuclear distances (-0.9985546 Hartrees at R = 100 bohrs) while the $^1\Sigma_u^+$ and $^1\Sigma_{g2}^+$ states converge to the energy of infinitely separated $H^+ + H^-$ (-0.4691839 Hartrees at R = 100 bohrs). The tensor product energies agree with full CI calculations to 0.1-0.2 microhartrees.

[1]The Σ signifies that the projection of the total orbital angular momentum of the electrons along the molecular axis is zero. The subscript *u* or *g* indicates that the eigenstate is odd or even with respect to inversion through the molecular center of gravity. The left superscript gives the spin multiplicity $2S + 1$ and the right superscript gives the sign of the wavefunction after reflection through the *yz* plane (where *z* corresponds to the bond axis).

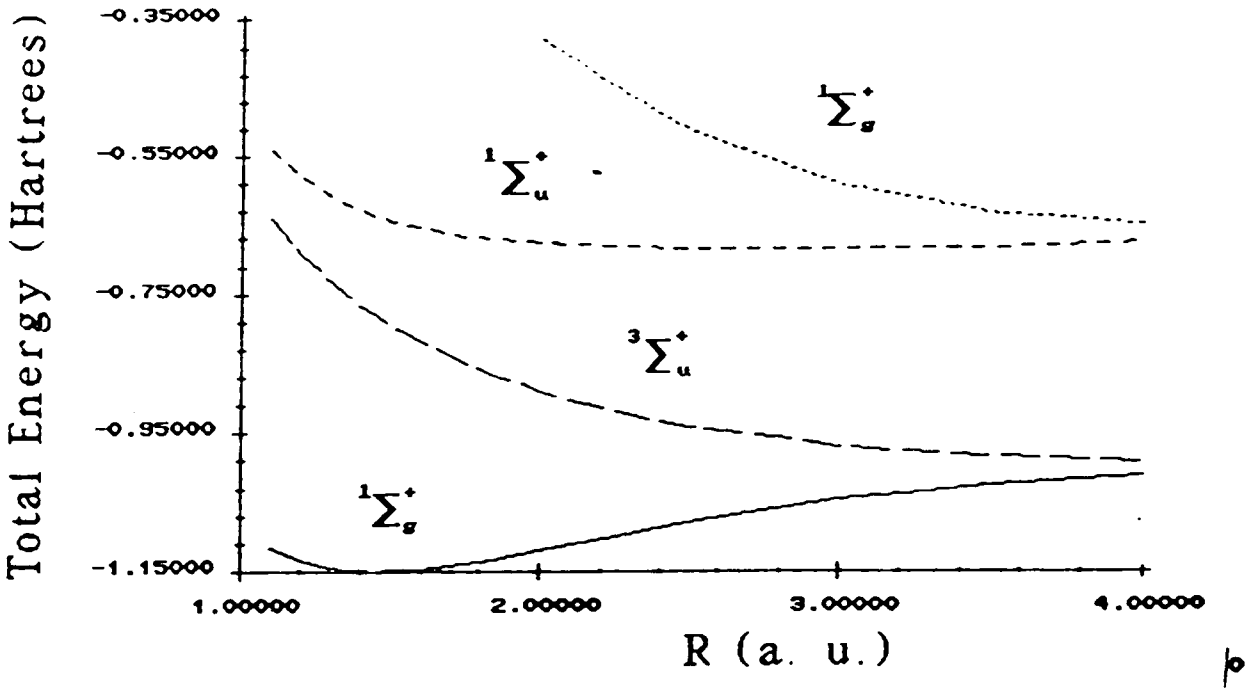

Figure 5.1: Ground and excited state potential energy curves for double-zeta H_2 computed by the tensor product approach

5.2 A Full Variational Hydrogen Dimer Potential Energy Surface

5.2.1 Background

The $(H_2)_2$ van der Waals dimer has been a frequent subject of both experimental and theoretical studies. Experimental H_2-H_2 interaction potentials can significantly deviate from one method to another, particularly when using state-selective methods (for example, molecular beam scattering methods). These deviations occur because of varying degrees of experimental sensitivity to different hydrogen isotopes, rotational forms, intermolecular potential ranges, and potential anisotropy. The variety of post-SCF and experimental results available and the relative simplicity of the system make the hydrogen molecule dimer a good first candidate for tensor product full variational studies. Although a number of FCI results are available for H_2 dimer structures of high symmetry, complete potential energy surfaces at the FCI level have not yet been computed. Construction of a highly accurate $(H_2)_2$ potential surface is worthwhile both theoretically and practically, given current interest in the low-temperature behavior of solid hydrogen in the development of hydrogen fuel and fusion technologies[78].

The first ab-initio calculations were performed in the late sixties and early seventies by Magnasco and Musso and Tapia and Bessis. The latter study involved 4 structures of $(H_2)_2$ at the SD- CI/[3s3p] level (see Figure 5.2.1.

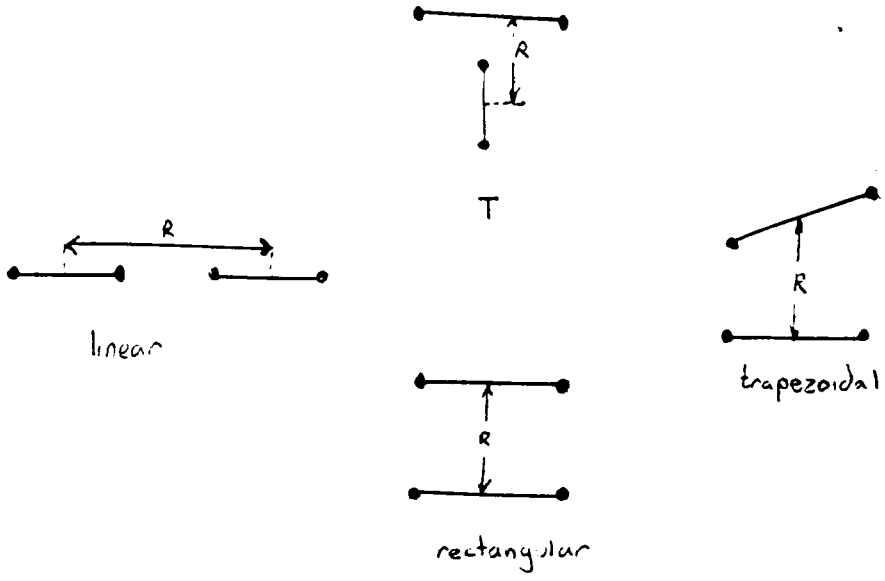

Figure 5.3. Hydrogen dimer structures considered by Tapia and Bessis

A series of computations involving these highly symmetric structures have been performed at both the SCF and post-SCF levels. Wilson and Goddard [96] computed fully correlated potential energy curves with a minimal Slater-type basis for the structures of Figure 5.2.1 (with an additional "crossed" or tetrahedral structure). Rubinstein and Shavitt[72] presented similar calculations using an unoptimized double-zeta basis set.

Of the four structures the T-structure is the most stable (due to the attractive quadrupole-quadrupole interaction) and has been the most extensively studied. Burton[18] obtained a minimum energy T-structure geometry using CEPA and PNO-SDCI with a large basis set (78 independent Gaussian functions). Harrison and Handy[35] performed a full CI calculation using Burton's geometry and basis set. Their computation included 912464 CSFs in C_{2v} symmetry; convergence to 10^{-5} hartree required 8 hours on a CRAY-1S using the GUGA-CI program of Saxe. Hobza et. al.[37] performed MP4 calculations on the T-structure with a variety of basis sets; their results indicate that basis set superposition errors (BSSE) are important in both SCF and post-SCF calculations. A [4s3p] basis set was recommended as an economical compromise between basis set size and completeness for extended calculations on the energy hypersurface.

Price and Stone [84] fitted a number of anisotropic pair potentials in the region of the van der Waals minimum to a 130-point rigid- rotor SDCI surface with a moderate (30 function) basis set. The SDCI calculations included corrections for both size consistency errors and BSSE. Using an exponential form for the short-range repulsive and S-function expansions for the long-range attractive portions of the pair potential, an extremely accurate fitting was obtained.

Schneider et. al. recently computed a rigid-rotor [4s3p] surface at the second-order Möller-Plesset and SDCI levels, corrected for basis set superposition error. Fifteen separate structures were included in the calculations. Their results indicate two equivalent T-structures as stationary points, connected by a saddle point with a rhomboid structure.

5.2.2 Model Geometry

Each $(H_2)_2$ geometry is completely specified by 6 parameters: The distance R between the molecular centers of mass; the H-H molecular bond lengths r_1 and r_2; the angles θ_1 and θ_2 between the line joining the centers of mass and the two molecular bond axes; and the torsional angle φ. The model geometry is shown in Figure 5.2.2.

The bond lengths r_1 and r_2 should be essentially equal for all but highly repulsive geometries, and will vary independently only when R is less than 2-3 bohr. Outside of this cutoff distance, $r_1 = r_2 = r_e = 1.4$ bohr (and the potential surface is that of a rigid rotor). The independent variation of the bond lengths at small intermolecular separations should allow a more accurate determination of the repulsive branch of the potential than has been previously obtained, since in this region higher order correlation effects become more prominent. Exploration of this region of the potential surface is deferred for a future study.

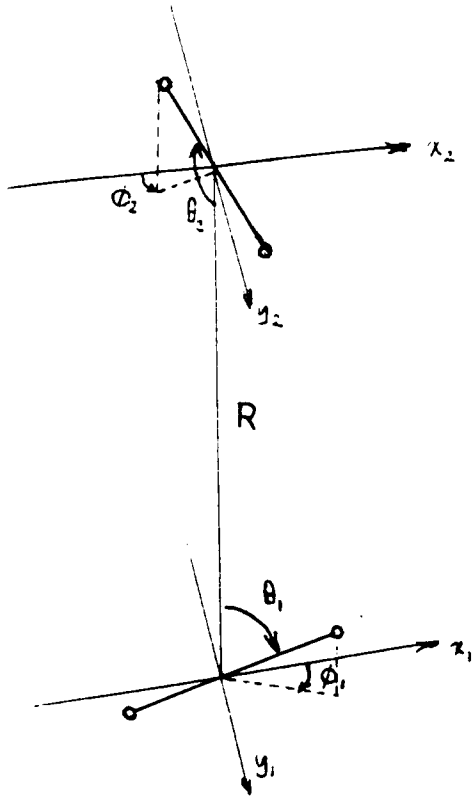

Figure 5.4: Molecular geometry of $(H_2)_2$

Energies are computed for the C_{2v} "T", D_{2h} rectangular, and $D_{\infty h}$ linear structures of Figure 5.2.1, and for a "crossed" D_{2d} configuration (with $\theta_1 = \theta_2 = \phi = 90°$). A large number of low-symmetry structures are computed, using the orientations selected by Price and Stone [84]. The orientations include angles chosen to facilitate polar Gauss-Legendre and azimuthal Gauss-Chebyshev integrations (see Appendix C).

5.2.3 Basis Sets

In any full variational calculation the choice of a basis set is necessarily a compromise between chemical accuracy and computational economy. Large basis sets are prohibitively expensive (and often contain near dependencies that may lead to numerical difficulties). Smaller basis sets inadequately model the charge distribution, leading to inaccurate prediction of polarizabilities and dipole moments and introducing *basis set superposition* errors. The basis set superposition error is a nonphysical variational lowering of the energy of one molecule in the presence of the virtual orbitals of another[13]. These errors result in a serious overestimation of interaction energies and are highly dependent on the geometry of the supermolecule. A simple estimate of the size of basis set superposition errors can be obtained by computing the energy of one molecule in the presence of the basis functions of the other, without the other's nuclei or electrons. The difference between the isolated molecule's true energy and its energy in the presence of the "ghost" orbitals of the other is usually taken is taken as the basis set superposition error. In truncated CI calculations the lack of size consistency complicates this simple estimate. Also note that the ghost orbitals include both occupied and virtual orbitals. Only the virtual orbitals cause the spurious lowering of the energy, so this procedure (sometimes referred to as the "counterpoise" method) slightly overestimates the basis set superposition error. When the occupied orbitals are compact (as in the case of the hydrogen molecular dimer) the counterpoise method should prove adequate. Although it would seem that the best remedy is an extended basis set, in the Möller-Plesset calculations of Hobza and Sauer [38] the basis set superposition error remained large relative to the interaction energy even with very large basis sets.

The expense of full variational computations increases rapidly with basis set size, motivating the use of highly optimized basis sets. While a large basis set can be conveniently optimized with respect to the energy of a single hydrogen molecule (for example, see Burton[18]) this approach is not feasible for small basis sets. Optimization with respect to the isolated molecule results in a contraction of the polarization functions which can lead to a poor description of the interaction potential. On the other hand, the use of diffuse polarization functions in small basis sets leads to higher basis set superposition errors [77].

In Table 5.2.3 tensor product variational energies reproduce Jankowski and Paldus' "H4" model hydrogen molecular dimer full CI energies to 1-2 microHartrees. The model consists of a pair of coplanar STO-3G hydrogen molecules with the atoms at the vertices of a trapezoid (see Figure 5.2.3). For a description of the basis set see Jankowski and Paldus [39].

Table 5.4: CI correlation energies for the $H4$ model (in mH, all signs reversed).

a	F-CI	This work	SD-CI	DQ-CI
0.500	53.690	-	--	53.511
0.200	57.260	57.259	55.871	57.163
0.100	65.221	65.220	63.545	65.227
0.050	76.129	76.127	73.789	76.401
0.020	92.148	92.146	88.807	92.124
0.015	96.711	96.710	93.246	96.686
0.005	109.196	109.195	105.556	109.188
0.000	—	117.620	113.972	—

F-CI. Full configuration interaction results taken from Jankowski and Paldus[39].
SD-CI: Configuration interaction including single and double excitations only, computed using the Gaussian 82 package[10]
DQ-CI: Configuration interaction with double and quadruple excitations only, taken from Jankowski and Paldus[39].

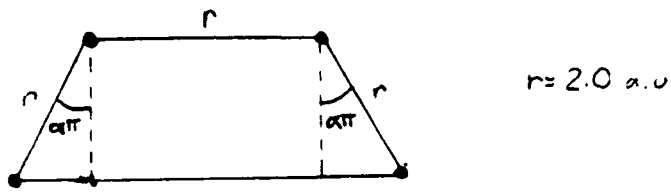

Figure 5.5: The STO-3G 'H4' model

In this preliminary study, the double zeta basis set of Table 5.1 is used without basis set superposition corrections. Table 5.5 compares restricted Hartree-Fock (RHF) and full configuration interaction calculations in the double zeta basis with more extensive basis sets (containing additional s and p functions) for the T-configuration of the hydrogen dimer, with a center-to-center intermolecular separation of 6.7 bohrs. These calculations suggest that (of these extended sets) the [$3s2p$] basis is a good comprimise between computational economy and accuracy. The total configuration interaction energies (with size-consistency corrections) successively decrease by 0.2%, 1.0% , and 0.1% with the addition of a first, a second, and a third polarization function, respectively. Addition of a third and fourth s function to the double zeta basis set successively decreases the corrected total configuration interaction energies by 0.5% and 0.09%, respectively. Restricted Hartree-Fock and limited configuration interaction (including all single and double excitations) calculations were performed for each point on the potential energy surface. The energies for the linear, "T", rectangular, and crossed structures are given in Tables 5.6, 5.7, 5.8, and 5.9, respectively. The corresponding potential energy curves are plotted in Figures 5.2.3, 5.2.3, 5.2.3, and 5.2.3. The energies for the low-symmetry structures are collected in Appendix D.

Note that the symmetry of the rectangular configurations in table 5.8 dictates that only pair excitations (doubles and quadruples) can contribute to the correlation energy [39], so the relative importance of the quadruple excitations can be gauged. The double excitations contribute 43.8 to 46.5 millihartrees to the correlation energy while the contribution of the quadruple excitations is 0.64-0.68 millihartrees.

The Davidson size-consistency correction was applied to the single-double configuration interaction energies for comparison with the fully variational energies obtained using the tensor product method. The Davidson correction [46] estimates the correlation energy due to "unlinked" quadruply excited configurations (which correspond to products of double replacements) as

$$\Delta E_q = (1 - c_0^2)\Delta E_d \tag{5.5}$$

where ΔE_d is the correlation energy for double-excitation CI and c_0 is the coefficient

Table 5.5. $(H_2)_2$ total energies in hartrees for the C_{2v} "T"-configuration with R = 6.7 a. u. for various basis sets.

Basis	RHF	SD-CI	SD-CI+SCC
$[2s]$	-2.249476	-2.295883	-2.296557
$[2s1p]$	-2.249846	-2.300263	-2.301047
$[3s1p]$	-2.257230	-2.311150	-2.311991
$[4s1p]$	-2.258117	-2.313136	-2.314013
$[3s2p]$	-2.265418	-2.335614	-2.336741
$[4s2p]$	-2.265936	-2.336764	-2.337914
$[4s3p]$	-2.266253	-2.339868	-2.341142

All energies computed using Gaussian-82[10].

RHF: Restricted Hartree-Fock.

SD-CI: Configuration interaction, including single and double excitations only.

SCC: Davidson's size-consistency correction.

TP: Tensor-product full variational energies.

The $3s$ and $4s$ sets are 3-1-1 and 3-1-1-1 contractions of Huzinaga's $5s$ and $6s$ sets, respectively; the $1p$, $2p$, and $3p$ functions have exponents $\{0.15\}$, $\{1.0, 0.08\}$, and $\{1.0, 0.15, 0.08\}$, respectively.

of the Hartree-Fock reference configuration. The corrected CI energies neglect triple excitations entirely, and do not entirely account for the fairly important quadruple excitations. Agreement between the corrected CI energies and the tensor product energies is very close at long range, the difference between the two energies rising to 10-15 microHartrees at intermolecular separations of 4 bohrs.

Price and Stone [84] describe a 6-parameter "S" potential function which was capable of fitting a SD-CI [3s1p] surface (with energies computed at identical orientations and intermolecular separations) with an unweighted root-mean-square error of 6 microhartrees; this potential model should be able to adequately distinguish full and truncated CI surfaces, particularly at closer intermolecular separations. Further studies will determine the feasibility of constructing an anisotropic model potential which can accurately reproduce full variational double zeta (and extended basis) surfaces.

Table 5.6: Double zeta $(H_2)_2$ total energies in hartrees for for the $D_{\infty h}$ linear configuration at various intermolecular separations.

$R(bohrs)$	RHF	SD-CI	SD-CI+SCC	TP
4.0	-2.2361802	-2.2826690	-2.2833287	-2.2833416
4.5	-2.2437115	-2.2902583	-2.2909256	-2.2909381
5.0	-2.2469736	-2.2936044	-2.2942788	-2.2942896
5.5	-2.2484073	-2.2950525	-2.2957303	-2.2957390
6.0	-2.2490361	-2.2956462	-2.2963247	-2.2963313
6.5	-2.2493070	-2.2958648	-2.2965425	-2.2965475
7.0	-2.2494225	-2.2959295	-2.2966062	-2.2966099
7.5	-2.2494724	-2.2959384	-2.2966142	-2.2966169
8.0	-2.2494949	-2.2959311	-2.2966062	-2.2966081
9.0	-2.2495108	-2.2959144	-2.2965887	-2.2965898
10.0	-2.2495151	-2.2959060	-2.2965800	-2.2965806
100.0	-2.2495203	-2.2958997	-2.2965733	-2.2965739

All energies computed using Gaussian-82[10] and TP.

RHF: Restricted Hartree-Fock.

SD-CI: Configuration interaction, including single and double excitations only.

SCC: Davidson's size-consistency correction.

TP: Tensor-product full variational energies.

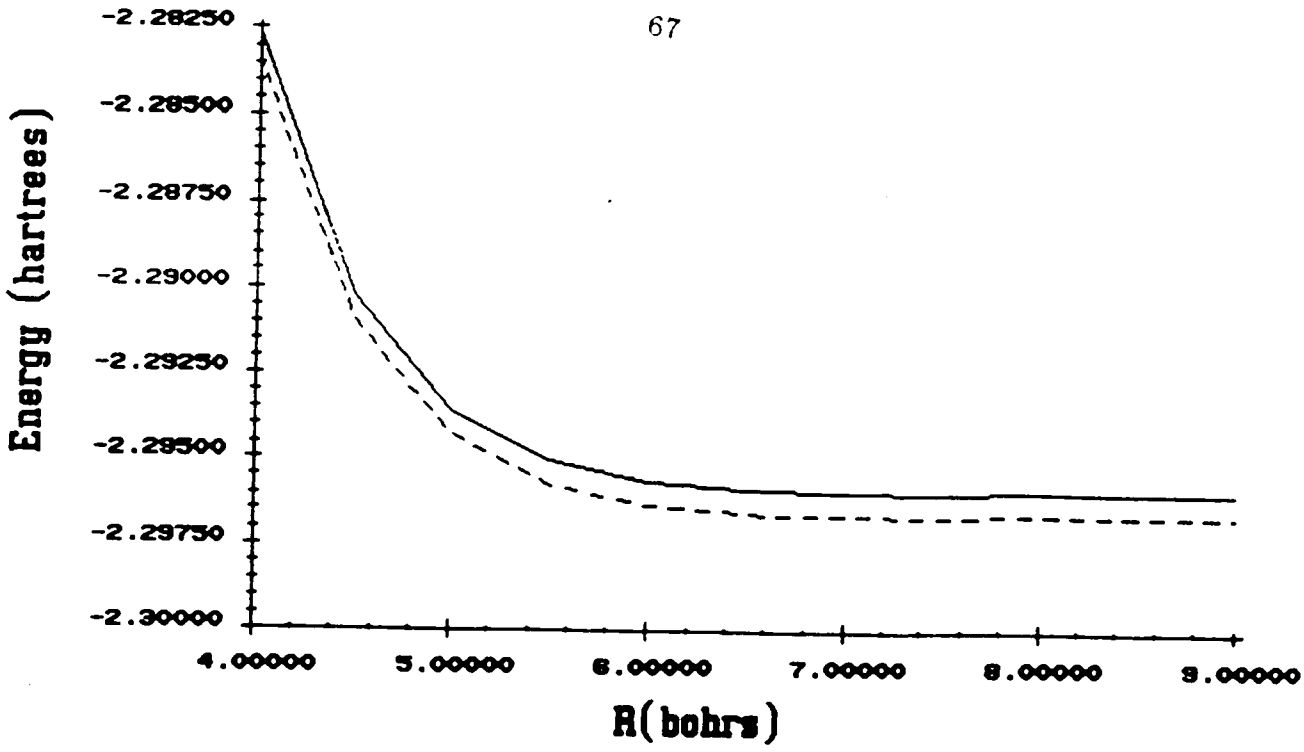

Figure 5.6: Ground state $\left({}^1\Sigma_g^+\right)$ potential energy curves for the $D_{\infty h}$ linear configuration.

The solid curve is the CI energy including single and double excitations; the dashed curve is the fully variational energy computed using the tensor product hamiltonian.

Table 5.7: Double zeta $(H_2)_2$ total energies in hartrees for for the C_{2v} "T"-configuration at various intermolecular separations.

R (bohrs)	RHF	SD-CI	SD-CI+SCC	TP
4.0	-2.2392804	-2.2857997	-2.2864665	-2.2864814
4.5	-2.2451155	-2.2916349	-2.2923058	-2.2923138
5.0	-2.2477323	-2.2942226	-2.2948953	-2.2948996
5.5	-2.2488420	-2.2953020	-2.2959754	-2.2959778
6.0	-2.2492814	-2.2957158	-2.2963895	-2.2963908
6.5	-2.2494456	-2.2958592	-2.2965329	-2.2965334
6.7	-2.2494765	-2.2958833	-2.2965570	-2.2965576
7.0	-2.2495041	-2.2959024	-2.2965760	-2.2965765
7.5	-2.2495233	-2.2959118	-2.2965854	-2.2965858
8.0	-2.2495284	-2.2959114	-2.2965850	-2.2965852
9.0	-2.2495271	-2.2959065	-2.2965801	-2.2965803
11.0	-2.2495224	-2.2959016	-2.2965752	-2.2965754
100.0	-2.2495203	-2.2958997	-2.2965733	-2.2965739

All energies computed using Gaussian-82[10] and TP.

RHF: Restricted Hartree-Fock.

SD-CI: Configuration interaction, including single and double excitations only.

SCC: Davidson's size-consistency correction.

TP: Tensor-product full variational energies.

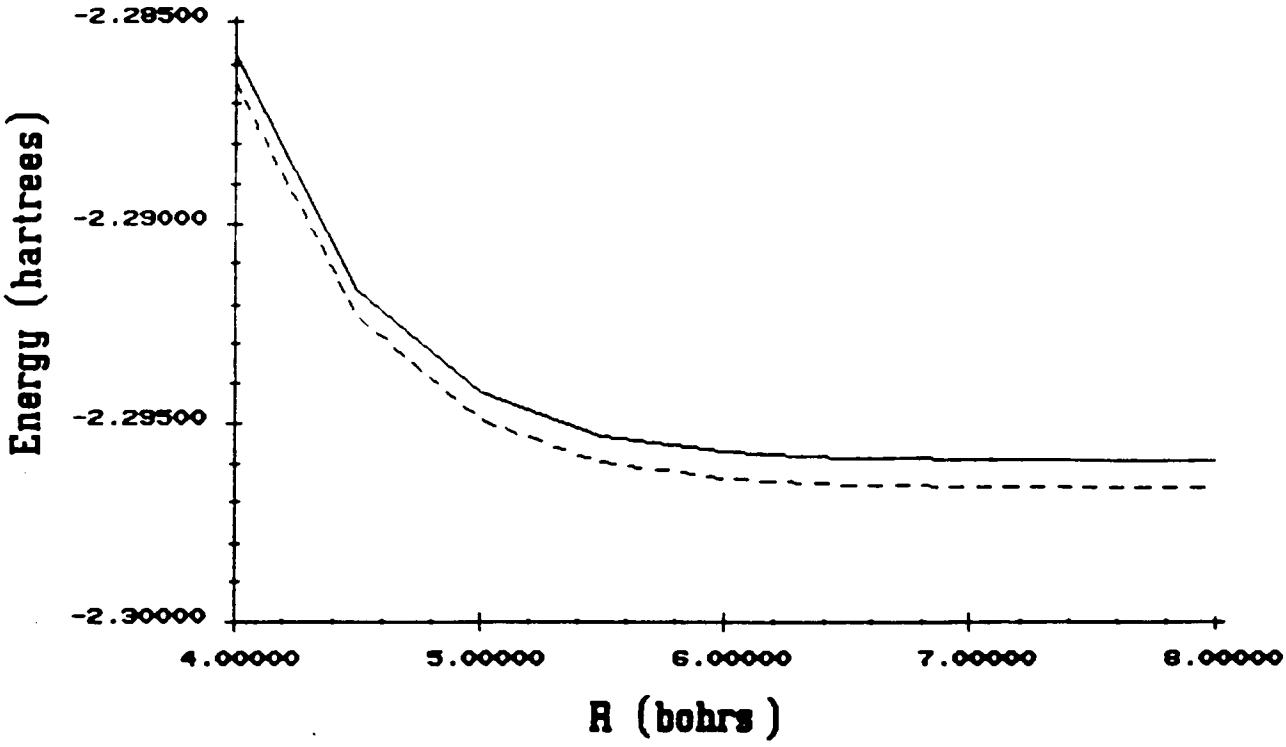

Figure 5.7: Ground state ($^3B_1$) potential energy curves for the C_{2v} "T" configuration.

Table 5.8. Double zeta $(H_2)_2$ total energies in hartrees for for the D_{2h} rectangular configuration at various intermolecular separations.

$R(bohrs)$	RHF	SD-CI	SD-CI+SCC	TP
5.5	-2.2488412	-2.2953611	-2.2960376	-2.2960408
6.0	-2.2492423	-2.2957021	-2.2963773	-2.2963794
6.5	-2.2494058	-2.2958316	-2.2965061	-2.2965076
7.0	-2.2494724	-2.2958790	-2.2965532	-2.2965543
7.5	-2.2494994	-2.2958954	-2.2965693	-2.2965701
8.0	-2.2495104	-2.2959003	-2.2965741	-2.2965748
9.0	-2.2495167	-2.2959011	-2.2965748	-2.2965752
10.0	-2.2495182	-2.2959002	-2.2965739	-2.2965743

All energies computed using Gaussian-82[10] and TP.

RHF: Restricted Hartree-Fock.

SD-CI: Configuration interaction, including single and double excitations only.

SCC: Davidson's size-consistency correction.

TP: Tensor-product full variational energies.

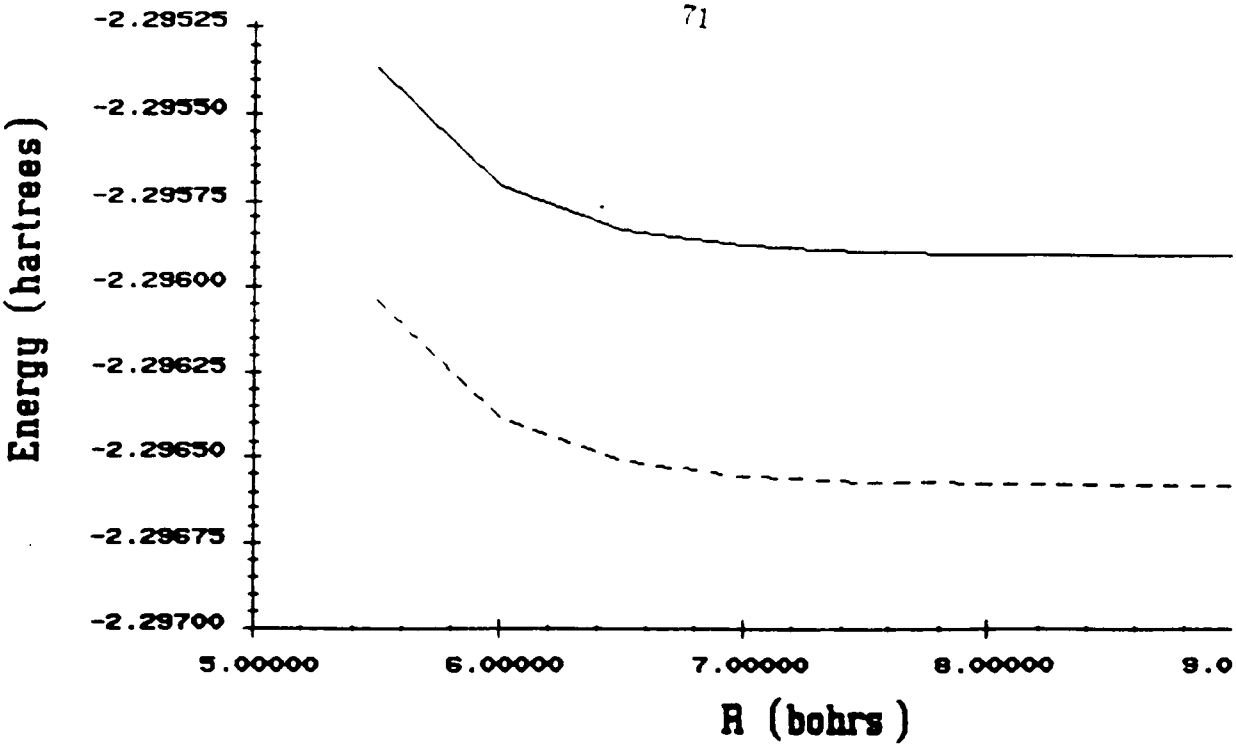

Figure 5.8: Ground state (^1A_g) potential energy curves for the D_{2h} rectangular configuration.

The solid curve is the CI energy including single and double excitations; the dashed curve is the fully variational energy computed using the tensor product hamiltonian.

Table 5.9: Double zeta $(H_2)_2$ total energies in hartrees for for the D_{2d} crossed configuration at various intermolecular separations.

R(bohrs)	RHF	SD-CI	SD-CI+SCC	TP
4.0	-2.2402958	-2.2872358	-2.2879241	-2.2879230
4.5	-2.2456109	-2.2922626	-2.2929423	-2.2929424
5.0	-2.2479155	-2.2944281	-2.2951042	-2.2951045
5.5	-2.2488728	-2.2953186	-2.2959931	-2.2959934
6.0	-2.2492618	-2.2956740	-2.2963479	-2.2963481
6.5	-2.2494187	-2.2958135	-2.2964872	-2.2964874
7.0	-2.2494813	-2.2958675	-2.2965411	-2.2965414
7.5	-2.2495057	-2.2958880	-2.2965616	-2.2965618
8.0	-2.2495515	-2.2958955	-2.2965691	-2.2965693
9.0	-2.2495192	-2.2958989	-2.2965725	-2.2965727
10.0	-2.2495197	-2.2958992	-2.2965728	-2.2965731
100.0	-2.2495203	-2.2958997	-2.2965733	-2.2965739

All energies computed using Gaussian-82[10] and TP.

RHF: Restricted Hartree-Fock.

SD-CI: Configuration interaction, including single and double excitations only.

SCC: Davidson's size-consistency correction.

TP: Tensor-product full variational energies.

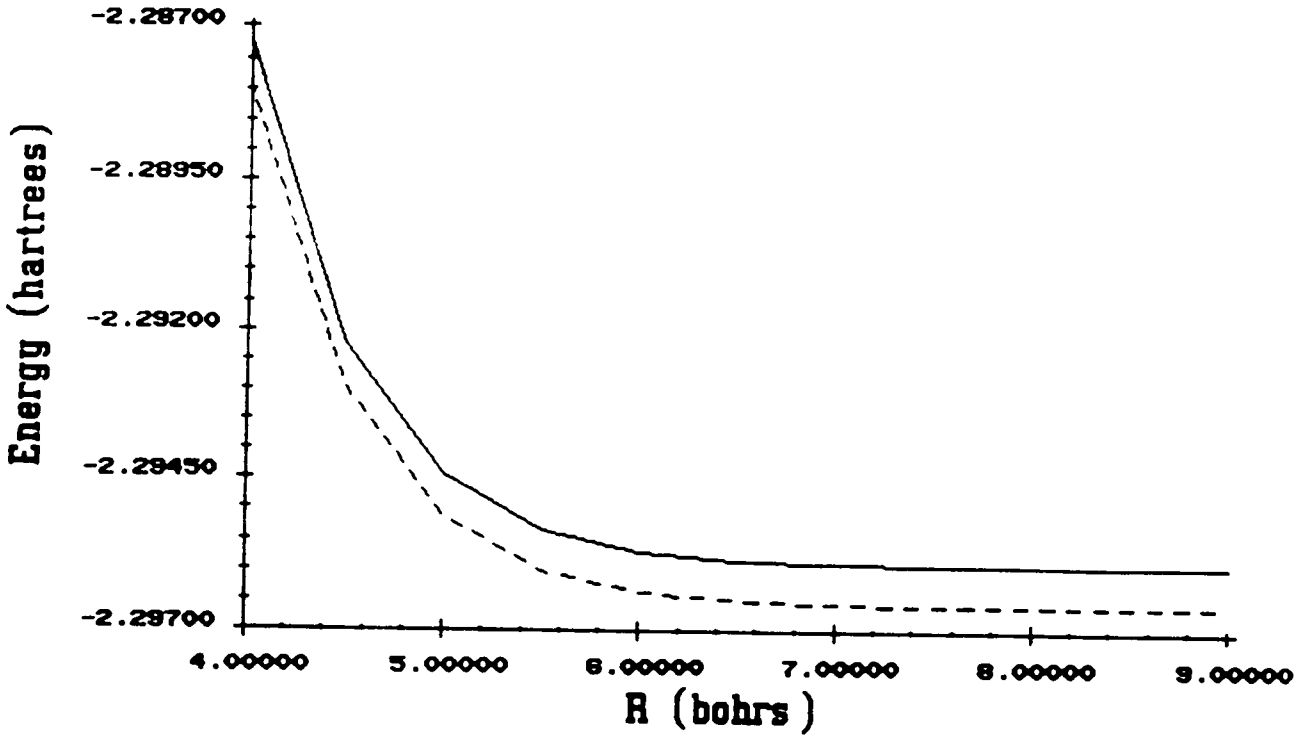

Figure 5.9: Ground state ($^1A_1$) potential energy curves for the D_{2d} crossed configuration.

The solid curve is the CI energy including single and double excitations; the dashed curve is the fully variational energy computed using the tensor product hamiltonian.

Chapter 6

Conclusions

In this work the tensor product approach has been realized as a fully variational method, with many of the attendant advantages and shortcomings common to all fully variational methods. While it may produce accurate results, the size of even the packed form of the eigenvector severely restricts the applicability of the method. In this work only applications involving small molecules with modest basis sets were feasible. In order to extend the scope of the method further approximations will be necessary. Development of the algorithm in a parallel environment (as outlined in Chapter 4) and the availability of high capacity storage devices may also allow the method to be applied to larger systems.

The incorporation of frozen core approximations will significantly extend the method, and allow it to be used within the framework of MCSCF calculations which involve configurations selected in a small active orbital space. The basic idea involves a partitioning of the orbital basis into a "core" set whose members remain relatively unperturbed by the chemical process being considered and a set of valence (or active or "peel" orbitals) which participate directly. Electrons occupying the core orbitals are uncorrelated; they experience only the averaged field of the other $N-1$ electrons, while the electrons in the peel orbitals are fully correlated.

Appendix A

The Kronecker Product and the vec Operator

The tensor (or Kronecker, or direct) product between matrices is defined as follows: Let $\mathbf{A} = [a_{i,j}]$ and $\mathbf{B} = [b_{i,j}]$ be $m \times n$ and $p \times q$ matrices, respectively. Then the Kronecker product $\mathbf{A} \otimes \mathbf{B}$ is the $mp \times nq$ partitioned matrix

$$\mathbf{A} \otimes \mathbf{B} = \begin{bmatrix} a_{11}\mathbf{B} & a_{12}\mathbf{B} & \dots & a_{1n}\mathbf{B} \\ a_{21}\mathbf{B} & a_{22}\mathbf{B} & \dots & a_{2n}\mathbf{B} \\ \vdots & \vdots & \ddots & \vdots \\ a_{m1}\mathbf{B} & a_{m2}\mathbf{B} & \dots & a_{mn}\mathbf{B} \end{bmatrix}.$$

In general the Kronecker product is associative and distributive over addition and multiplication but it is not commutative. For arbitrary matrices $\mathbf{A}$, $\mathbf{B}$, $\mathbf{C}$, and $\mathbf{D}$ and scalars α and β, the Kronecker product has the following properties (see [34, 60] for proofs):

$$\mathbf{A} \otimes (\mathbf{B} + \mathbf{C}) = \mathbf{A} \otimes \mathbf{B} + \mathbf{A} \otimes \mathbf{C} \tag{A.1}$$

$$(\mathbf{A} \otimes \mathbf{B})(\mathbf{C} \otimes \mathbf{D}) = (\mathbf{AC}) \otimes (\mathbf{BD}) \tag{A.2}$$

$$(\alpha\mathbf{A}) \otimes (\beta\mathbf{B}) = \alpha\beta(\mathbf{A} \otimes \mathbf{B}) \tag{A.3}$$

$$(\mathbf{A} \otimes \mathbf{B})^t = \mathbf{A}^t \otimes \mathbf{B}^t \tag{A.4}$$

and when $\mathbf{A}$ and $\mathbf{B}$ are square, invertible matrices,

$$(\mathbf{A} \otimes \mathbf{B})^{-1} = \mathbf{A}^{-1} \otimes \mathbf{B}^{-1} \tag{A.5}$$

The Kronecker product matrix inherits the sparsity patterns of its factor matrices. For example, the tensor product of diagonal matrices is a diagonal matrix; the tensor product of upper (lower) triangular matrices is again an upper (lower) triangular matrix.

If the square $n \times n$ and $m \times m$ matrices $\mathbf{A}$ and $\mathbf{B}$ have the spectral decompositions $\mathbf{A} = \mathbf{UDU}^t$ and $\mathbf{B} = \mathbf{VEV}^t$, the spectral decomposition of the Kronecker product $\mathbf{A} \otimes \mathbf{B}$ is

$$\begin{aligned} \mathbf{A} \otimes \mathbf{B} &= (\mathbf{UDU}^t) \otimes (\mathbf{VEV}^t) \\ &= (\mathbf{U} \otimes \mathbf{V})(\mathbf{D} \otimes \mathbf{E})(\mathbf{U}^t \otimes \mathbf{V}^t) \\ &= (\mathbf{U} \otimes \mathbf{V})(\mathbf{D} \otimes \mathbf{E})(\mathbf{U} \otimes \mathbf{V})^t \end{aligned}$$

so that if $\mathbf{Au} = \alpha\mathbf{u}$ and $\mathbf{Bv} = \beta\mathbf{v}$, where $\mathbf{u}$ and v are columns of $\mathbf{U}$ and $\mathbf{V}$ and α, β are the corresponding eigenvalues, then

$$(\mathbf{A} \otimes \mathbf{B})(\mathbf{u} \otimes \mathbf{v}) = \alpha\beta(\mathbf{u} \otimes \mathbf{v}) \tag{A.6}$$

The *Kronecker sum* of $\mathbf{A}$ and $\mathbf{B}$ is defined as

$$\mathbf{A} \oplus \mathbf{B} = \mathbf{I_m} \otimes \mathbf{A} + \mathbf{B} \otimes \mathbf{I_n} \tag{A.7}$$

where $\mathbf{I_m}$ and $\mathbf{I_n}$ denote $m \times m$ and $n \times n$ identity matrices. For the matrices $\mathbf{A}$ and $\mathbf{B}$ described above, the spectral decomposition of their Kronecker sum is

$$\mathbf{A} \oplus \mathbf{B} = (\mathbf{U} \otimes \mathbf{V})(\mathbf{D} \oplus \mathbf{E})(\mathbf{U} \otimes \mathbf{V})^t \tag{A.8}$$

so $(\mathbf{A} \oplus \mathbf{B})(\mathbf{u} \otimes \mathbf{v}) = (\alpha + \beta)(\mathbf{u} \otimes \mathbf{v})$.

The **vec** operator maps an $m \times n$ matrix $\mathbf{A} = [a_{i,j}]$ onto a vector $\mathbf{vec}(\mathbf{A})$ of length mn by joining the columns of $\mathbf{A}$:

$$\mathbf{vec}(\mathbf{A}) = \begin{bmatrix} a_{11} \\ \vdots \\ a1n \\ a21 \\ \vdots \\ a_{mn} \end{bmatrix} \tag{A.9}$$

The vec operator is linear ($\mathrm{vec}(\alpha\mathbf{A} + \beta\mathbf{B}) = \alpha\,\mathrm{vec}(\mathbf{A}) + \beta\,\mathrm{vec}(\mathbf{B})$) and it preserves the Euclidean norm of its operand ($\|\mathrm{vec}(\mathbf{A})\|_E = \|\mathbf{A}\|_E = \sqrt{\sum_{i=1}^{m}\sum_{j=1}^{n} A_{ij}^2}$).

Appendix B

Total Energies for Low-Symmetry $(H_2)_2$ Configurations

The orientation angles θ_1, θ_2, and ϕ are defined in figure 5.2.2. The orientations were chosen by Price and Stone [84] to facilitate Gauss-Legendre integration; the values of the Gauss-Legendre integration angles are: 25.0173397°, 42.1379871°, 57.4205012°, 66.0559004°, 113.9440996°, 122.5794988°, and 154.9826603°.

Table B.1. Double zeta $(H_2)_2$ total energies in hartrees for for various low-symmetry configurations. R = 4.3 to R = 5.1

θ_1	θ_2	ϕ	R(bohrs)	RHF	SD-CI	SD-CI+SCC	TP
57.4	57.4	90.0	4.3	-2.24344424	-2.2900928	-2.2907692	-2.2907732
90.0	90.0	54.0	4.3	-2.24393686	-2.2907500	-2.2914341	-2.2914363
150.0	30.0	0.0	4.4	-2.2435045	-2.2899914	-2.2906584	-2.2906664
57.4	57.4	18.0	4.4	-2.2441776	-2.2909885	-2.2916693	-2.2916787
25.0	25.0	18.0	4.6	-2.2448765	-2.2915115	-2.2921837	-2.2921954
122.6	57.4	18.0	4.6	-2.2460065	-2.2925801	-2.2932554	-2.2932604
57.4	90.0	54.0	4.6	-2.2460809	-2.2927090	-2.2933869	-2.2933903
25.0	57.4	54.0	4.7	-2.2461028	-2.2927002	-2.2933742	-2.2933815
25.5	90.0	90.0	4.7	-2.2464757	-2.2929986	-2.2936717	-2.2936765
45.0	45.0	45.0	4.7	-2.2460650	-2.2927199	-2.2933961	-2.2934039
25.0	25.0	90.0	4.8	-2.2462479	-2.2928333	-2.2935058	-2.2935143
155.0	57.4	54.0	4.8	-2.2467646	-2.2932773	-2.2939496	-2.2939545
115.0	35.0	10.0	4.8	-2.2469694	-2.2934785	-2.2941516	-2.2941561
25.0	57.4	18.0	4.9	-2.2470659	-2.2936835	-2.2943592	-2.2943667
57.4	90.0	18.0	4.9	-2.2474829	-2.2940879	-2.2947656	-2.2947703
122.6	57.4	54.0	4.9	-2.2474446	-2.2939542	-2.2946285	-2.2946310
66.1	66.1	12.0	5.1	-2.2480110	-2.2946273	-2.2953056	-2.2953109
155.0	25.0	54.0	5.1	-2.2475812	-2.2941502	-2.2948243	-2.2948307

Table B.2: Double zeta $(H_2)_2$ total energies in hartrees for for various low-symmetry configurations. R = 5.2 to R = 6.1

θ_1	θ_2	ϕ	R(bohrs)	RHF	SD-CI	SD-CI+SCC	TP
57.4	90.0	90.0	5.2	-2.2483650	-2.2948439	-2.2955187	-2.2955197
57.4	25.0	90.0	5.2	-2.2481393	-2.2946662	-2.2953362	-2.2953401
25.0	90.0	18.0	5.4	-2.2486918	-2.2951692	-2.2958432	-2.2958460
25.0	57.4	90.0	5.6	-2.2488607	-2.2953582	-2.2960330	-2.2960359
25.0	25.0	18.0	5.6	-2.2486503	-2.2952714	-2.2959493	-2.2959565
42.1	90.0	12.0	5.6	-2.2489554	-2.2954322	-2.2961070	-2.2961094
155.0	25.0	54.0	5.7	-2.2488400	-2.2953940	-2.2960702	-2.2960748
57.4	57.4	18.0	5.7	-2.2489686	-2.2954998	-2.2961764	-2.2961802
25.0	90.0	54.0	5.7	-2.2490649	-2.2955142	-2.2961880	-2.2961897
90.0	90.0	18.0	5.8	-2.2491253	-2.2955997	-2.2962752	-2.2962775
113.9	42.1	12.0	5.8	-2.2491490	-2.2955843	-2.2962581	-2.2962593
25.0	57.4	54.0	5.9	-2.2491248	-2.2956274	-2.2963030	-2.2963060
25.0	90.0	90.0	5.9	-2.2492190	-2.2956536	-2.2963274	-2.2963285
57.4	90.0	18.0	6.1	-2.2492980	-2.2957406	-2.2964152	-2.2964169
122.6	57.4	54.0	6.1	-2.2493109	-2.2957296	-2.2964034	-2.2964040

Table B.3. Double zeta $(H_2)_2$ total energies in hartrees for for various low-symmetry configurations, R = 6.2 to R = 7.1

θ_1	θ_2	ϕ	R(bohrs)	RHF	SD-CI	SD-CI+SCC	TP
155.0	57.4	18.0	6.2	-2.2493369	-2.2957745	-2.2964486	-2.2964498
120.0	30.0	45.0	6.2	-2.2493403	-2.2957731	-2.2964447	-2.2964481
25.0	25.0	54.0	6.2	-2.2492153	-2.2957658	-2.2964431	-2.2964477
57.4	57.4	54.0	6.3	-2.2493465	-2.2957947	-2.2964695	-2.2964711
90.0	90.0	54.0	6.3	-2.2493671	-2.2957802	-2.2964543	-2.2964550
57.4	90.0	90.0	6.4	-2.2494036	-2.2958063	-2.2964800	-2.2964803
25.0	57.4	18.0	6.4	-2.2493567	-2.2958351	-2.2965106	-2.2965133
30.0	30.0	10.0	6.4	-2.2493056	-2.2958362	-2.2965131	-2.2965173
80.0	30.0	10.0	6.6	-2.2494407	-2.2958656	-2.2965398	-2.2965411
145.0	30.0	0.0	6.7	-2.2494357	-2.2958819	-2.2965567	-2.2965582
25.1	90.0	18.0	6.7	-2.2494690	-2.2958773	-2.2965511	-2.2965518
57.4	57.4	90.0	6.7	-2.2494518	-2.2958653	-2.2965391	-2.2965346
155.0	25.0	18.0	6.7	-2.2494126	-2.2958879	-2.2965635	-2.2965659
122.6	57.4	18.0	6.8	-2.2494779	-2.2958743	-2.2965479	-2.2965484
57.4	90.0	54.0	6.8	-2.2494663	-2.2958744	-2.2965488	-2.2965396
42.1	42.1	12.0	6.8	-2.2494249	-2.2958932	-2.2965688	-2.2965714
155.0	57.4	54.0	6.9	-2.2494793	-2.2958950	-2.2965691	-2.2965700
25.0	25.0	90.0	6.9	-2.2494338	-2.2959105	-2.2965863	-2.2965890
155.0	25.0	54.0	7.1	-2.2494650	-2.2959199	-2.2965952	-2.2965973
57.0	90.0	18.0	7.1	-2.2494882	-2.2958887	-2.2965627	-2.2965635

Table B.4: Double zeta $(H_2)_2$ total energies in hartrees for for various low-symmetry configurations, R = 7.2 to R = 8.0

θ_1	θ_2	ϕ	R(bohrs)	RHF	SD-CI	SD-CI+SCC	TP
113.9	42.1	12.0	7.2	-2.2495089	-2.2958992	-2.2965728	-2.2965732
25.0	90.0	18.0	7.3	-2.2495130	-2.2959060	-2.2965796	-2.2965801
57.4	57.4	54.0	7.3	-2.2494934	-2.2958993	-2.2965735	-2.2965744
150.0	30.0	45.0	7.4	-2.2494960	-2.2959215	-2.2965961	-2.2965975
25.0	25.0	18.0	7.4	-2.2494738	-2.2959295	-2.2966049	-2.2966073
122.6	57.4	54.0	7.6	-2.2495171	-2.2959021	-2.2965757	-2.2965760
42.1	90.0	12.0	7.6	-2.2495143	-2.2959046	-2.2965784	-2.2965789
30.0	60.0	45.0	7.7	-2.2495067	-2.2959143	-2.2965885	-2.2965895
25.0	57.4	18.0	7.7	-2.2495052	-2.2959163	-2.2965906	-2.2965918
66.1	90.0	64.0	7.8	-2.2495137	-2.2958971	-2.2965707	-2.2965710
25.0	90.0	90.0	7.8	-2.2495244	-2.2959084	-2.2965819	-2.2965822
57.4	57.4	18.0	7.9	-2.2495071	-2.2959076	-2.2965816	-2.2965826
155.0	57.4	54.0	7.9	-2.2495215	-2.2959132	-2.2965870	-2.2965875
25.0	57.4	18.0	8.0	-2.2495113	-2.2959148	-2.2965889	-2.2965899
120.0	30.0	80.0	8.0	-2.2495207	-2.2959105	-2.2965848	-2.2965853

Table B.5: Double zeta $(H_2)_2$ total energies in hartrees for for various low-symmetry configurations. R = 8.2 to R = 12.0

θ_1	θ_2	ϕ	R(bohrs)	RHF	SD-CI	SD-CI+SCC	TP
25.0	25.0	54.0	8.2	-2.2495060	-2.2959212	-2.2965957	-2.2965970
66.1	66.1	12.0	8.2	-2.2495121	-2.2959043	-2.2965818	-2.2965788
155.0	25.0	18.0	8.4	-2.2495160	-2.2959176	-2.2965917	-2.2965926
25.0	90.0	54.0	8.4	-2.2495263	-2.2959075	-2.2965810	-2.2965813
60.0	90.0	80.0	8.8	-2.2495213	-2.2959012	-2.2965747	-2.2965750
25.0	57.4	54.0	8.8	-2.2495196	-2.2959085	-2.2965823	-2.2965829
57.4	90.0	90.0	9.0	-2.2495214	-2.2959010	-2.2965746	-2.2965748
42.1	42.1	12.0	9.0	-2.2495149	-2.2959076	-2.2965815	-2.2965822
57.4	57.4	90.0	9.2	-2.2495217	-2.2959027	-2.2965763	-2.2965766
155.0	57.4	18.0	9.2	-2.2495250	-2.2959063	-2.2965799	-2.2965859
120.0	30.0	45.0	9.4	-2.2495194	-2.2959049	-2.2965787	-2.2965787
90.0	90.0	54.0	9.4	-2.2495188	-2.2958997	-2.2965733	-2.2965729
57.4	90.0	54.0	9.6	-2.2495207	-2.2959027	-2.2965746	-2.2965748
122.6	57.4	18.0	9.6	-2.2495234	-2.2959057	-2.2965763	-2.2965765
25.0	25.0	90.0	9.8	-2.2495178	-2.2959057	-2.2965796	-2.2965801

Appendix C

Software

This appendix lists the software used to generate the double-zeta hydrogen dimer potential energy surface in the sample calculations described in Chapter 5. The program was implemented to demonstrate the use of the tensor product structure specifically for a small 4 electron system; a more efficient and general program is presently under development.

The program TP4 requires several data files. The molecular integrals are computed using POLYATOM modules PA20a, PA20b, PA30a and PA30b, which place the one- and two- electron integrals with their packed indices on a tape connected to TP4 through logical unit 14. The Hartree-Fock molecular orbitals are read from logical unit 10 (see subroutine GUESS) to construct an initial eigenvector estimate. The initial eigenvector estimate is then spin-adapted using subroutine PROJ, which reads the permutations which characterize a desired structure projector from unit 13. Alternatively, an initial eigenvector estimate (which has been spin projected and transformed) may be provided on unit 9; the final transformed eigenvector estimate is written to unit 9. All other output is written to unit 6.

A file on unit 5 contains miscellaneous input parameters; the first record holds the 6-character label of the POLYATOM integral tape. The second record holds an initial eigenvalue estimate, an estimate of the half-width of the interval where the eigenvalue is to be found, and the maximum residual norm which TLIME will use as a stopping criterion. The third record holds two flags: MOGUES (which

selects a Hartree-Fock starting vector if zero, or an initial vector read from unit 9 otherwise) and VERBOS (for verbose output). The fourth record holds control parameters for TLIME: MINIT (the minimum number of iterations before a switch in the case of a stationary Rayleigh quotient), MAXITN (the maximum number of shift/eigenvector refinements allowed), ND (a negative power of 10 such that when the eigenvalue estimates converge to within 10^{-ND} TLIME switches from inverse to Rayleigh quotient iterations), and K0 (the number of components at each end of the trial vector to print, each iteration).

```
C TP4 v1.1
C
C TP4 demonstrates fully variational electronic structure calculations
C using a tensor product decomposition of the Hamiltonian.
C
      IMPLICIT REAL*8 (A-H,O-Z)
      INTEGER P
      PARAMETER (M=8,P=4,M2=M*M,MP=M**P,LREC = 128)
      DIMENSION AL(M,M),C(M),SS(M,M),WERK(M2,M2)
      DIMENSION W1(MP),W2(MP),W3(MP),W4(MP),W5(MP)
      LOGICAL VERBOS,PARAND,DBUG,PRECON,GEN,GOTVEC,GOTVAL,SPECTR
      REAL*8 NAMTAP
      EXTERNAL ATIMES,ASB
      COMMON /INTGRL/ H(M,M),G(M2,M2)
      COMMON /OVRLP/ S(M,M)
      COMMON /HYMULT/ INDEX(MP)
      COMMON /CFLAGS/ VERBOS,PARAND,DBUG,GOTVEC,GOTVAL,SPECTR,PRECON,
     1                IOUT,INTSRC,INTPRT,ND,KPRINT
      COMMON /PATAP/ PKDLBL(LREC),VALINT(LREC)
      COMMON /ENERGY/ ENUC
      COMMON /EIGEN/ W(MP),X(MP)
      IOUT = 6
      IMO = 10
      IPROJ = 13
      NTAPE = 14
      VERBOS = .TRUE.
      PARAND = .TRUE.
      READ(5,1100) NAMTAP
      READ(5,*) SPIN
      READ(5,*) GAMMA,HWIDTH,RNORM
      READ(5,*) MOGUES,VERBOS,PARAND
```

```
      READ(5,*) MINIT,MAXITN,ND,KO
1100  FORMAT(A6)
      CALL PATAPE(NTAPE,NAMTAP,S,H,G,M,M2)
      IF (VERBOS) THEN
         WRITE (6,*) 'THE OVERLAP MATRIX: '
         CALL MATPRT(S,M)
         WRITE (6,*) 'THE HAMILTONIAN CORE: '
         CALL MATPRT(H,M)
         WRITE (6,*) 'THE TWO ELECTRON MATRIX: '
         CALL MATPRT(G,M2)
      END IF
      CALL DECOM(S,AL,W,INDEX,M)
      IF (VERBOS) THEN
         WRITE (6,*) 'CHOLESKY FACTOR OF S: '
         CALL MATPRT(AL,M)
      END IF
      CALL TRANSF(AL,H,W,M,1,M)
      CALL TRANSF(AL,G,W,M,2,M2)
      IF (MOGUES .EQ. 0) THEN
         CALL GUESS(SPIN,IOUT,IMO,IPROJ)
         CALL MULTTY(AL,X,W,M,P,MP,10,W2)
      ELSE
         READ(9,*)X
      ENDIF
      PRECON = .FALSE.
      GEN = .FALSE.
      GOTVEC = .TRUE.
      GOTVAL = .TRUE.
      SPECTR = .TRUE.
      GAMMA = GAMMA - ENUC
      EPS = 16.D0 ** (-13)
```

```
      ASIZE = 0.0D0
      CALL TLIME(MP,W,W1,W2,W3,W4,W5,
     &           X,ATIMES,ATIMES,PRECON,ATIMES,ASB,
     &           MINIT,GEN,GOTVEC,GOTVAL,
     &           HWIDTH,SPECTR,ND,GAMMA,EPS,
     &           MAXITN,NOUT,KO,INFO,ASIZE,RNORM)

C
C     TLIME  IS DESIGNED TO FIND AN EIGENPAIR OF A SPARSE SYMMETRIC
C     PENCIL (A,B) USING A COMBINATION OF INVERSE AND RAYLEIGH-
C     QUOTIENT ITERATIONS.
C     THE MAIN OPERATION IS TO APPLY THE SYMMETRIC
C     INDEFINITE EQUATION SOLVER  SYMMLQ  TO SYSTEMS OF THE FORM
C
C           (A - SHIFT*B) * X(NEW)  =  X
C
C     TO REFINE THE EIGENVECTOR APPROXIMATION  X.  THE EIGENVALUE
C     APPROXIMATION SHIFT MAY THEN BE REFINED USING THE RAYLEIGH
C     QUOTIENT CORRESPONDING TO  X(NEW).
C
C     MORE SPECIFICALLY TLIME  WILL TRY TO FIND AND EIGENPAIR
C     SO THAT THE EIGENVALUE LIES IN THE INTERVAL CENTERED IN
C     GAMMA (IF GOTVAL=.TRUE.) WITH WIDTH 2*HWIDTH
C
C
C     PROVISION IS MADE FOR PRECONDITIONING THE ABOVE SYSTEM OF
C     EQUATIONS.
C
C     PARAMETERS
C     ----------
C
```

```
C     N        INPUT      THE DIMENSION OF THE MATRIX  A.
C
C     B1(N)    WORKSPACE
C     P(N)     WORKSPACE
C     R1(N)    WORKSPACE     (ONLY USED IN SYMMLQ)
C     R2(N)    WORKSPACE              "
C     V(N)     WORKSPACE              "
C     W(N)     WORKSPACE              "
C
C     X(N)     INPUT      IF  GOTVEC = .TRUE. ,  X  IS ASSUMED TO
C                         CONTAIN AN INITIAL APPROXIMATION TO THE
C                         REQUIRED EIGENVECTOR.  OTHERWISE  X  WILL
C                         BE INITIALIZED TO A STANDARD VECTOR.
C
C              OUTPUT     ON RETURN,  X  WILL CONTAIN THE FINAL
C                         APPROXIMATION TO AN EIGENVECTOR, NORMALIZED
C                         TO HAVE B-NORM 1.
C
C     ATIMES   EXTERNAL   A SUBROUTINE DEFINING THE MATRIX  A.
C                         FOR A GIVEN VECTOR  V,  THE STATEMENT
C
C                               CALL ATIMES( N,V,P )
C
C                         SHOULD RETURN THE PRODUCT  P = A*V.
C                         ATIMES  MUST NOT ALTER THE VECTOR  V.
C
C     MSOLVE   EXTERNAL   AN OPTIONAL SUBROUTINE DEFINING A
C                         PRECONDITIONING MATRIX  M,  WHICH MUST BE
C                         POSITIVE DEFINITE AND WILL USUALLY
C                         APPROXIMATE  (A - SHIFT*B)  IN SOME SENSE.
C                         FOR A GIVEN VECTOR  V,  THE STATEMENT
```

```
C
C                              CALL MSOLVE( N,V,X )
C
C                        SHOULD SOLVE THE LINEAR SYSTEM  M*X = V.
C                        MSOLVE  MUST NOT ALTER THE VECTOR  V.
C
C     BTIMES  EXTERNAL   A SUBROUTINE THAT PERFORMS THE MULTIPLICATION
C                        OF THE MATRIX B TIMES THE VECTOR V IN THE
C                        FORM    CALL BTIMES(N,V,P)      WHERE P IS
C                        THE VECTOR CONTAINING THE RESULT.
C                        BTIMES MUST NOT ALTER THE VECTOR V.
C
C     ASB      EXTERNAL  A SUBROUTINE THAT PERFORMS P=(A-SHIFT*B)*V
C                        NOTE THAT SHIFT IS PASSED THROUGH THE COMMON
C                        BLOCK /ASBCOM/.
C
C                        **NOTE. THE PROGRAM CALLING TLIME MUST DECLARE
C                        **ATIMES, BTIMES, ASB AND MSOLVE TO BE EXTERNA
C
C     PRECON   INPUT     IF  PRECON = .TRUE. ,  PRECONDITIONING WILL
C                        BE INVOKED.  OTHERWISE, SUBROUTINE  MSOLVE
C                        WILL NOT BE REFERENCED.  IN THIS CASE THE
C                        ACTUAL PARAMETER CORRESPONDING TO  MSOLVE  MAY
C                        BE THE SAME AS THAT CORRESPONDING TO  ATIMES.
C
C     MINIT    INPUT     MINIMUM NUMBER OF ITERATIONS BEFORE SWITCH
C                        IN THE CASE OF STATIONARY RAYLEIGH-QUOTIENT.
C
C     GEN      INPUT     LOGICAL VARIABLE SET TO TRUE IF THE
C                        MATRIX B IS DIFFERENT FROM THE IDENTITY, I.E.
C                        IF WE ARE DEALING WITH A TRUE GENERALIZED
```

```
C                       EIGENVALUE PROBLEM. IF GEN=.FALSE., THEN
C                       THE SUBROUTINE BTIMES IS NOT REFERENCED.
C
C
C     GOTVEC  INPUT     LOGICAL VARIABLE, DEFINED ABOVE IN THE DEFINIT
C
C     GOTVAL  INPUT     IF  GOTVAL = .TRUE. ,  GAMMA  IS USED
C                       AS INITIAL ESTIMATE OF AN
C                       EIGENVALUE OF THE MATRIX  A.  OTHERWISE
C                       GAMMA  WILL BE INITIALIZED TO THE
C                       RAYLEIGH-QUOTIENT  X(T)*A*X/X(T)*B*X
C                       CORRESPONDING TO THE INITIAL  X.
C
C     HWIDTH  INPUT     HALF WIDTH OF THE INTERVAL WHERE THE EIGENVALU
C                       IS TO BE FOUND. IF KNOWN IT SHOULD BE SET TO
C                       AN ESTIMATE FOR 1/8 OF MINIMUM LOCAL GAP
C                       BETWEEN EIGENVALUES, I.E. 1/8 OF THE MINIMUM D
C                       BETWEEN THE EIGENVALUE SOUGHT AND ITS NEIGHBOR
C                       IN THE LATTER CASE SPECTR SHOULD BE SET TO TRU
C                       IF HWIDTH.LE.0 IT ASSUMED THAT THE USER IS SEE
C                       TO FIND ANY EIGENVALUE, SO HWIDTH IS RESET TO
C
C     SPECTR  INPUT     LOGICAL VARIABLE. IF ITS VALUE IS TRUE, IT MEA
C                       HWIDTH IS KNOWN TO BE A LOWER BOND TO 1/8 OF T
C                       LOCAL MINIMUM GAP BETWEEN EIGENVALUES NEAR GAM
C
C     ND      INPUT     NEGATIVE POWER OF 10 SUCH THAT WHEN
C                       DIF.LT.10**(-ND) WE SWITCH TO RQI
C
C     GAMMA   INPUT     SEE DEFINITION OF GOTVAL.IT IS THE MIDPOINT OF
C                       THE INTERVAL WHERE THE EIGENVALUE IS TO BE FOU
```

```
C
C             OUTPUT     ON RETURN, GAMMA WILL CONTAIN THE FINAL
C                        APPROXIMATION TO AN EIGENVALUE OF A,
C                        CORRESPONDING TO THE EIGENVECTOR X.
C
C     EPS     INPUT      THE RELATIVE MACHINE PRECISION.
C                        FOR EXAMPLE,
C                        BURROUGHS B6700       EPS = 2.0**(-37)
C                        CDC 6600, 7600        EPS = 2.0**(-47)
C                        IBM 370 (SINGLE)      EPS = 16.0**(-5)
C                        IBM 370 (DOUBLE)      EPS = 16.0**(-13)
C
C     MAXITN  INPUT      AN UPPER LIMIT ON THE NUMBER OF REFINEMENTS OF
C                        SHIFT AND/OR X. A TYPICAL VALUE IS 10.
C
C     NOUT    INPUT      IF NOUT IS POSITIVE, INFORMATION WILL BE
C                        PRINTED ON UNIT NOUT.
C
C     KO      INPUT      NUMBER OF COMPONENTS AT EACH END OF THE
C                        CURRENT ITERATION VECTOR TO BE PRINTED. A TYPI
C                        VALUE IS 15. IF KO .LE.0 NO COMPONENT IS PRINT
C
C     INFO    OUTPUT     AN INTEGER DEFINING THE RESULT OF TLIME ...
C
C               1        SHIFT AND X CONVERGED SATISFACTORILY
C                        TO AN EIGENVALUE AND EIGENVECTOR OF THE PENCIL
C
C               2        SHIFT AND X DID NOT CONVERGE WITHIN
C                        MAXITN REFINEMENTS.
C
C               3        THE APPROXIMATE EIGENVECTOR IN X WAS
```

```
C                       IDENTICALLY ZERO. TLIME STOPS.
C
C                  4    BTIMES DOES NOT REPRESENT
C                       A POSITIVE DEFINITE MATRIX. TLIME STOPS.
C
C     ASIZE    INPUT    ON ENTRY,  ASIZE  SHOULD CONTAIN AN
C                       ESTIMATE OF  NORM(A).  IT IS USED TO
C                       TEST IF THE INITIAL  X  IS AN ACCEPTABLE
C                       APPROXIMATION TO AN EIGENVECTOR OF  A.
C
C              OUTPUT   IF  PRECON = .FALSE.,  ASIZE WILL BE CHANGED T
C                       THE FINAL ESTIMATE OF  NORM(A - SHIFT*B)
C                       AS GIVEN BY SUBROUTINE  SYMMLQ.
C
C     RNORM    INPUT    THE MAXIMUM RESIDUAL NORM TO BE USED AS
C                       STOPING CRITERIA
C
C              OUTPUT   THE FINAL VALUE OF THE NORM OF THE RESIDUAL
C                       VECTOR  (A - SHIFT*B)*X.
C
      WRITE(9,*) X
      WRITE(IOUT,*) 'TOTAL ENERGY:',ENUC+GAMMA
      STOP
 1000 FORMAT(' ',4D22.15)
 1001 FORMAT(//' EIGENVALUE #',I2,': ',D22.15)
      END
C-----------------------------------------------------------------------
C
C
      SUBROUTINE TRANSP(A,N)
      IMPLICIT REAL*8 (A-H,O-Z)
```

```
      DIMENSION A(N,N)
      DO 10 I=1,N-1
         DO 5 J=I+1,N
            SWAP = A(I,J)
            A(I,J) = A(J,I)
            A(J,I) = SWAP
 5       CONTINUE
 10    CONTINUE
      RETURN
      END
C-----------------------------------------------------------------------
C
      SUBROUTINE DECOM(S,AL,WORK,JPIVOT,M)
      IMPLICIT REAL*8(A-H,O-Z)
      INTEGER JPIVOT(1),M
      REAL*8 S(M,M),AL(M,M),WORK(1)
C
C     THIS ROUTINE PERFORMS A CHOLESKY DECOMPOSITION ON THE OVERLAP
C     MATRIX
C
C  ON ENTRY:
C
C     AL        REAL*8(M,M). AL CONTAINS THE OVERLAP MATRIX ON ENTRY.
C               ONLY THE UPPER TRIANGULAR PORTION IS REFERENCED.
C
C     WORK      SEE THE LINPACK ROUTINES DCHDC,DTRCO
C
C     JPIVOT    SEE THE LINPACK ROUTINE DCHDC.
C
C     M         INTEGER. DIMENSION OF THE OVERLAP MATRIX.
C  ON EXIT:
```

```
C
C       AL        CONTAINS TRANSPOSE(L) IN THE UPPER TRIANGULAR PORTION.
C
C  SUBROUTINES: DCHDC,DTRCO,DTRDI
C
       DO 7 J = 1,M
          DO 4 I = 1,M
             AL(I,J) = S(I,J)
 4        CONTINUE
 7     CONTINUE
       DO 10 I = 1,M
          JPIVOT(I) = 0
 10    CONTINUE
C      CHOLESKY DECOMPOSITION ON THE OVERLAP MATRIX... REQUEST NO PIVOT
       CALL DCHDC(AL,M,M,WORK,JPIVOT,0,INFO)
       IF (INFO .NE. M) WRITE (6,1000) INFO
C      CHECK FOR ZERO DIAGONAL ELEMENTS, AND SHOW JPIVOT.
       WRITE(7,1004)
       DO 20 INFO = 1,M
          WRITE(7,1003) INFO,JPIVOT(INFO)
          IF (AL(INFO,INFO) .NE. 0.D0) GO TO 20
          WRITE(7,1001) INFO
          STOP
 20    CONTINUE
       DO 30 I = 1,M
          DO 25 J = I,M
             AL(J,I) = AL(I,J)
 25       CONTINUE
 30    CONTINUE
       CALL DTRCO(AL,M,M,RCOND,WORK,1)
       MM1 = M-1
```

```
      DO 90 I = 1,MM1
         IP1 = I + 1
         DO 91 J = IP1,M
            AL(I,J) = 0
   91    CONTINUE
   90 CONTINUE
      WRITE(7,1002) RCOND
 1000 FORMAT(' DECOMO1 WARNING: INDEX OF THE LAST POSITIVE DIAGONAL'/
     &       '          ELEMENT OF THE CHOLESKY FACTOR OF S IS ',I10)
 1001 FORMAT(' DECOMO2 ERROR  : CHOLESKY FACTOR OF S IS SINGULAR.'/
     &       '          FIRST ZERO DIAGONAL ELEMENT FOUND AT ',I10)
 1002 FORMAT(' CONDITION NUMBER OF THE CHOLESKY FACTOR L: ',D10.5)
 1003 FORMAT(1X,2I5)
 1004 FORMAT(' DECOM: PIVOT ELEMENTS'//'  M   PIVOT(M)'/)
      RETURN
      END
C
C-----------------------------------------------------------------
C
      SUBROUTINE TRANSF(T,A,B,M,P,MP)
      IMPLICIT REAL*8 (A-H,O-Z)
      INTEGER M,P,MP

      REAL*8 T(M,M),A(MP,MP),B(1)
C
C FORMS THE PRODUCT
C                          P                                    P
C               INVERSE( (X) T) * A * INVERSE(TRANSPOSE( (X) T))
C
C WHERE (X)P DENOTES A P-FOLD TENSOR PRODUCT OF IDENTICAL LOWER TRIANGU
C MATRICES T OF RANK M AND A IS A SYMMETRIC MATRIX WITH DIMENSION MP. T
C PRODUCT IS RETURNED IN A. B IS A WORK VECTOR WITH LENGTH AT LEAST MP.
```

```
C
      INTEGER ICOL,INFO
C
C SOLVE THE SYSTEM T * TRANSPOSE(X) = A; STORE TRANSPOSE(X) IN A
C
      DO 10 ICOL = 1,MP
         CALL SOLVTY(T,A(1,ICOL),B,M,P,MP,00,INFO)
 10   CONTINUE
      CALL TRANSP(A,MP)
C
C SOLVE THE SYSTEM T * A = X
C
      DO 20 ICOL = 1,MP

        CALL SOLVTY(T,A(1,ICOL),B,M,P,MP,00,INFO)
 20   CONTINUE
      RETURN
      END
C
C-----------------------------------------------------------------------
C
      SUBROUTINE SOLVTY(T,X,WORK,M,P,MP,JOB,INFO)
      IMPLICIT REAL*8 (A-H,0-Z)
      INTEGER M,P,MP,JOB,INFO
      REAL*8 T(M,M),X(MP),WORK(MP)
C
C  SOLVES SYSTEMS OF THE TYPE
C     (T TENSOR T TENSOR ... TENSOR T)Y = X
C
C  ON INPUT:
C
C  P     (INTEGER) THE NUMBER OF FACTORS IN THE TENSOR PRODUCT
```

```
C         (THE NUMBER OF ELECTRONS IN FULLCI)
C  T     (REAL*8) A TRIANGULAR M BY M MATRIX
C         (THE CHOLESKY FACTOR OF THE OVERLAP MATRIX IN FULLCI)
C  X      (REAL*8) MP-LENGTH VECTOR CONTAINING THE RIGHT HAND SIDE OF
C         OF THE SYSTEM. ON EXIT X CONTAINS THE SOLUTION.
C         (IN FULLCI, X IS AN STANDARD EIGENVECTOR ESTIMATE.)
C  M      (INTEGER) THE DIMENSION OF THE MATRICES AL
C         (THE NUMBER OF BASIS FUNCTIONS IN FULLCI.)
C  MP     (INTEGER) M**P.
C  JOB    (INTEGER) DEPENDS ON THE NATURE OF THE SYSTEM TO BE SOLVED:
C         JOB = 00  SOLVE (T TENSOR ... TENSOR T)Y=X, T LOWER TRIANGULAR
C         JOB = 01           '', T UPPER TRIANGULAR
C         JOB = 10 SOLVE TRANS(T TENSOR...TENSOR T)Y=X, T LOWER TRIANGUL
C         JOB = 11           '', T UPPER TRIANGULAR
C
C
      INTEGER MPMM,MPM1,I,J,K,L
C
      MPM1 = MP/M
      DO 40 K = 1,P
         DO 10 J = 1,MP,M
            CALL DTRSL(T,M,M,X(J),JOB,INFO)
10       CONTINUE
         CALL DCOPY(MP,X,1,WORK,1)
         L = 1
         DO 30 J = 1,MPM1
            DO 20 I = 1,M

               LL = (I-1)*MPM1 + J
               X(LL) = WORK(L)
               L = L+1
20          CONTINUE
```

```
 30       CONTINUE
 40    CONTINUE
       RETURN
       END
C
C-----------------------------------------------------------------------
C
       SUBROUTINE MULTTY(T,X,Y,M,P,MP,JOB,TT)
       IMPLICIT REAL*8 (A-H,O-Z)
       INTEGER M,P,MP,JOB,INFO
       REAL*8 T(M,M),X(1),Y(1),TT(1)
C
C      FORMS PRODUCTS X = (T TENSOR ... TENSOR T)Y
C
C  ON INPUT:
C
C  P      (INTEGER) THE NUMBER OF FACTORS IN THE TENSOR PRODUCT
C         (THE NUMBER OF ELECTRONS IN FULLCI)
C  T     (REAL*8) A TRIANGULAR M BY M MATRIX
C         (THE CHOLESKY FACTOR OF THE OVERLAP MATRIX IN FULLCI)
C  TT     (REAL*8) A WORK VECTOR OF LENGTH AT LEAST M*(M-1)/2
C  Y      (REAL*8) MP-LENGTH VECTOR TO BE RIGHT MULTIPLIED BY THE
C         P-FOLD TENSOR PRODUCT.
C         (IN FULLCI, X IS AN STANDARD EIGENVECTOR ESTIMATE.)
C  M      (INTEGER) THE DIMENSION OF THE MATRICES AL
C         (THE NUMBER OF BASIS FUNCTIONS IN FULLCI.)
C  MP     (INTEGER) M**P.
C  JOB    (INTEGER) DEPENDS ON THE NATURE OF THE SYSTEM:
C         JOB = 00  SOLVE (T TENSOR ... TENSOR T)Y=X, T LOWER TRIANGULAR
C         JOB = 01          '', T UPPER TRIANGULAR
C         JOB = 10 SOLVE TRANS(T TENSOR...TENSOR T)Y=X, T LOWER TRIANGUL
```

```
C         JOB = 11          ", T UPPER TRIANGULAR
C
C  ON EXIT:
C
C  X      CONTAINS THE SOLUTION IF INFO .EQ. 0; OTHERWISE X IS UNCHANGED
C
C
C BLAS: DAXPY, DDOT,  DCOPY
C
      INTEGER MPM1,I,J,K,L,II,JJ,KK,LL
      REAL*8 SUM
C
C  USE FULL MATRIX STORAGE FOR NOW...
C
      K=1
      DO 10 I = 1,M
         DO 5 J = 1,M
            TT(K)= T(J,I)
            K = K+1
 5       CONTINUE
 10   CONTINUE
      MPM1 = MP/M
      DO 50 II = 1,P
         K = 1
         I = 1
         DO 40 JJ = 1,M
            J = 1
            DO 30 KK = 1,MPM1
               L = I
               SUM = 0.DO
               DO 20 LL = 1,M
```

```
                  SUM = SUM + T(L)*Y(J)
                  L = L + 1
                  J = J + 1
20             CONTINUE
               X(K) = SUM
               K = K + 1
30          CONTINUE
            I = L
40       CONTINUE
         CALL DCOPY(MP,X,1,Y,1)
50    CONTINUE
      RETURN
      END

       SUBROUTINE CLRVEC(X,N)
       IMPLICIT REAL*8 (A-H,O-Z)
       REAL*8 X(*)
C
C SETS THE FIRST N ENTRIES OF THE VECTOR X TO ZERO.
C
       INTEGER M, MP1, I, MOD
       ZERO = 0.DO
       M = MOD(N,7)
       IF (M .EQ. 0) GOTO 20
       DO 10 I = 1,M
          X(I) = ZERO
10     CONTINUE
       IF (N .LT. 7) RETURN
20     MP1 = M + 1
       DO 30 I = MP1,N,7
          X(I) = ZERO
```

```
            X(I+1) = ZERO
            X(I+2) = ZERO
            X(I+3) = ZERO
            X(I+4) = ZERO
            X(I+5) = ZERO
            X(I+6) = ZERO
 30     CONTINUE
        RETURN
        END
C
C-----------------------------------------------------------------------
C
        SUBROUTINE INORDR(INDEX,N)
        IMPLICIT INTEGER(A-Z)
        INTEGER INDEX(*),N
C
C SETS THE FIRST N ENTRIES OF THE VECTOR X TO ZERO.
C
        INTEGER M, MP1, I, MOD
        M = MOD(N,7)
        IF (M .EQ. 0) GOTO 20
        DO 10 I = 1,M
           INDEX(I) = I
 10     CONTINUE
        IF (N .LT. 7) RETURN
 20     MP1 = M + 1
        DO 30 I = MP1,N,7
           INDEX(I) = I
           INDEX(I+1) = I+1
           INDEX(I+2) = I+2
           INDEX(I+3) = I+3
```

```
            INDEX(I+4) = I+4
            INDEX(I+5) = I+5
            INDEX(I+6) = I+6
 30     CONTINUE
        RETURN
        END

C
C-------------------------------------------------------------- - --
C
        SUBROUTINE ATIMES( N,Y,HY)
        IMPLICIT REAL*8 (A-H,O-Z)
        INTEGER P
        PARAMETER (M=8,P=4,M2=M*M,MP=M**P)
        REAL*8 Y(N),HY(N)
        COMMON /INTGRL/ H1(M,M),H2(M2,M2)
        COMMON /HYMULT/ INDEX(MP)
C
C ATIMES MULTIPLIES A VECTOR Y BY THE TRANSFORMED HAMILTONIAN MATRIX
C WITHOUT FORMING THE HAMILTONIAN MATRIX EXPLICITLY.
C
C ON ENTRY:
C
C  H1 REAL*8(M,M); TRANSFORMED ONE ELECTRON MATRIX.
C        H2       REAL*8(M2,M2); TRANSFORMED TWO ELECTRON MATRIX.
C        Y        REAL*8(MP); VECTOR TO BE MULTIPLIED.
C        M        INTEGER; NUMBER OF BASIS FUNCTIONS
C        M2       INTEGER; M**2
C        P        INTEGER; NUMBER OF ELECTRONS
C        MP       INTEGER; M**P (DIMENSION OF THE HAMILTONIAN MATRIX)
C        INDEX    INTEGER(MP); WORK VECTOR
C
```

```
C ON EXIT:
C
C       HY REAL*8(MP); CONTAINS THE PRODUCT
C              (INVERSE(L)*H*INVERSE(TRANSPOSE(L)))Y, WHERE L IS THE
C          CHOLESKY FACTOR OF THE OVERLAP MATRIX AND H IS THE FULL
C          CI MATRIX.
C
C SUBROUTINES: IAIY,INORDR,PERMUT,PAIPY
C
       INTEGER PM1,J,K,MJM1,MPMJM1,MPM2,MPMJ,PM2
C
       CALL CLRVEC(HY,MP)
C
C FORM THE ONE-ELECTRON PRODUCT
C
       MJM1 = 1
       MPMJ = MP/M
       DO 10 J = 1,P
          CALL IAIY(H1,Y,HY,MJM1,M,MPMJ,MP)
          MJM1 = MJM1*M
          MPMJ = MPMJ/M
 10    CONTINUE
C
C FORM THE TWO-ELECTRON PRODUCT
C
C FORM ADJACENT TERMS (I TENSOR ... TENSOR H2 TENSOR ... TENSOR I)Y
C (TERMS INVERSE(P(J,J+1))*(H2 TENSOR I)*P(J,J+1)*Y)
C
       MJM1 = 1
       MPM2 = MP/M2
       MPMJM1 = MPM2
```

```
      PM1 = P-1
      DO 20 J = 1,PM1
         CALL IAIY(H2,Y,HY,MJM1,M2,MPMJM1,MP)
         MJM1 = MJM1*M
         MPMJM1 = MPMJM1/M
20    CONTINUE
      DO 50 J = 1,P-2
         DO 40 K = J+2,P
            CALL INORDR(INDEX,MP)
            CALL PERMUT(INDEX,J+1,K,M,P,MP)
            CALL PIAIPY(H2,Y,HY,M**(J-1),M2,M**(P-J-1),INDEX)
40       CONTINUE
50    CONTINUE
      RETURN
      END
C
C-----------------------------------------------------------------
C
      SUBROUTINE MATPRT(A,M)
      IMPLICIT REAL*8(A-H,O-Z)
      DIMENSION A(M,M),II(4),JJ(4),AA(4)
C
C     PRINTS ALL NONZERO ENTRIES IN THE LOWER TRIANGULAR PART OF
C
      K=1
      DO 10 I=1,M
         DO 5 J=1,I
           IF (A(I,J) .NE. 0) THEN
              II(K)=I
              JJ(K)=J
              AA(K)=A(I,J)
```

```
                K=K+1
                IF (K .GT. 4) THEN
                   WRITE (6,1000) (II(K),JJ(K),AA(K),K=1,4)
                   K = 1
                ENDIF
             ENDIF
  5       CONTINUE
  10   CONTINUE
       IF (K .GT. 1) WRITE(7,1000) (II(I),JJ(I),AA(I),I=1,K-1)
 1000  FORMAT(4(' (',I3,',',I3,')',1PD12.5))
       RETURN
       END
C
C-----------------------------------------------------------------
C
       SUBROUTINE IAIY(A,Y,X,J,K,L,JKL)
       IMPLICIT REAL*8 (A-H,O-Z)
       INTEGER J,K,L,JKL
       REAL*8 A(K,K),Y(JKL),X(JKL)
C
C FORMS MATRIX-VECTOR PRODUCTS OF THE FORM
C
C       X <=   (I  (X) A  (X) I ) Y  + X
C                J      K      L
C
C WHERE I DENOTES AN IDENTITY MATRIX, X & Y ARE VECTORS OF LENGTH
C A IS A SYMMETRIC MATRIX. THE SUBSCRIPTS J,K,AND L ARE THE RANKS
C RESPECTIVE MATRICES. (X) REPRESENTS A DIRECT (TENSOR) PRODUCT.
C
       INTEGER LM1,KL,ISTART,IROW,JSTART,JCOL,IBLOCK,IBLEND,LL
       REAL*8 AIJ
```

```
      LM1 = L - 1
      KL = K * L
      ISTART = 0
      DO 40 IROW = 1,K
         JSTART = 0
         DO 30 JCOL = 1,K
            AIJ = A(IROW,JCOL)
            DO 20 IBLOCK = 1,JKL,KL
               IBLEND = IBLOCK + LM1
               DO 10 LL = IBLOCK,IBLEND
                  X(JSTART+LL) = X(JSTART+LL) + AIJ * Y(ISTART+LL)
10             CONTINUE
20          CONTINUE
            JSTART = JSTART + L
30       CONTINUE
         ISTART = ISTART + L

40    CONTINUE
      RETURN
      END
C
C
C-----------------------------------------------------------------------
C
      SUBROUTINE PIAIPY(A,Y,X,J,K,L,INDEX)
      IMPLICIT REAL*8 (A-H,O-Z)
      INTEGER J,K,L,INDEX(1)
      REAL*8 A(K,K),Y(1),X(1)
C
C FORMS MATRIX-VECTOR PRODUCTS OF THE FORM
C
C       X <=   P (I  (X) A  (X) I ) P Y  + X
```

```
C                   J       K       L
C
C WHERE I DENOTES AN IDENTITY MATRIX, X & Y ARE VECTORS OF LENGTH J*K*L
C A IS A SYMMETRIC MATRIX. THE SUBSCRIPTS J,K,AND L ARE THE RANKS OF TH
C RESPECTIVE MATRICES. (X) REPRESENTS A DIRECT (TENSOR) PRODUCT.
C
      INTEGER LM1,KL,ISTART,IROW,JSTART,JCOL,IBLOCK,IBLEND,LL
      REAL*8 AIJ
      LM1 = L - 1
      KL = K * L
      JKL = J * KL
      ISTART = 0
      DO 40 IROW = 1,K
         JSTART = 0
         DO 30 JCOL = 1,K
            AIJ = A(IROW,JCOL)
            DO 20 IBLOCK = 1,JKL,KL
               IBLEND = IBLOCK + LM1
               DO 10 LL = IBLOCK,IBLEND
                  IX = INDEX(JSTART+LL)
                  X(IX) = X(IX) + AIJ * Y(INDEX(ISTART+LL))
10             CONTINUE
20          CONTINUE
            JSTART = JSTART + L
30       CONTINUE
         ISTART = ISTART + L
40    CONTINUE
      RETURN
      END
C-------------------------------------------------------------------------
C
```

```
      SUBROUTINE PAIPY(A,Y,X,K,L,INDEX)
      IMPLICIT REAL*8 (A-H,O-Z)
      INTEGER K,L,INDEX(1)
      REAL*8 A(K,K),Y(1),X(1)
C
C FORMS MATRIX-VECTOR PRODUCTS OF THE FORM
C
C      X <=  X +   INVERSE(P) * ( A  (X) I ) * P * Y
C                                  K      L
C
C WHERE I DENOTES AN IDENTITY MATRIX, X & Y ARE VECTORS OF LENGTH J*K*L
C A IS A SYMMETRIC MATRIX. THE SUBSCRIPTS K AND L ARE THE RANKS OF THE
C RESPECTIVE MATRICES. (X) REPRESENTS A DIRECT (TENSOR) PRODUCT. P IS A
C PERMUTATION MATRIX; MULTIPLICATION OF A VECTOR BY P IS EQUIVALENT TO
C INDIRECT ADDRESSING OF THE VECTOR BY INDEX.
C
      INTEGER ISTART,IROW,JSTART,JCOL,LL
      REAL*8 AIJ
C
      ISTART = 0
      DO 30 IROW = 1,K

         JSTART = 0
         DO 20 JCOL = 1,K
            AIJ = A(IROW,JCOL)
            DO 10 LL = 1,L
               II = INDEX(JSTART + LL)
               X(II) = X(II) + AIJ * Y(INDEX(ISTART+LL))
10          CONTINUE
            JSTART = JSTART + L
20       CONTINUE
         ISTART = ISTART + L
```

```
 30     CONTINUE
        RETURN
        END
        SUBROUTINE PERMUT(IVEC,J,K,M,P,MP)
C
C FORMS THE PRODUCT OF P(J,K) AND IVEC, WHERE IVEC IS A VECTOR OF LENGT
C AND P(J,K) IS A PERMUTATION MATRIX. IF C(I(1),I(2),..,I(J),..,I(K),..
C I(P)) MAPS ONTO IVEC(I) USING A LEXOGRAPHICAL ORDER HASHING FUNCTION
C
C           I = 1 + SUMMATION(K) (I(K)-1) * M **(P-K),K=1,..,P
C
C THEN THE OPERATION P(J,K)IVEC EFFECTIVELY SWAPS ALL ELEMENTS
C
C  C(I(1),..,I(J),..,I(K),..,I(P)) <=> C(I(1),...I(K),..,I(J),..,I(P))
C
C WHERE I(J) = 1,...,M-1, I(K) = I(J)+1,...,M, J<K, AND ALL OTHER
C SUBSCRIPTS I(L) WITH L<>J AND L<>K ARE STEPPED FROM 1 TO M.
C
C ON ENTRY:
C
C    IVEC       INTEGER(MP). THE VECTOR TO BE PERMUTED
C
C    J,K        INTEGER. INDICES OF THE INDICES OF THE PARTITIONED IVEC
C               TO BE SWAPPED.
C
C    M          INTEGER. LENGTH OF THE INDIVIDUAL PARTITIONED INDICES
C               I(N):       1 <= I(N) <= M
C
C    P          INTEGER. NUMBER OF PARTITIONED INDICES OF IVEC.
C               IVEC(I) <=> IVEC(I(1),I(2),...,I(P))
C
```

```
C     MP         INTEGER. LENGTH OF IVEC. MP = M ** P.
C
C     ON EXIT:
C
C     IVEC       CONTAINS THE PERMUTED VECTOR.
C
      DIMENSION IVEC(MP)
      INTEGER P
      MPMJ = M ** (P-J)
      MPMK = M ** (P-K)
      MPMJ1 = M * MPMJ
      MPMK1 = M * MPMK
      LAST3 =MP - MPMJ1 + 1
      LAST2 =MPMJ - MPMK1 + 1
      LAST1 = MPMK
      IJJ = 1
      IJK = 1
      IKK = MPMK
      IKJ = MPMJ
      MM1 = M-1
      DO 50 IJ = 1,MM1
         JK = IJJ + IKK - 3
         KJ = IJK + IKJ - 3
         IJP1 = IJ+1
         DO 40 IK = IJP1, M
            DO 30 L3 = 1, LAST3 , MPMJ1

               JK3 = JK + L3
               KJ3 = KJ + L3
               DO 20 L2 = 1 , LAST2 , MPMK1
                  JK23 = JK3 + L2
                  KJ23 = KJ3 + L2
```

```
                  DO 10 L1 = 1, LAST1, 1
                     JK123 = JK23+ L1
                     KJ123 = KJ23 + L1
                     SWAP = IVEC(JK123)
                     IVEC(JK123) = IVEC(KJ123)
                     IVEC(KJ123) = SWAP
 10                CONTINUE
 20              CONTINUE
 30            CONTINUE
               JK = JK + MPMK
               KJ = KJ + MPMJ
 40          CONTINUE
             IJJ = IJJ + MPMJ
             IJK = IJK + MPMK
             IKJ = IKJ + MPMJ
             IKK = IKK + MPMK
 50      CONTINUE
         RETURN
         END
C
C These routines interface TENSER with the PolyAtom
C package.  Note that the parameter LREC is the record length in the
C PolyAtom integral tape.
C
C-----------------------------------------------------------------------
C
      SUBROUTINE PATAPE(NTAPE,NAMTAP,OVRLAP,H,G,M,M2)
      IMPLICIT DOUBLE PRECISION (A-H,O-Z)
C     PARAMETER (M=8,M2 = M*M)
      PARAMETER (LREC = 128)
      LOGICAL VERBOS,PARAND,DBUG,GOTVEC,GOTVAL,SPECTR,PRECON
```

```
      DOUBLE PRECISION NAMTAP,OVRLAP(M,M),H(M,M),G(M2,M2)
      COMMON /CFLAGS/ VERBOS,PARAND,DBUG,GOTVEC,GOTVAL,SPECTR,PRECON
     1               ,IOUT,INTSRC,INTPRT,ND,KPRINT
      COMMON /PATAP/ PKDLBL(LREC),VALINT(LREC)
      COMMON /ENERGY/ ENUC

C     COMMON /INTGRL/ H(M,M), G(M2,M2)
C     COMMON /OVRLP/  OVRLAP(M,M)
C
C This routine reads the 1- and 2-electron integrals from a tape created by
C the POLYATOM modules PA30A and PA30B.
C
C PATAPECALLS THE ASSEMBLY LANGUAGE ROUTINE UNPACK FROM THE POLYATOM PACKAGE
C to unpack the two-electron integral labels.
C
      DOUBLE PRECISION FNAME(5),FLABEL(12)
      DATA FNAME/6HETA+VL, 6HG-INTS, 6HT-INTS, 6HV-INTS,6HM-INTS/

C
C     Initialize the tape and check to see that its name is correct.
C
      CALL CHKTAP(NTAPE,NAMTAP)
C
C      Read in the nuclear repulsion energy, ENUC.
C
      CALL FILE(NTAPE,NAMTAP,FNAME(1),FLABEL)
      READ (NTAPE)
      READ (NTAPE)
      READ (NTAPE)
      READ (NTAPE) ENUC
      IF (VERBOS) WRITE(IOUT,1000) ENUC
```

```
C
C       Read in the overlap integrals.
C
      CALL MATCLR(OVRLAP,M)
      CALL RDINT1(NTAPE,NAMTAP,OVRLAP,M,FNAME(2),FLABEL)
C
C       Read in the Hamiltonian core integrals.
C
      CALL MATCLR(H,M)
      CALL RDINT1(NTAPE,NAMTAP,H,M,FNAME(3),FLABEL)
      CALL RDINT1(NTAPE,NAMTAP,H,M,FNAME(4),FLABEL)
C
C       Read in the matrix of two electron integrals.  It
C       would be much better to store this big m**2 x m**2 matrix
C       implicitly, but we will only be dealing with
C       fairly small systems for now.
C
      CALL MATCLR(G,M2)
      CALL RDINT2(NTAPE,NAMTAP,G,M,M2,FNAME(5),FLABEL)
      RETURN
 1000 FORMAT(' READ THE NUCLEAR REPULSION ENERGY: ',D22.15,' HARTREES')
 1010 FORMAT(' READ THE OVERLAP MATRIX: ')
 1020 FORMAT(' READ THE HAMILTONIAN CORE MATRIX: ')
 1030 FORMAT(' READ THE TWO ELECTRON INTEGRALS: ')
      END
C
C-----------------------------------------------------------------------
C
      SUBROUTINE CHKTAP(NTAPE,NAMTAP)
      IMPLICIT DOUBLE PRECISION (A-H,O-Z)
      PARAMETER (LREC = 128)
```

```
      LOGICAL VERBOS,PARAND,DBUG,GOTVEC,GOTVAL,SPECTR,PRECON
      DOUBLE PRECISION NAMTAP,IEOF,NAME,IWRD
      COMMON /CFLAGS/ VERBOS,PARAND,DBUG,GOTVEC,GOTVAL,SPECTR,PRECON,
     1                ICUT,INTSRC,INTPRT,ND,KPRINT
      COMMON /PATAP/ PKDLBL(LREC),VALINT(LREC)
C
C CHKTAP rewinds a PolyAtom integral tape and checks its label.
C If the correct tape has not been mounted, the program is aborted.
C Adapted from PolyAtom module PA30A.
C
      DATA IEOF /6H***EOF/
      REWIND NTAPE
C
C     Read until an end-of-file marker is found.
C
 10   READ(NTAPE) IWRD
      IF(IWRD.NE.IEOF) GOTO 10
C
C     Read the name of the tape, and rewind to the point just over the
C     last end-of-file mark.
C
      READ(NTAPE) NAME
      CALL EFSKIP(NTAPE,-1)
C
      IF (NAME .NE. NAMTAP) THEN
         WRITE(ICUT,1000) NTAPE, NAMTAP, NAME
         CALL ABRT
      ELSE IF (VERBOS) THEN
         WRITE(ICUT,1010) NAMTAP,NAME
      ENDIF
      RETURN
```

```
 1000  FORMAT(' *** ERROR *** (From CHKTAP)'/
     1       ' The tape on unit ',I3,' is named ',A6,' not ',A6,
     1       ' as expected.'/' Was the wrong tape mounted? ')
 1010  FORMAT(' POLYATOM INTEGRAL TAPE ',A6,' WAS LOADED ON UNIT ',I4,
     1       '.')

       END
C
C-----------------------------------------------------------------------
C
       SUBROUTINE EFSKIP(NTAPE,NFILS)
       IMPLICIT DOUBLE PRECISION (A-H,O-Z)
       PARAMETER (LREC = 128)
       LOGICAL VERBOS,PARAND,DBUG,GOTVEC,GOTVAL,SPECTR,PRECON
       COMMON /CFLAGS/ VERBOS,PARAND,DBUG,GOTVEC,GOTVAL,SPECTR,PRECON,
     1                 IOUT,INTSRC,INTPRT,ND,KPRINT
       COMMON /CPARMS/ HWIDTH,RNORM
       COMMON /PATAP/ PKDLBL(LREC),VALINT(LREC)
       PARAMETER (MAXREC = 50)
C
C      This subroutine moves tape no. ntape just over nfils number of
C      end-of-file marks, either forward or backwards depending on the
C      sign of nfils. If nfils=0, the subroutine does nothing.
C
C      Note that PolyAtom imposes a limit MAXREC = 50 on the
C     number of records in each file in the record tape.
C
      DOUBLE PRECISION EOF,WORD1
      DATA EOF/6H***EOF/
C
      NT=NTAPE
      IF (NFILS .GT. 0) THEN
```

```
C
C        Forward space over nfils end-of-files on tape ntape
C
         DO 20 K=1,NFILS
 10         READ(NT) WORD1
            IF(WORD1.NE.EOF) GO TO 10
 20      CONTINUE
      ELSE
C
C        Backspace file unit ntape over nfils file marks
C
         N = -NFILS
         DO 40 K=1,N
            KOUNT=0
 30         BACKSPACE NT
            KOUNT=KOUNT+1
            READ(NT) WORD1
            BACKSPACE NT
            IF (KOUNT .GT. MAXREC) THEN
               WRITE(IOUT,1000) K,MAXREC
               IF (PARAND) CALL ABRT
            ENDIF
            IF (WORD1.NE.EOF) GO TO 30
 40      CONTINUE
      ENDIF
      RETURN
 1000 FORMAT(' *** WARNING *** (from EFSKIP).'/' File number ',I3,
     1       ' on the PolyAtom integral tape contains more than ',
     1       I5,' records.')
      END
C
```

```
C-----------------------------------------------------------------------
C
      SUBROUTINE FILE(NTAPE,NAMTAP,FILNAM,FLABEL)
      IMPLICIT DOUBLE PRECISION (A-H,O-Z)
      PARAMETER (LREC = 128)
      LOGICAL VERBOS,PARAND,DBUG,GOTVEC,GOTVAL,SPECTR,PRECON
      DOUBLE PRECISION FILNAM,FLABEL,NAMTAP,XNOFIL
      DIMENSION FLABEL(*)
      COMMON /CFLAGS/ VERBOS,PARAND,DBUG,GOTVEC,GOTVAL,SPECTR,PRECON,
     1                IOUT,INTSRC,INTPRT,ND,KPRINT
      COMMON /CPARMS/ HWIDTH,RNORM
      COMMON /PATAP/ PKDLBL(LREC),VALINT(LREC)
C
C     This subroutine searches the integral tape on unit ntape for the data
C     file named FILNAM.  If it finds it the file unit is positioned to
C     read or rewrite the file . Otherwise a new identification record
C     for the new file is written after the last file, followed by an
C     eof mark, and the tape is left in a position to write this data
C     file.
C     Adapted from PolyAtom module PA30A.
C
      EQUIVALENCE (NOFILE,XNOFIL)
C
      IF (VERBOS) WRITE(IOUT,1000) NTAPE,FILNAM
      M=3
C
C     Skip to the next end-of-file marker and read directory info.
C
 10   CALL EFSKIP(NTAPE,1)
      READ(NTAPE) NAMTAP,NOFILE,(FLABEL(I),I=3,NOFILE)
C
```

```
C     Start searching for the file name.
C
      DO 20 I = M,NOFILE
         IF(FLABEL(I).EQ.FILNAM) GO TO 30
 20   CONTINUE
      IF (FLABEL(NOFILE) .EQ. 0) THEN
C
C        Assign a new file.
C
         CALL EFSKIP(NTAPE,-1)
         CALL EFSKIP(NTAPE,1)
         FLABEL(NOFILE)=FILNAM
         WRITE(NTAPE) NAMTAP,NOFILE,(FLABEL(I),I=3,NOFILE)
         CALL EOFILE(NTAPE)
         CALL EFSKIP(NTAPE,-1)
         IF (VERBOS) THEN
            WRITE(IOUT,1010)
            WRITE(IOUT,1020) NAMTAP,NOFILE,FLABEL(3)
            IF(NOFILE .GT. 3) WRITE(IOUT,1040) (FLABEL(I),I=4,NOFILE)
            WRITE(IOUT,1030)
         ENDIF
         FLABEL(1) = NAMTAP
         FLABEL(2) = XNOFIL
         RETURN
      ENDIF
      M = NOFILE + 1
      GO TO 10
C
C     The file was found.
C
 30   IF (VERBOS) WRITE(IOUT,1050)
```

```
      IF (NOFILE .NE. I) THEN
         REWIND NTAPE
         CALL EFSKIP (NTAPE,I-2)
         READ(NTAPE) NAMTAP,NOFILE,(FLABEL(I),I=3,NOFILE)
         IF (FLABEL(NOFILE) .NE. FILNAM) THEN
            WRITE(IOUT,1070) NTAPE,FILNAM
            CALL ABRT
         ENDIF
      ENDIF
 9    FLABEL(1)=NAMTAP
      FLABEL(2)=XNOFIL
      RETURN
C
 1000 FORMAT(' Searching the PolyAtom integral tape on unit ',I3,
     1       ' for file ',A6)

 1010 FORMAT(' A new file has been assigned.'/' The new directory'
     1       ,' IS:'//'TAPE NAME',T22,'FILE NUMBER',T36,'FILE NAME'/)
 1020 FORMAT(2X,A6,9X,I3,8X,A6)
 1030 FORMAT('...End...'//)
 1040 FORMAT((28X,A6))
 1050 FORMAT(' The file name has been found. ')
 1070 FORMAT(' *** ERROR *** (from FILE).'/' File number ',I3,' is ',
     1       'apparently mislabelled.'/' The file label ',A6,' can not'
     1       ,' be found.')
      END

C
C---------------------------------------------------------------------
C
      SUBROUTINE RDINT1(NTAPE,NAMTAP,ARRAY,M,FILNAM,FLABEL)
      IMPLICIT DOUBLE PRECISION (A-H,O-Z)
```

```
      PARAMETER (LREC = 128)
      LOGICAL VERBOS,PARAND,DBUG,GOTVEC,GOTVAL,SPECTR,PRECON
      DOUBLE PRECISION FILNAM,NAMTAP
      DIMENSION FLABEL(*),ARRAY(M,M)
      COMMON /CFLAGS/ VERBOS,PARAND,DBUG,GOTVEC,GOTVAL,SPECTR,PRECON,
     1                IOUT,INTSRC,INTPRT,ND,KPRINT
      COMMON /CPARMS/ HWIDTH,RNORM
      COMMON /PATAP/ PKDLBL(LREC),VALINT(LREC)

C
C Reads one electron integrals from the PolyAtom integral tape into
C the upper triangular half of the M x M matrix ARRAY.  The integrals
C are found in the file FILNAM on the tape. ILABEL is an array of
C labels dimensioned in the calling program.
C Adapted from the PolyAtom routine ADDT in module BTL40.
C
C     Find the file FILNAM that holds the binary records that hold
C     the integral labels and values.
C
      CALL FILE(NTAPE,NAMTAP,FILNAM,FLABEL)
C
C     Read a record of integral labels and values.  Abort if the
C     number of integrals makes no sense.
C
 10   READ (NTAPE) NINTS, LASTRC, PKDLBL, VALINT
      IF (NINTS .GT. LREC .OR .NINTS. LE. 0) THEN
         WRITE(IOUT,1000)
         CALL ABRT
      ENDIF
C
C     For each integral and its labels,  call the assembly language
C     routine UNPACK to unpack the labels and put the integral into
```

```
C     the upper triangular part of ARRAY. Keep it up until LASTRC
C     is nonzero, indicating that this is the last record.
C
      DO 20 K = 1, NINTS
         CALL UNPACK(PKDLBL(K),I,J,IZ,IZ,IZ,ITAG)
         ARRAY(J,I) = ARRAY(J,I) + VALINT(K)
         ARRAY(I,J) = ARRAY(J,I)
 20   CONTINUE
      IF (LASTRC .EQ. 0) GO TO 10
      RETURN
 1000 FORMAT(' *** ERROR *** (in RDINT1)'/' A record on the integral'
     1       ,' tape makes no sense.'/' Tape read error?')
      END
C
C-----------------------------------------------------------------------
C
      SUBROUTINE RDINT2(NTAPE,NAMTAP,G,M,M2,FILNAM,FLABEL)
      IMPLICIT DOUBLE PRECISION (A-H,O-Z)
      PARAMETER (LREC = 128)
      LOGICAL VERBOS,PARAND,DBUG,GOTVEC,GOTVAL,SPECTR,PRECON
      DOUBLE PRECISION FILNAM,LAB,NAMTAP

      DIMENSION FLABEL(*),G(M2,M2)
      COMMON /CFLAGS/ VERBOS,PARAND,DBUG,GOTVEC,GOTVAL,SPECTR,PRECON,
     1                IOUT,INTSRC,INTPRT,ND,KPRINT
      COMMON /PATAP/ PKDLBL(LREC),VALINT(LREC)
C
C Reads one electron integrals from the PolyAtom integral tape into
C the upper triangular half of the M x M matrix ARRAY.  The integrals
C are found in the file FILNAM on the tape. ILABEL is an array of
C labels dimensioned in the calling program.
C Adapted from the PolyAtom routine ADDT in module BTL40.
```

```
C
      NINTOT = 0
      NRECS = 0
C
C     Find the file FILNAM that holds the binary records that hold
C     the two electron integral labels and values.
C
      CALL FILE(NTAPE,NAMTAP,FILNAM,FLABEL)
C
C     Read each record of integral labels and values.  Abort if the
C     number of integrals makes no sense.
C
 10   READ (NTAPE) NINTS, LASTRC, PKDLBL, VALINT
      IF (NINTS .GT. LREC .OR .NINTS. LE. 0) THEN
         WRITE(IOUT,1000)
         CALL ABRT
      ENDIF
C
C     For each integral and its labels,  call the assembly language
C     routine UNPACK to unpack the labels and put the integral into
C     A. Keep it up until LASTRC
C     is nonzero, indicating that this is the last record.
C
      DO 20 K = 1, NINTS
         CALL UNPACK(PKDLBL(K),I1,I2,I3,I4,MU,ITA)
         IF ((I1.GT.M.OR. I2.GT.M.OR. I3.GT.M.OR. I4.GT.M) .OR.
     1       (I1.LE.0 .OR. I2.LE.0 .OR. I3.LE.0 .OR. I4.LE.0)) THEN
           WRITE(IOUT,1000)
           CALL ABRT
         ENDIF
         IK = M * (I1-1) + I3
```

```
         IL = M * (I1-1) + I4
         JK = M * (I2-1) + I3
         JL=  M * (I2-1) + I4
         KI=  M * (I3-1) + I1
         LI=  M * (I4-1) + I1
         KJ=  M * (I3-1) + I2
         LJ = M * (I4-1) + I2
         G(IK,JL) = VALINT(K)
         G(IL,JK) = VALINT(K)
         G(KI,LJ) = VALINT(K)
         G(LI,KJ) = VALINT(K)
         G(JK,IL) = VALINT(K)
         G(JL,IK) = VALINT(K)
         G(KJ,LI) = VALINT(K)
         G(LJ,KI) = VALINT(K)
 20    CONTINUE
       NINTOT = NINTOT + NINTS
       NRECS = NRECS + 1
       IF (LASTRC .EQ. 0) GO TO 10
       IF (VERBOS) WRITE(IOUT,1010) NINTOT,FILNAM,NAMTAP,NRECS
       RETURN
 1000  FORMAT(' *** ERROR *** (IN RDINT2)'/' A RECORD ON THE INTEGRAL'
      1        ,' tape makes no sense.'/' Tape read error?')
 1010  FORMAT(' A total of ',I10,' integrals were read from file ',A6,
      1       ' on tape ',A6,'.'/' A total of ',I5,' records were read.')
       END

C
C-----------------------------------------------------------------------
C
       SUBROUTINE EOFILE(NTAPE)
       LOGICAL VERBOS,PARAND,DBUG,GOTVEC,GOTVAL,SPECTR,PRECON
```

```
      COMMON /CFLAGS/ VERBOS,PARAND,DBUG,GOTVEC,GOTVAL,SPECTR,PRECON,
     1                IOUT,INTSRC,INTPRT,ND,KPRINT
C
C     Simulate an end of file mark.
C
      DOUBLE PRECISION EOF
      DATA EOF/6H***EOF/
      WRITE(NTAPE) EOF
      RETURN
      END
C
C
C This routine builds a starting estimate of the eigenvector given
C the Hartree-Fock MO coefficients (in HF).
C
C SPECIFIC FOR 4 ELECTRONS IN THIS VERSION.
C
      SUBROUTINE GUESS(SPIN,IOUT,IMO,IPROJ)
      IMPLICIT REAL*8 (A-H,O-Z)
      PARAMETER (M=8,N=4,MN=M**N,M3=M*M*M,M2=M*M)
      CHARACTER*20 LABEL
      DIMENSION CA(M,N),CB(M,N)
      COMMON /EIGEN/ X(MN),W(MN)
C
      WRITE(IOUT,1010)
      IF (SPIN .NE. 0.D0) WRITE(IOUT,*) 'Alpha coefficients:'
      DO 5 I = 1,M
         READ(IMO,1000,ERR=9000) LABEL,(CA(I,J),J=1,N)
         WRITE(IOUT,1020) LABEL, (CA(I,J),J=1,N)
 5    CONTINUE
```

```
      IF (SPIN .NE. 0.D0) THEN
      WRITE(IOUT,*) 'Beta coefficients:'
      DO 6 I = 1,M
         READ(IMO,1000,ERR=9000) LABEL,(CB(I,J),J=1,N)
         WRITE(IOUT,1020) LABEL, (CB(I,J),J=1,N)
 6    CONTINUE
      ENDIF
      IF (N .EQ. 4) THEN
         DO 10 I = 1,M
         DO 10 J = 1,M
         DO 10 K = 1,M
         DO 10 L = 1,M
 10   W(M3*(I-1)+M2*(J-1)+M*(K-1)+L) = CA(I,1)*CA(J,1)*CA(K,2)*CA(L,2)
      ENDIF
      CALL PROJ(SPIN,IPROJ)
      RETURN
 9000 WRITE(IOUT,1030) IMO
      CALL ABRT
      RETURN
 1000 FORMAT(A20,4F10.5)
 1010 FORMAT(//' ---The Hartree-Fock orbitals--- '/)
 1020 FORMAT(1X,A20,4F9.5)
 1030 FORMAT(/' *** ERROR *** (IN GUESS)'/' SOMETHING IS WRONG',
     +       ' on unit ',i2,' containing HF MO coefficients.'/)
      END

C
C---------------------------------------------------------------------
C
       SUBROUTINE PROJ(S,IPROJ)
C
C Applies the first singlet 4 electron structure projector to a trial
```

```
C eigenvector.
C
      IMPLICIT REAL*8(A-H,O-Z)
      INTEGER P
      PARAMETER (M=8,P=4,M2=M*M,MP=M**P)
      COMMON /EIGEN/ PY(MP),Y(MP)
      DIMENSION KET(P)
      INTEGER IYNGOP(16,5)
C
      IHASH(I,J,K,L) = M*(M*(M*(I-1) + (J-1)) + (K-1)) + L
      NPERM = DFLOAT(P)/2.D0 - S
      NTERMS = 16
      C1 = 1.D0/DSQRT(DFLOAT(NTERMS))
      C2 = 1.D0/DSQRT(DFLOAT(MP))
      DO 5 I = 1,MP
         PY(I) = 0.D0
 5    CONTINUE
      REWIND IPROJ
      DO 6 I = 1,NTERMS
        READ(IPROJ,*) (IYNGOP(I,J),J=1,5)
 6    CONTINUE
      DO 10 I = 1,M
        KET(1) = I
        DO 20 J = 1,M
          KET(2) = J
          DO 30 K = 1,M
            KET(3) = K
            DO 40 L = 1,M
              KET(4) = L
              INDEX = IHASH(I,J,K,L)
              C = C1*Y(INDEX)
```

```
                DO 50 II = 1,NTERMS
                  I1 = KET(IYNGOP(II,1))
                  I2 = KET(IYNGOP(II,2))
                  I3 = KET(IYNGOP(II,3))
                  I4 = KET(IYNGOP(II,4))
                  INDEX = IHASH(I1,I2,I3,I4)
                  PY(INDEX)=PY(INDEX)+IYNGOP(II,5)*C
 50             CONTINUE
 40           CONTINUE
 30         CONTINUE
 20       CONTINUE
 10     CONTINUE
C1000   FORMAT(//' INDEX',3X,'KET',8X,'BEFORE PROJECTION',6X,'AFTER ',
C     &         'PROJECTION')
C1001   FORMAT(1X,I5,1X,4I2,2X,1PD22.15,2X,1PD22.15)
        RETURN
        END
C
C-----------------------------------------------------------------------
C
      SUBROUTINE MATCLR(A,N)
      DOUBLE PRECISION A(N,N)
C
      DO 20 I = 1,N
         DO 10 J = 1,N
             A(I,J) = 0.DO
 10      CONTINUE
 20   CONTINUE
      RETURN
      END
```

```
C
C-----------------------------------------------------------------------
C
      SUBROUTINE ABRT
      IMPLICIT DOUBLE PRECISION (A-H,O-Z)
      LOGICAL VERBOS,PARAND,DBUG,GOTVEC,GOTVAL,SPECTR,PRECON
      COMMON /CFLAGS/ VERBOS,PARAND,DBUG,GOTVEC,GOTVAL,SPECTR,PRECON,
     1                IOUT,INTSRC,INTPRT,ND,KPRINT
      WRITE (IOUT,1000)
 1000 FORMAT(' The last error was fatal... aborting.')
      STOP
      END
```

Bibliography

[1] Mulliken, R. S., "Diatomic Molecules: Results of *Ab- Initio* Calculations", Academic Press, New York (1977).

[2] Almlöf, J., Taylor, P. R., "Computational Aspects of Direct SCF and MCSCF Methods", in "Advanced Theories and Computational Approaches to the Electronic Structure of Molecules", ed. C. E. Dykstra, D. Reidel Publishing, Dordrecht (1984).

[3] Bartlett, R. J., Purvis, G. D., *Ann. N. Y. Acad. Sci.*, **62**, 367 (1981).

[4] Bauschlicher, C. W., Langhoff, S. R., *Theor. Chim. Acta*,**73**, 43 (1988).

[5] Bauschlicher, C. W., *J. Chem. Phys.*, **92**, 3020 (1988).

[6] Beattie, C., Schug, J. C., Viers, J. W., Watson, L., "A Vector Method For Large Scale CI Calculations", *SIAM Conference on Numerical Linear Algebra*, Rayleigh, N. C. (May 1986).

[7] Beattie, C., in Numerical Treatment of Eigenvalue Problems,*Int. Series Num. Math.*, 69, 9 (1984)

[8] Bender, C. F., Davidson, E. R., *J. Chem. Phys.*, **70**, 2675 (1966).

[9] Berezanskii, I. M., "Expansions in Eigenfunctions of Selfadjoint Operators", American Mathematical Society, Providence, Rhode Island (1968).

[10] Binkley, J. S., De Frees, M. J., Frisch, Raghavachari, K, Whiteside, R. A., Schlegel, H. A., Fluder, E. M., Pople, J. A., *Gaussian 82 (release H version)*, Carnegie Mellon University, Pittsburgh, PA. (1982).

[11] Born, M., Oppenheimer, J. R., *Ann. Phys., Liepzig*, **84**, 457 (1927).

[12] Born, M., Huang, K., "Dynamical Theory of Crystal Lattices", Oxford Press, Oxford (1954).

[13] Boys, S. F., Benardi, F., *Molec. Phys.*, **19**, 553 (1970).

[14] Breit, G., *Phys. Rev.*, **39**, 616 (1932).

[15] Brooks, B. K., Schaeffer, H. F. III, *J. Chem. Phys.*, **70**, 5092 (1979).

[16] Buenker, R. J., *Theor. Chim. Acta*, **35**, 33 (1974).

[17] Buenker, R. J., Peyerinhoff, S. D., in "Excited States in Quantum Chemistry", eds. C. A. Nicolaides and D. R. Beck, D. Reidel Publishing, Dordrecht, Holland (1979).

[18] Burton, P. G., *Int. J. Quant. Chem.*, **14**, 561 (1978).

[19] Burton, P. G., Senff, U. E., *J. Chem. Phys.*, **78**, 6073 (1983).

[20] Carbo, R., Riera. J. M., "A General SCF Theory", *Lecture Notes in Chemistry, No 5*, Springer-Verlag, Berlin (1978).

[21] Cauchy, A., "Cours D'Analyse de L'Ecole Polytechnique", *Oeuvres Complètes*, v. 2-3 (1821).

[22] ,Coleman, A. J., "The Symmetric Group Made Easy", *Adv. Quant. Chem.*, **4**, 83 (1968).

[23] Cook, J. M., *Trans. Am. Math. Soc.*, **44**, 222 (1953).

[24] Cooper, J. L. B., *Quart. Appl. Math.*,**6**, 179 (1948).

[25] Davidson, E. R., in Methods for Computational Molecular Physics, ed. G. H. F. Diercksen, S. Wilson, D. Reidel Publishing, Dordrecht, Holland (1983).

[26] Davidson, E. R., *J. Comp. Phys.*, **17**, 87 (1975).

[27] Epstein, S. T., "The Variational Method in Quantum Chemistry", Academic Press, New York (1974).

[28] Fox, D. W.,*SIAM Jour. Math. Anal.*, 3, 617 (1972).

[29] Fripiat, J. G., DeHalle, J., André, J. M., *Int. J. Quant. Chem.*, **23**, 1179 (1980).

[30] Froese-Fischer, C. F., "The Hartree-Fock Method for Atoms", Wiley-Interscience, New York (1976).

[31] Gaunt, J. A., *Proc. R. Soc. London*, **122**, 513 (1929).

[32] Gerratt, J., Raimondi, M., *Proc. R. Soc. London*, bf 371 A, 525 (1980).

[33] Golub, G. H., van Loan, C. F., "Matrix Computations", John Hopkins University Press, Baltimore (1983).

[34] Graham, A., "The Kronecker Product and Matrix Calculus: with Applications", Wiley & Sons, New York (1986).

[35] Harrison, R. J., Handy, N. C., *Chem. Phys. Lett.*, **95**, 386 (1983).

[36] Huzinaga, S., *J. Chem. Phys.*, **42**, 1293 (1965).

[37] Hobza, P., Schneider, B., Sauer, J.,Čársky, P., Zahradník, R., *Chem. Phys. Lett.*, **134**, 418 (1986).

[38] Hobza, P., Sauer, J., *Theor. Chim. Acta*,**65**, 279 (1984); *Theor. Chim. Acta*,**65**, 291 (1984)

[39] Jankowski, K., Paldus, J., *Int. J. Quant. Chem.*,**18**, 1243 (1980).

[40] Jorgensen, P., Simons, J., "Second Quantization-Based Methods in Quantum Chemistry", Academic Press, New York (1981).

[41] Kaplan, I. G., "Symmetry of Many-Electron Systems", transl. J. Gerratt, Academic Press, New York (1973).

[42] Knowles, P. J., Handy, N. C., "A New Determinant-Based Full Configuration Interaction Method",*Chem. Phys. Lett.*, 11, 315 (1984).

[43] Kolos, W., Wolniewicz, I., "Improved Theoretical Ground State Energy of the Hydrogen Molecule", *J. Chem. Phys.*,**49**,1 (1969).

[44] Kronig, R. de. L., "Band Spectra and Molecular Structure", Cambridge University Press (1930).

[45] Lanczos, C., *J. Res. Nat. Bur. Stand.*, **45**, 255 (1950).

[46] Langhoff, S. R., Davidson, E. R., *Int. J. Quant. Chem.*, **8**, 61 (1974).

[47] Lengsfield, B. H., *J. Chem. Phys.*, **73**, 382(1980).

[48] Lewis, J. G., Technical Report STAN-CS-77-595, Computer Science Department, Stanford University, Stanford, California (March 1977).

[49] Lischka, H., Sherpard, R., Brown, F. B., Shavitt, I.,*Int. J. Quant. Chem.*, S15, 91 (1981).

[50] Liu, B., Yoshimine, M.,*J. Chem. Phys.*, 74, 612 (1981).

[51] Longuet-Higgens, H. C., *Adv. Spectr.*, **2**, 429 (1961).

[52] Löwdin, P. O., *Adv. Chem. Phys.*, **2**, 207 (1959).

[53] Löwdin, P. O.,*Rev. Mod. Phys.*, 32, 328 (1962).

[54] MacDonald, J. K. L.,*Phys. Rev.*, 43, 830 (1933).

[55] March, N. H., "Self-Consistent Fields in Atoms", Pergamon Press, Oxford (1975).

[56] Matsen, F. A., Pauncz, R., "The Unitary Group in Quantum Chemistry", Elsevier, New York (1986).

[57] Matsen, F. A., Cantu, A. A., Poshusta, R. D., *J. Chem. Phys.*, **70**, 1558 (1966).

[58] Moshinsky, M., Seligman, T. H., *Ann. Phys.*, **66**, 311 (1971).

[59] Nesbet, *J. Chem. Phys.*, **43**, 311 (1965).

[60] Neudecker, H., *SIAM J. Appl. Math.*, **17**, 3 (1969).

[61] Paige, C. C., Saunders, M. A.,*SIAM J. Numer. Anal.*, 12, 617 (1975).

[62] Paldus, J.,*J. Chem. Phys.*, 61, 5321 (1974)

[63] Paldus, J.,*Theor. Chem: Adv. Perspect.*, 2, 131 (1976)

[64] Paldus, J., in The Unitary Group for the Evaluation of Electronic Energy Matrix Elements, ed. J. Hinze, Lecture Notes in Chemistry, 22, Springer-Verlag, Berlin (1981)

[65] Paldus, J., Jeziorski, B.,*Theor. Chim. Acta.*, 73, 81 (1988).

[66] Parlett, B. N., "The Symmetric Eigenvalue Problem", Prentice Hall, Englewood Cliffs, New Jersey (1980).

[67] Pauncz, R., "Spin Eigenfunctions", Plenum Press, New York (1979).

[68] Pereyra, V., Scherer, G., *Math. Anal.*, 595

[69] Pitzer, K., *Acc. Chem. Res.*,**12**, 271 (1979).

[70] Pyykkö, P., *Adv. Quant. Chem.*, **11**, 353 (1978).

[71] Richards, W. G., Walker, T. E. H., Hinkley, R. K., *A Bibliography of Ab Initio Molecular Wave Functions*, Oxford University Press, 1971; Supplement for 1970-73, Richards, W.G., Walker, T. E. H., Farnell, L., Scott, P.R. (1974); Supplement for 1974-1977, Richards, W. G., Scott, P. R., Colbourn, E. A., Marchington, A. F. (1978).

[72] Rubinstein, M., Shavitt, I., *J. Chem. Phys.*, **51**, 2014 (1969).

[73] Russell, D. M., "The Calculation of Lower Bounds to Atomic Energies", Dissertation, University of Arizona (1983)

[74] Saunders, V. R., van Lenthe, J. H.,*Mol. Phys.*, 48, 923 (1983)

[75] Saxe, P., Fox, J., Schaefer, H. F., Handy, N. C.,*J. Chem. Phys.*, 77, 5584 (1982).

[76] Schecter, M., "Operator Methods in Quantum Mechanics", Elsevier North Holland, New York (1981).

[77] Schneider, B., P. Hobza, R. Zahradnik, *Theor. Chim. Acta*,**73**, 201 (1988).

[78] Souers, P. C., "Hydrogen Properties for Fusion Energy", University of California Press, Berkeley (1986).

[79] Shavitt, I., in The Unitary Group for the Evaluation of Electronic Energy Matrix Elements, ed. J. Hinze, Springer-Verlag, Berlin (1981)

[80] Shavitt, I., Bender, C.F., Pipano, A.,*J. Comp. Phys*, 11, 90 (1973)

[81] Siegbahn, P. E. M.,*J. Chem. Phys.*, 72, 1647 (1980)

[82] Roos, B. O., Taylor, P., Siegbahn, P. E. M., *Chem. Phys.*, **48**, 157(1980); Siegbahn, P. E. M., Heiberg, A., Roos, B. O., Levy, B., *Phys. Scr.*, **29**, 323 (1980); Siegbahn, P. E. M., Almhof, J., Heiberg, A., Roos, B. O.,*J. Chem. Phys.*, 74, 2384 (1981)

[83] Siegbahn, P. E. M.,*Chem. Phys. Lett.*, **109**, 417 (1984).

[84] Price, S. L., Stone, A. J., *Mol. Phys.*, **40**, 805 (1980).

[85] Soulé, J. L., "Linear Operators in Hilbert Space", Gordon and Breach, New York (1968).

[86] Szabo, A., Ostland, N. L., "Modern Quantum Chemistry: Introduction to Advanced Electronic Structure Theory". Macmillan, New York (1982).

[87] Szyld, D. B., in "Innovative Numerical Methods in Engineering", ed. R. P. Shaw, J. Periaux, A. Chaudouet, J. Wu, C. Marino, C. Brebbia, Springer-Verlag, Berlin (1986).

[88] Szyld, D. B., Widlund, O. B., in "Advances in Computer Methods for Partial Differential Equations - III", IMACS, 167 (1979).

[89] Tapia, O., Bessis, G., *Theor. Chim. Acta*,**25**, 130(1972)

[90] Veillard, A., Clementi, E., *J. Chem. Phys*, **49**, 2415(1968)

[91] von Neumann, J., "Mathematical Foundations of Quantum Mechanics", Princeton University Press, Princeton (1955).

[92] Wahl, C., Das, G., in "Methods of Electronic Structure Theory", ed. H. F. Schaefer III, Plenum Press, New York (1972).

[93] Watts, J. D., Dupuis, M.,*J. Comp. Chem.*, 9, 158 (1988).

[94] Wilkinson, J. H., "The Algebraic Eigenvalue Problem", Oxford University Press, London (1965).

[95] Wilson, S., "Electron Correlation in Molecules", Clarendon Press, Oxford (1984).

[96] Wilson, C. W., Goddard, W. A., *J. Chem. Phys.*, **51**, 715 (1969).

[97] Wilson, S., Silver, D. M., in Proceedings of the Fourth Seminar on Computational Problems in Quantum Chemistry, ed. B. Roos and G. H. F. Diercksen, Max-Planck-Institut fur Physik und Astrophysik, Munich (1978)

The vita has been removed from the scanned document